

# **Computational Identification and Evaluation of Potential QaCA Inhibitors in *Staphylococcus aureus* using Structure-Based Drug Discovery Techniques**

G Shreyasree

## **Table of Contents**

S.no.	Title		Page Number
1	Introduction		4
2	Background of the Study		5
2	1	Antimicrobial Resistance	5
2	2	ESKAPE Pathogens	6
2	3	Staphylococcus Aureus: Biology and Resistance Mechanisms	7
2	4	Multidrug Resistance and Role of Efflux Pumps	7
2	5	QacA Efflux Pump: Structure, Function and Relevance	8
3	Target Selection and Potential Ligands		10
3	1	Target Protein: QacA Structure and Function	11
	2	Ligand Selection from Literature Review	11
4	ADMET Analysis of the Compounds		15
	1	ADMET Analysis of Primary Ligands	15
	2	ADMET Analysis of Secondary Ligands	18
5	Protein Preparation and Active Site Preparation		50
	1	Active Site Prediction	50
6	Grid Box Setting and Molecular Docking		52
	1	Grid Box Setting	52
	2	Docking Results	53
7	Post-Docking Analysis		67
8	Challenges and Limitations		104
9	References		105

## List of Figures

S.No.	Title
1	How Antibiotic Resistance Works
2	ESKAPE Pathogens
3	Methicillin-resistant <i>Staphylococcus aureus</i>
4	Multidrug resistance and the role of efflux pumps
5	QacA Efflux Pump
6	CryoEM structure of QacA (D411N), an antibacterial efflux transporter from <i>Staphylococcus aureus</i>
7 - 9	Structures of Primary Ligands
10 - 12	ADME Analysis of Primary Ligands
13	ADME Analysis of Secondary Ligands for 1,8-naphthyridine-3-carboxamide
14 - 32	ADME Analysis of Secondary Ligands for Carnosic Acid
33 - 45	ADME Analysis of Secondary Ligands for Carnosol
46	3-Dimensional Structure of the QacA Protein
47	Binding Site with the Highest Surface Area (P_0)
48	Grid Box Setting

## List of Tables

S.no.	Title
1	Compounds inhibiting QacA efflux activity in <i>Staphylococcus aureus</i> - Primary Ligands Summary
2	Similar compounds to 1,8-Naphthyridine-3-carboxamide, as retrieved from ChEMBL Web Resource Client API
3	Similar compounds to Carnosic acid, as retrieved from ChEMBL Web Resource Client API
4	Similar compounds to Carnosol, as retrieved from ChEMBL WebResource Client API
5	Drug-Likeness Comparison of Primary Ligands (SwissADME Metrics)
6	Compounds selected for further analysis by docking
7	Active Sites Predicted in QacA Efflux Protein
8	Grid Box Conformations
9 – 11	Primary Ligands Docking Results
12 – 26	Secondary Ligands Docking Results – Carnosic Acid
27	Secondary Ligands Docking Results – 1,8-Naphthyridine-3-Carboxamide
28 – 40	Secondary Ligands Docking Results – Carnosol
41 – 42	Post Docking Analysis Results of Primary Ligands - Hydrogen Bonds and Hydrophobic Interaction Data
43 – 44	Post-Docking Analysis Results – Secondary Ligands of Naphthyridine-3-Carboxamide – Hydrogen Bonds and Hydrophobic Interaction Data
45 – 46	Post-Docking Analysis of Secondary Ligands of Carnosic Acid – Hydrogen Bond Interactions and Hydrophobic Interaction Data
47 – 48	Post-Docking Analysis of Secondary Ligands of Carnosol – Hydrogen Bond Interactions and Hydrophobic Interaction Data

## **INTRODUCTION**

Antimicrobial resistance (AMR) has become a critical global health concern, with certain bacterial pathogens evolving mechanisms that render conventional antibiotics ineffective. Among these, the ESKAPE group of pathogens are notorious for their ability to "escape" the effects of antimicrobial agents, leading to persistent and hard-to-treat infections. *Staphylococcus aureus*, a key member of this group, contributes significantly to hospital- and community-acquired infections through its multidrug resistance (MDR) capabilities. One of the molecular mechanisms underlying MDR in *S. aureus* is the expression of efflux pumps such as QaCA, which actively transport a wide range of antimicrobial compounds out of the bacterial cell. In this study, the objective was to design a structure-based drug discovery pipeline to identify potential QaCA inhibitors, thus targeting the efflux mechanism as a strategy to restore antibiotic efficacy.

## BACKGROUND OF THE STUDY

### Antimicrobial Resistance

Antimicrobial resistance (AMR) is widely recognized as one of the most pressing global public health challenges of the 21st century. It undermines the effectiveness of treatments and preventive measures against a growing spectrum of infections caused by bacteria, viruses, parasites, and fungi that have become resistant to the drugs traditionally used to combat them. Antimicrobial agents—including antibiotics, antivirals, antifungals, disinfectants, and food preservatives—are designed to either inhibit microbial growth or kill the microorganisms. However, AMR is an inevitable consequence of evolutionary adaptation, arising as organisms acquire genetic mutations that enable them to withstand the selective pressure imposed by these agents.

Bacteria can develop resistance to antibiotics through three primary mechanisms: intrinsic, acquired, and adaptive resistance.

- Intrinsic resistance refers to a bacterium's natural, inherent ability to resist certain classes of antibiotics due to specific chromosomal genes. This form of resistance exists without requiring genetic mutation or the acquisition of new genes
- Acquired resistance develops when a previously susceptible bacterium becomes resistant due to mutations in its chromosomal DNA or through the acquisition of external genetic material via horizontal gene transfer (HGT). The major modes of HGT include transformation, transposition, and conjugation.
- Adaptive resistance is a temporary or sometimes permanent resistance phenotype that emerges in response to environmental stressors. Its stability depends on the nature and duration of the selective pressure.

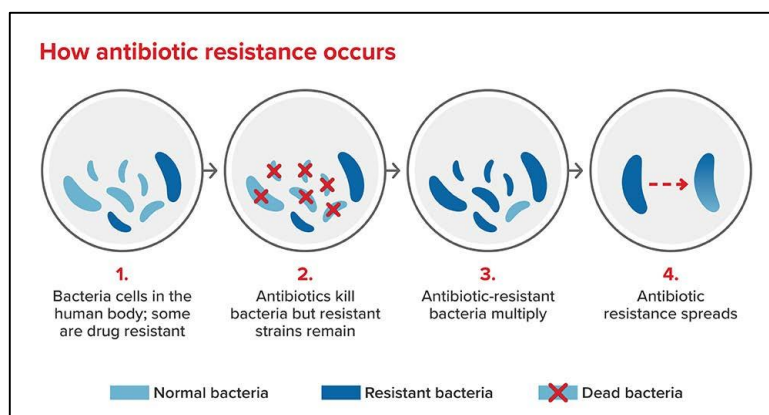


Figure 1: How Antibiotic Resistance Occurs

The spread and acquisition of AMR predominantly occur through human-to-human transmission, both in healthcare settings and within the broader community. The risk is further exacerbated by environmental hotspots, including urban wastewater and sewage sludge, as well as agricultural sources such as pig slurry, cow manure, and poultry-derived fertilizers, all of which serve as reservoirs and vectors for resistant microorganisms.

Addressing AMR effectively demands a unified, global response. This includes the active collaboration of international and national governments, public health authorities, scientific researchers, pharmaceutical industries, hospital systems, agricultural stakeholders, and the general public. With strong political will and

coordinated action, this multifaceted alliance can slow the progression of AMR and alleviate the associated health and economic burdens on societies worldwide.

## ESKAPE Pathogens

Nosocomial infections are caused by a variety of organisms, and can be derived from both exogenous and endogenous sources and are transferred by either direct or indirect contact. Growing numbers of antimicrobialresistant pathogens are increasingly associated with nosocomial infections. Recent reports from hospital-based surveillance studies have begun to refer to a group of nosocomial pathogens as ESKAPE pathogens.

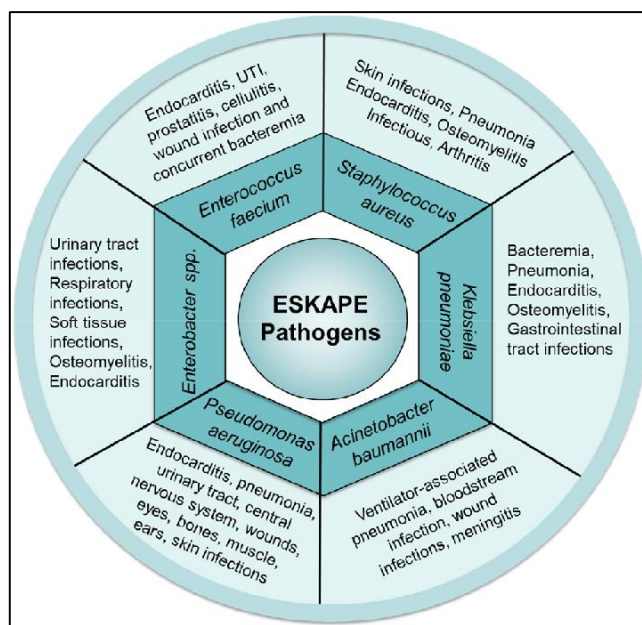


Figure 2: ESKAPE Pathogens

These are a group of bacteria, including both gram-positive and gram-negative species, made of the following six bacterial species:

- *Staphylococcus aureus*
- *Enterococcus faecium*
- *Klebsiella pneumoniae*
- *Acinetobacter baumannii*
- *Pseudomonas aeruginosa*
- *Enterobacter* species

These pathogens are associated with the highest risk of death, resulting in higher healthcare costs. Multiple alternative therapies are being tried and in practice include the use of antibiotics in combination or with adjuvants, bacteriophage therapy, antibacterial antibodies, phytochemicals, and nanoparticles as antibacterial agents. However, there remains an insufficiency of effective antibiotic combinations, in addition to the dry pipeline of new drugs. A uniform research methodology used to test the efficacy of these therapeutic agents, well-defined standards and well-performed clinical trials can aid in understanding the therapeutic potential of these agents.

## *Staphylococcus aureus*: Biology and Resistance Mechanisms

*Staphylococcus aureus* is a Gram-positive catalase-positive coccus that commonly colonizes human skin and mucous membranes, but is also a major opportunistic pathogen responsible for a wide spectrum of diseases, from superficial skin infections to severe systemic diseases such as bacteremia, pneumonia, and endocarditis. Its success as both a commensal and a pathogen is attributed to its adaptability and the arsenal of virulence factors it produces, including surface proteins that mediate adhesion, enzymes that facilitate tissue invasion, and toxins that damage host cells and modulate immune responses. The regulation of virulence in *S. aureus* is complex and involves several global regulatory systems, notably the accessory gene regulator (agr) quorum sensing system, which controls the expression of many toxins and exoenzymes in response to cell density. Additional regulatory systems, such as SarA and Rot, further fine-tune the expression of virulence determinants, enabling the bacterium to adapt to changing host environments and evade immune defenses.

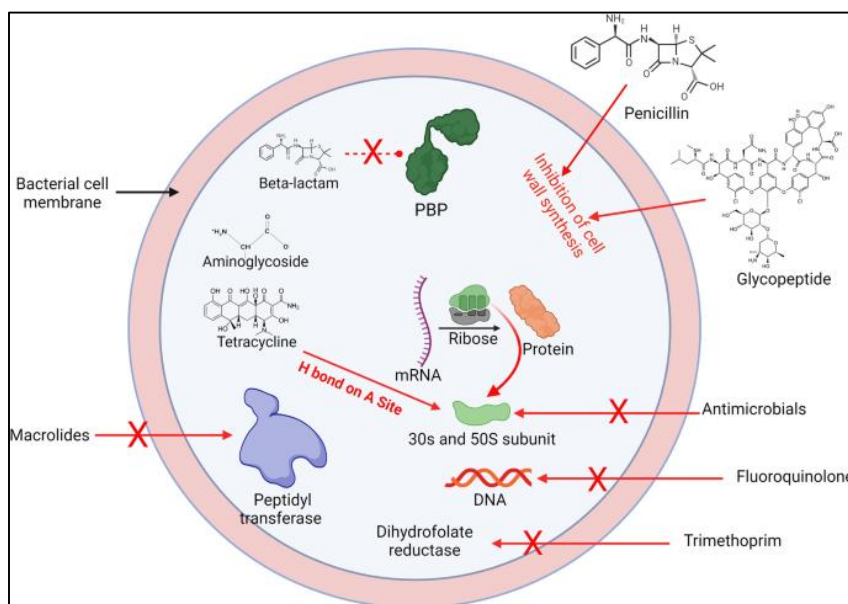


Figure 3: Methicillin-resistant *Staphylococcus aureus*

*S. aureus* has developed multiple mechanisms of antibiotic resistance, most notably the production of  $\beta$ -lactamases that inactivate penicillins and the acquisition of the *mecA* gene, which encodes an altered penicillin binding protein (PBP2a) with low affinity for  $\beta$ -lactam antibiotics, resulting in methicillin resistance (MRSA). Resistance is further enhanced by biofilm formation, which protects bacterial communities from both antibiotics and immune attacks, and by the horizontal transfer of resistance genes via mobile genetic elements, making *S. aureus* a persistent and evolving threat to public health.

## Multidrug Resistance and the Role of Efflux Pumps

Multidrug resistance (MDR) in bacteria is a growing global health threat, largely driven by the action of efflux pumps—membrane-bound transport proteins that actively expel a wide variety of antibiotics and toxic compounds from the cell, thereby reducing intracellular drug concentrations to sub-lethal levels. Efflux pumps are found in both Gram-positive and Gram-negative bacteria and play a crucial role in intrinsic and acquired resistance by exporting structurally diverse antimicrobial agents, detergents, dyes, and even heavy metals. These systems are classified into several major families, including the ATP-binding cassette (ABC) superfamily, major facilitator superfamily (MFS), multidrug and toxic compound extrusion (MATE) family, resistance-nodulation-division (RND) family, small multidrug resistance (SMR) family, and the

proteobacterial antimicrobial compound efflux (PACE) family, each differing in structure, energy source, and substrate specificity.

Efflux pumps not only contribute to antibiotic resistance but also play broader physiological roles in bacterial survival, such as the extrusion of metabolic waste products, signaling molecules involved in quorum sensing, and factors necessary for biofilm formation and virulence. The RND family, for instance, is particularly important in Gram-negative bacteria like *Pseudomonas aeruginosa*, where pumps such as MexAB-OprM and MexXY are linked to high-level resistance and enhanced biofilm-associated tolerance. Overexpression of efflux pumps can be triggered by environmental stressors, sub-inhibitory antibiotic concentrations, and genetic mutations, leading to co-selection of resistance traits and increased pathogenicity. Furthermore, substrate redundancy means that a single efflux pump can export multiple antibiotic classes, while several pumps may act on the same drug, making inhibition of resistance particularly challenging.

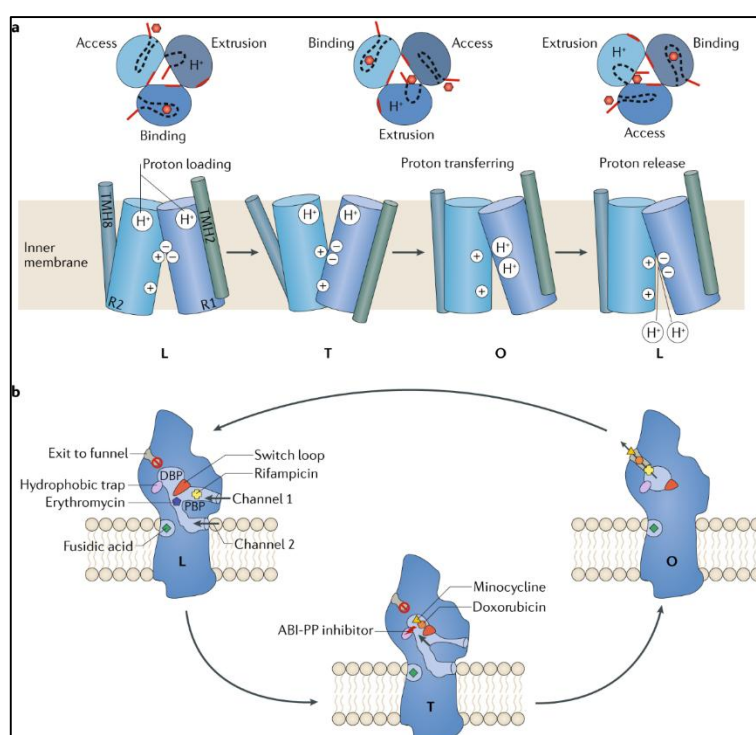


Figure 4: Multidrug resistance and the role of efflux pumps

The clinical significance of efflux-mediated MDR is profound, as it limits the effectiveness of existing antibiotics and complicates infection management, especially in hospital settings where multidrug-resistant pathogens are prevalent. While efflux pump inhibitors (EPIs) have been proposed as adjunct therapies to restore antibiotic efficacy, the development of broad-spectrum, clinically effective EPIs remains difficult due to the pumps' structural diversity and overlapping substrate profiles. Ongoing research focuses on unravelling the regulatory networks controlling efflux pump expression and identifying novel inhibitors, with the goal of countering MDR and preserving the utility of current and future antimicrobial agents.

### **QacA Efflux Pump: Structure, Function and Relevance**

The QacA efflux pump is a membrane protein found predominantly in *Staphylococcus aureus* and is a member of the major facilitator superfamily (MFS) of transporters. Structurally, QacA is composed of 14 transmembrane helices and operates as a proton-coupled antiporter, utilizing the proton motive force to extrude a broad spectrum of monovalent and divalent cationic antimicrobial agents—including quaternary ammonium compounds, intercalating dyes, diamidines, and biguanidines—out of the bacterial cell. The

recent cryo-EM structure of QacA, resolved at 3.6 Å, reveals an outward-open conformation with a unique extracellular helical hairpin loop (EL7) between transmembrane helices 13 and 14, which is conserved in a subset of DHA2 transporters and plays a critical role in substrate efflux.

Functionally, QacA mediates resistance by exporting toxic compounds from the bacterial cytoplasm, thereby lowering their intracellular concentrations and protecting the cell from their effects. The pump's substrate promiscuity is facilitated by multiple acidic residues in the vestibule, which enable the transport of structurally diverse cationic drugs through a competition-driven proton/substrate antiport cycle. The presence of the EL7 hairpin loop and its interaction with other extracellular loops are essential for the structural integrity and activity of QacA; removal or disruption of this motif significantly impairs efflux function. Importantly, QacA's ability to extrude a wide variety of antimicrobial agents contributes to high-level multidrug resistance in clinical isolates of *S. aureus*.

The clinical relevance of QacA lies in its contribution to the survival of *S. aureus* in environments with high concentrations of disinfectants and antiseptics, particularly in healthcare settings where quaternary ammonium compounds are frequently used. Inhibition of QacA and related efflux pumps has been shown to sensitize bacteria to antibacterial agents, suggesting that efflux pump inhibitors could be a promising strategy to combat multidrug resistance. Understanding the structure-function relationship of QacA, especially the role of conserved structural motifs like EL7, is crucial for the development of targeted inhibitors and for addressing the ongoing challenge of efflux-mediated resistance in pathogenic bacteria.

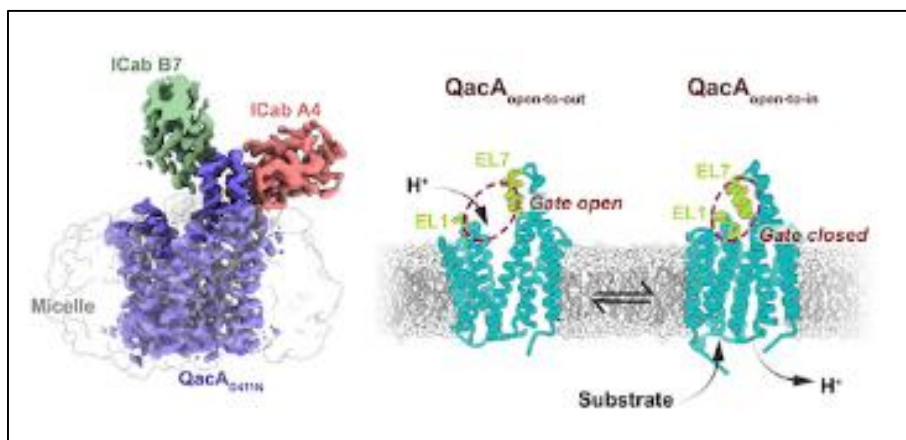


Figure 5: QacA Efflux Pump

## Target Selection and Potential Ligands

### Target Protein: QacA Structure and Function

#### **QacA Protein Structure**

- QacA is a membrane-bound multidrug efflux protein found in *Staphylococcus aureus*
- It belongs to the major facilitator superfamily (MFS) of transporters and consists of 14 transmembrane helices arranged in two helical bundles, with a unique extracellular  $\alpha$ -helical hairpin loop (EL7) between helices 13 and 14.
- The protein is composed of 514 amino acids and has a molecular weight of approximately 55 kDa
- The EL7 loop plays an allosteric role, essential for efficient drug efflux; its removal or disruption impairs transporter function.
- The overall structure supports a rocker-switch mechanism for substrate transport, typical of MFS antiporters.

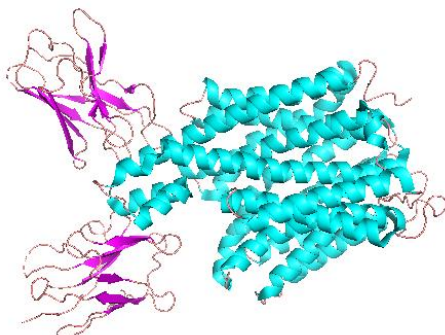


Figure 6: CryoEM structure of QacA (D411N), an antibacterial efflux transporter from *Staphylococcus aureus*

#### **Function**

- QacA confers resistance to a broad range of cationic antimicrobial agents, including:
  - Quaternary ammonium compounds (e.g., benzalkonium chloride, chlorhexidine)
  - Intercalating dyes (e.g., ethidium bromide, acriflavine)
  - Diamidines and biguanidines
- It operates as a proton-coupled antiporter, using the proton motive force to export toxic compounds out of the bacterial cell in exchange for protons.
- QacA can recognize and expel both monovalent and divalent cationic substrates; distinct binding sites exist for these substrate types, with specific acidic residues (e.g., D323) being crucial for divalent cation recognition.
- This efflux activity is a major contributor to multidrug resistance in *S. aureus*, allowing survival in the presence of disinfectants and antiseptics.
- The expression of qacA is regulated by the QacR protein, a TetR-family transcriptional repressor that binds to the qacA operator region and modulates gene expression in response to environmental signals.

## Ligand Selection from Literature Review

### Primary Ligands

1,8-naphthyridine-3-carboxamide is a synthetic compound of the 1,8-naphthyridine class that has been demonstrated to inhibit efflux pumps in *Staphylococcus aureus*, including QacA. Studies show that these compounds, when combined with antibiotics, significantly reduce the minimum inhibitory concentrations (MICs) of ethidium bromide and  $\beta$ -lactam antibiotics in QacA-expressing strains, indicating effective inhibition of pump and restoration of antibiotic susceptibility.

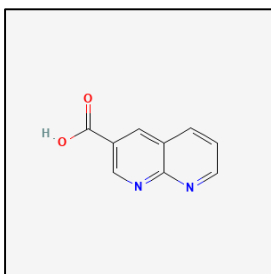


Figure 7: Structure of 1,8-Naphthyridine-3-carboxamide

Carnosic acid is a phenolic diterpene derived from rosemary (*Rosmarinus officinalis*) that has been shown to act as an efflux pump inhibitor in *S. aureus*. Experimental evidence demonstrates that carnosic acid can dissipate membrane potential and inhibit the activity of efflux pumps, including QacA, thereby enhancing the intracellular accumulation of antimicrobial agents and reducing bacterial resistance.

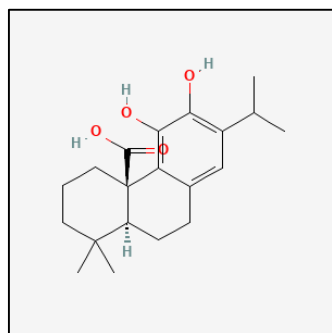


Figure 8: Structure of carnosic acid

Carnosol, another phenolic diterpene from rosemary, has been evaluated for its anti-efflux pump activity in multidrug-resistant *S. aureus*. In laboratory studies, carnosol significantly suppressed efflux pump activity in extensively drug-resistant *S. aureus* strains, as evidenced by reduced efflux in flow cytometry assays and potentiation of gentamicin activity, supporting its role as a QacA inhibitor.

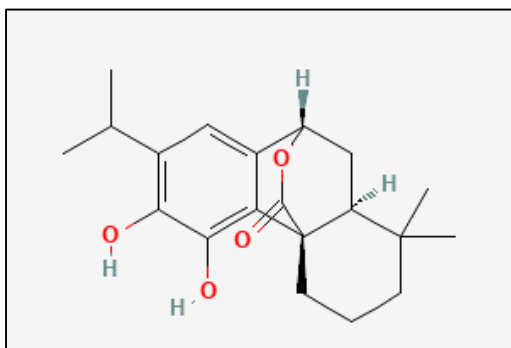


Figure 9: Structure of Carnosol

Compound Name	PubChem CID	Description
1,8-Naphthyridine-3-carboxamide	23435869	This synthetic compound inhibits QacA efflux activity in <i>Staphylococcus aureus</i> , reducing resistance to antibiotics and ethidium bromide. Its use in combination with antibiotics has been shown to lower MICs in QacA-expressing strains, supporting its role as an efflux pump inhibitor.
Carnosic acid	65126	Carnosic acid, a phenolic diterpene from rosemary, has demonstrated the ability to inhibit efflux pumps such as QacA by dissipating membrane potential. This action increases the intracellular concentration of antibiotics, thereby enhancing their effectiveness against resistant <i>S. aureus</i> .
Carnosol	442009	Carnosol, another diterpene from rosemary, has been shown to suppress QacA-mediated efflux in multidrug-resistant <i>S. aureus</i> . Laboratory studies report that carnosol potentiates antibiotic activity by reducing efflux pump function, as evidenced by flow cytometry assays.

Table 1: Compounds inhibiting QacA efflux activity in *Staphylococcus aureus* - Primary Ligands Summary

## Secondary Ligands

To broaden the chemical landscape surrounding the primary hits, secondary ligands were identified using the ChEMBL web resource client, with Tanimoto similarity employed as the basis for compound selection. A threshold of 0.50 was applied to allow moderate structural flexibility while retaining core molecular features, facilitating the exploration of potentially diverse yet functionally relevant analogs. This similarity-based expansion was initiated from three primary ligands, resulting in a set of eighteen secondary ligands. Such an approach is commonly used in early-stage drug discovery to identify structurally related candidates that may exhibit comparable binding profiles or biological activity.

The code can be found in the following link:

[https://github.com/shrek-28/DockingStudies/tree/main/Code/ligand\\_selection](https://github.com/shrek-28/DockingStudies/tree/main/Code/ligand_selection)

**Table 2: Similar compounds to 1,8-Naphthyridine-3-carboxamide, as retrieved from ChEMBL Web Resource Client API**

ChEMBL ID	Similarity (%)	SMILES
<b>CHEMBL216226</b>	60.00	NC(=O)c1nc2ccccc2c1

**Table 3: Similar compounds to Carnosic acid, as retrieved from ChEMBL Web Resource Client API**

ChEMBL ID	Similarity (%)	SMILES
<b>CHEMBL4868012</b>	80.39	COc1c(C(C)C)cc2c(c1O)[C@]1(C(=O)O)CCCC(C)(C)[C@@H]1CC2

<b>CHEMBL1096627</b>	80.39	COc1c(C(C)C)cc2c(c1O)[C@@@]1(C(=O)O)CCCC(C)(C)[C@@H]1CC2
<b>CHEMBL4471445</b>	78.00	CNC(=O)[C@]12CCCC(C)(C)[C@@H]1CCc1cc(C(C)C)c(O)c(O)c12
<b>CHEMBL2333537</b>	78.00	COC(=O)[C@]12CCCC(C)(C)[C@@H]1CCc1cc(C(C)C)c(O)c(O)c12
<b>CHEMBL4519804</b>	76.47	CC(C)c1cc2c(c(O)c1O)[C@@@]1(C(=O)NN)CCCC(C)(C)[C@@H]1CC2
<b>CHEMBL4515503</b>	75.00	CC(=O)NC(=O)[C@]12CCCC(C)(C)[C@@H]1CCc1cc(C(C)C)c(O)c(O)c12
<b>CHEMBL4574206</b>	73.58	CC(C)c1cc2c(c(O)c1O)[C@@@]1(C(=O)NC(N)=O)CCCC(C)(C)[C@@H]1CC2
<b>CHEMBL4451825</b>	72.22	CC(C)c1cc2c(c(O)c1O)[C@@@]1(C(=O)NC3CCCCC3)CCCC(C)(C)[C@@H]1CC2
<b>CHEMBL4471914</b>	70.91	CC(C)c1cc2c(c(O)c1O)[C@@@]1(C(=O)NCCO)CCCC(C)(C)[C@@H]1CC2
<b>CHEMBL4447764</b>	68.97	CC(C)c1cc2c(c(O)c1O)[C@@@]1(C(=O)NCc3cccc3)CCCC(C)(C)[C@@H]1CC2
<b>CHEMBL4468065</b>	67.24	CC(C)c1cc2c(c(O)c1O)[C@@@]1(C(=O)NCCN(C)C)CCCC(C)(C)[C@@H]1CC2
<b>CHEMBL221380</b>	66.07	COc1cc2c(c(O)c1O)[C@@@]1(C(=O)O)CCCC(C)(C)[C@@H]1CC2
<b>CHEMBL2376099</b>	65.38	CC(C)c1cc2c(c(O)c1O)[C@@@]1(C(=O)O)CCCC(C)(C)[C@@H]1CC2
<b>CHEMBL4447390</b>	65.00	CC(C)c1cc2c(c(O)c1O)[C@@@]1(C(=O)NC(=O)c3ccc(Br)cc3)CCCC(C)(C)[C@@H]1CC2
<b>CHEMBL479111</b>	63.64	COc1cc2c(cc1C(C)C)CC[C@H]1C(C)(C)CCC[C@]21C(=O)O
<b>CHEMBL4576693</b>	63.46	CC(C)c1cc2c(c(O)c1O)[C@@@]1(CO)CCCC(C)(C)[C@@H]1CC2
<b>CHEMBL4544242</b>	60.94	CC(C)c1cc2c(c(O)c1O)[C@@@]1(C(=O)NC(=O)[C@H](C)NC(=O)OC(C)(C)C)CCCC(C)(C)[C@@H]1CC2
<b>CHEMBL4436108</b>	60.00	CC(C)c1cc2c(c(O)c1O)[C@@@]1(C(=O)NCc3ccnc3)CCCC(C)(C)[C@@H]1CC2
<b>CHEMBL2374044</b>	100.00	CC(C)c1cc2c(c(O)c1O)[C@]1(C(=O)O)CCCC(C)(C)C1CC2
<b>CHEMBL484853</b>	100.00	CC(C)c1cc2c(c(O)c1O)[C@@@]1(C(=O)O)CCCC(C)(C)[C@@H]1CC2
<b>CHEMBL5407683</b>	100.00	CC(C)c1cc2c(c(O)c1O)[C@@@]1(C(=O)O)CCCC(C)(C)C1CC2

**Table 4: Similar compounds to Carnosol, as retrieved from ChEMBL WebResource Client API**

ChEMBL ID	Similarity (%)	SMILES
CHEMBL483017	82.35	CC1(C)CCC[C@@]23C(=O)OC(C[C@@H]12)c1cc(C(CO)CO)c(O)c13
CHEMBL491307	82.35	CC(CO)c1cc2c(c(O)c1O)[C@@]13CCCC(C)(C)[C@@H]1C[C@H]2OC3=O
CHEMBL478933	73.58	COc1c(C(C)C)cc2c(c1OC)[C@@]13CCCC(C)(C)[C@@H]1C[C@H]2OC3=O
CHEMBL1079367	66.07	C[C@H]1COc2c1cc1c(c2O)[C@@]23CCCC(C)(C)[C@@H]2C[C@H]1OC3=O
CHEMBL2376097	64.81	CC(C)c1cc2c(c(O)c1O)[C@@]13CCCC(C)(C)[C@@H]1[C@H](O)C3=O)[C@@H]2O
CHEMBL2333536	64.81	CC(C)c1cc2c(c(O)c1O)[C@@]13CCCC(C)(C)[C@@H]1[C@H](O)[C@@H]2OC3=O
CHEMBL507166	64.81	CC(C)c1cc2c(c(O)c1O)[C@@]13CCCC(C)(C)[C@@H]1[C@H](O)C3=O)[C@H]2O
CHEMBL494659	64.81	CC(C)c1cc2c(c(O)c1O)[C@@]13CCCC(C)(C)[C@@H]1[C@H](O)[C@@H]2OC3=O
CHEMBL1081338	61.40	CO[C@@H]1c2cc(C(C)C)c(O)c(O)c2[C@@]23CCCC(C)(C)[C@@H]2[C@@H]1OC3=O
CHEMBL464376	61.40	CO[C@H]1c2cc(C(C)C)c(O)c(O)c2[C@@]23CCCC(C)(C)[C@@H]2[C@@H]1OC3=O
CHEMBL4544522	61.11	CC(C)c1cc2c(c(O)c1O)[C@@]13CCCC(C)(C)[C@@H]1CC2OC3
CHEMBL491879	61.11	CC(C)c1cc2c(c(O)c1O)[C@@]13CCCC(C)(C)[C@@H]1C[C@@H]2OC3
CHEMBL1514916	100.00	CC(C)c1cc2c(c(O)c1O)[C@@]13CCCC(C)(C)C1CC2OC3=O
CHEMBL519970	100.00	CC(C)c1cc2c(c(O)c1O)[C@@]13CCCC(C)(C)[C@@H]1CC2OC3=O
CHEMBL218693	100.00	CC(C)c1cc2c(c(O)c1O)[C@@]13CCCC(C)(C)[C@@H]1C[C@@H]2OC3=O

The ChEMBL Webresource Client was obtained from the following link:  
[https://github.com/chembl/chembl\\_webresource\\_client](https://github.com/chembl/chembl_webresource_client)

## ADMET Analysis of the Compounds

ADMET properties—Absorption, Distribution, Metabolism, Excretion, and Toxicity—are essential factors that determine the fate of a drug candidate in the body and its likelihood of success as a therapeutic agent. According to Cheng et al. (2012), ADMET evaluation is critical not only in drug discovery but also in the safety assessment of chemicals in various industries, as these properties influence both efficacy and potential adverse effects.

- Absorption refers to how well a compound enters systemic circulation from its administration site, impacting its bioavailability.
- Distribution describes how the compound spreads through body compartments and tissues, affecting which organs or systems are exposed to the drug.
- Metabolism involves the chemical transformation of the drug, often in the liver, which can activate, deactivate, or sometimes generate toxic metabolites.
- Excretion is the process by which the drug and its metabolites are eliminated from the body, typically via the kidneys (urine) or liver (bile/feces), determining how long the compound remains active.
- Toxicity assesses the potential of the compound or its metabolites to cause harmful effects at therapeutic or higher concentrations, which is a major reason for late-stage drug attrition.

The *admetSAR* database described by Cheng et al. provides curated experimental data and predictive models for a wide range of ADMET endpoints, supporting both qualitative and quantitative assessment of these properties for thousands of compounds. This comprehensive approach enables researchers to identify and optimize drug candidates with favorable ADMET profiles early in development, reducing the risk of failure in later clinical stages and improving the overall efficiency of drug discovery.

## ADMET Analysis of Primary Ligands

### 1,8-naphthyridine-3-carboxamide

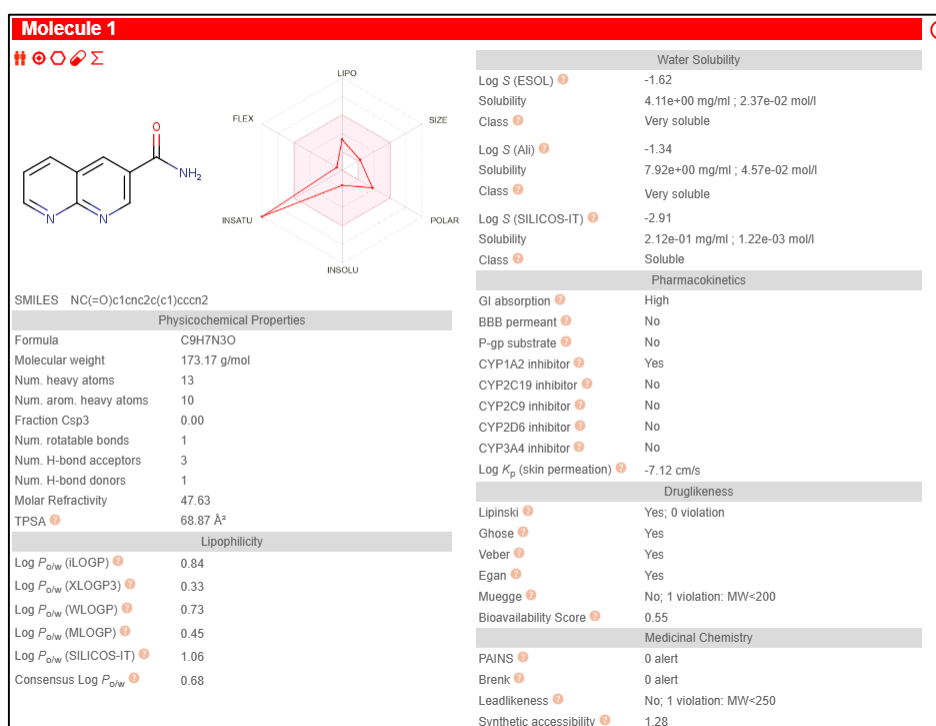


Figure 10: ADME Profile of 1,8-naphthyridine-3-carboxamide

The molecule ( $C_9H_7N_3O$ ) exhibits strong potential as a drug-like candidate based on its favorable ADME and medicinal chemistry profile. It has a low molecular weight (173.17 g/mol), good water solubility across multiple models, and a balanced lipophilicity (consensus log P of 0.68), supporting oral bioavailability. Key pharmacokinetic properties are encouraging, with high gastrointestinal absorption and no interaction with major efflux transporters like P-gp. It inhibits only CYP1A2 among the tested enzymes, indicating minimal risk for drug-drug interactions. The compound passes all major drug-likeness filters (Lipinski, Ghose, Veber, and Egan), with a single violation of the Muegge filter due to its low molecular weight. Importantly, it is free from PAINS and Brenk alerts, and its low synthetic accessibility score (1.28) suggests ease of synthesis. While it does not permeate the blood-brain barrier, making it unsuitable for CNS-targeted therapies, **it remains a strong oral lead candidate for peripheral targets, with room for further optimization.**

## Carnosic Acid

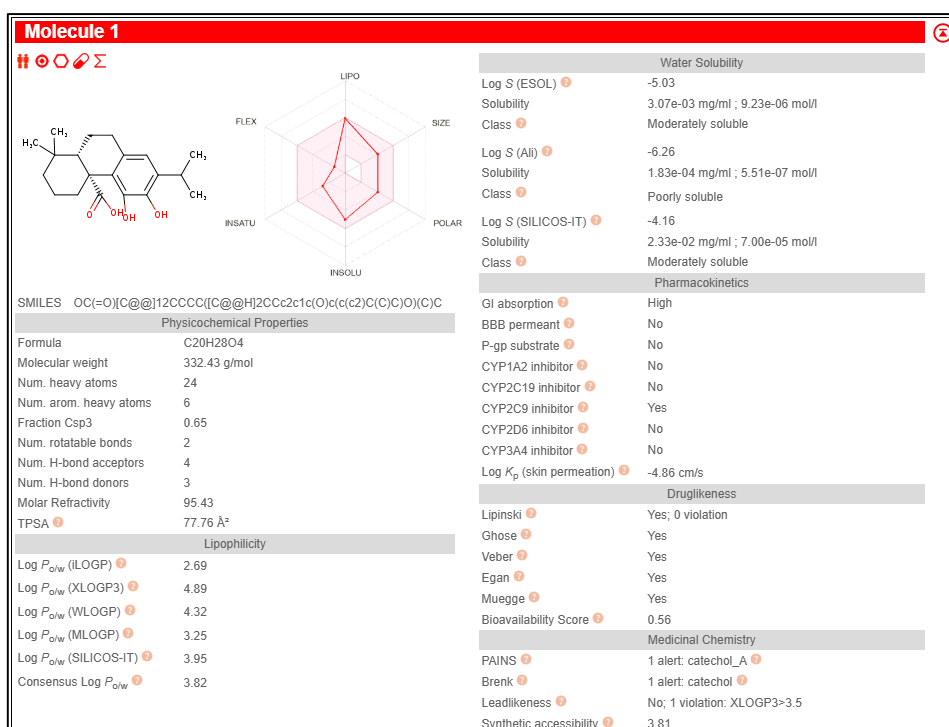


Figure 11: ADME Profile of Carnosic Acid

The molecule ( $C_{20}H_{28}O_4$ ) demonstrates generally favorable ADME properties, though it presents a few medicinal chemistry concerns. It has a moderate molecular weight (332.43 g/mol), low polarity (TPSA = 77.76 Å<sup>2</sup>), and a consensus log P of 3.82, indicating lipophilicity within acceptable bounds for oral bioavailability. Despite poor solubility according to the Ali model and moderate solubility by ESOL and SILICOSIT, its high gastrointestinal absorption is promising. It does not permeate the blood-brain barrier and is not a P-gp substrate, but it inhibits CYP2C9, which may lead to drug-drug interactions. The molecule passes all major drug-likeness rules (Lipinski, Ghose, Veber, Egan, Muegge), and has a good bioavailability score (0.56). However, it triggers PAINS and Brenk alerts due to the catechol moiety, and fails the lead-likeness filter due to its high XLOGP3 value. With a moderate synthetic accessibility score of 3.81, **the compound remains a viable lead for peripheral targets, though structural modifications may be necessary to reduce reactivity and CYP liabilities.**

## Carnosol

The molecule ( $C_{20}H_{26}O_4$ ) shows a favorable ADME profile with strong drug-likeness, although a few red flags exist in its medicinal chemistry. It has a molecular weight of 330.42 g/mol and a consensus log P of 3.72, indicating good membrane permeability and oral absorption potential. All water solubility models predict moderate solubility, and gastrointestinal absorption is high. It can permeate the blood-brain barrier and is a P-gp substrate, which may influence its CNS activity and efflux profile. It inhibits CYP2C9, which may pose interaction concerns. The molecule satisfies all major drug-likeness filters, including Lipinski, Ghose, Veber, Egan, and Muegge, and has a decent bioavailability score of 0.55. However, PAINS and Brenk filters both raise alerts due to the catechol structure, and lead-likeness is compromised by its high XLOGP3 value. Its synthetic accessibility score of 4.88 indicates moderate complexity. **Overall, the molecule appears to be a promising candidate, particularly for CNS indications, but may require chemical refinement to reduce liabilities related to reactivity and CYP inhibition.**

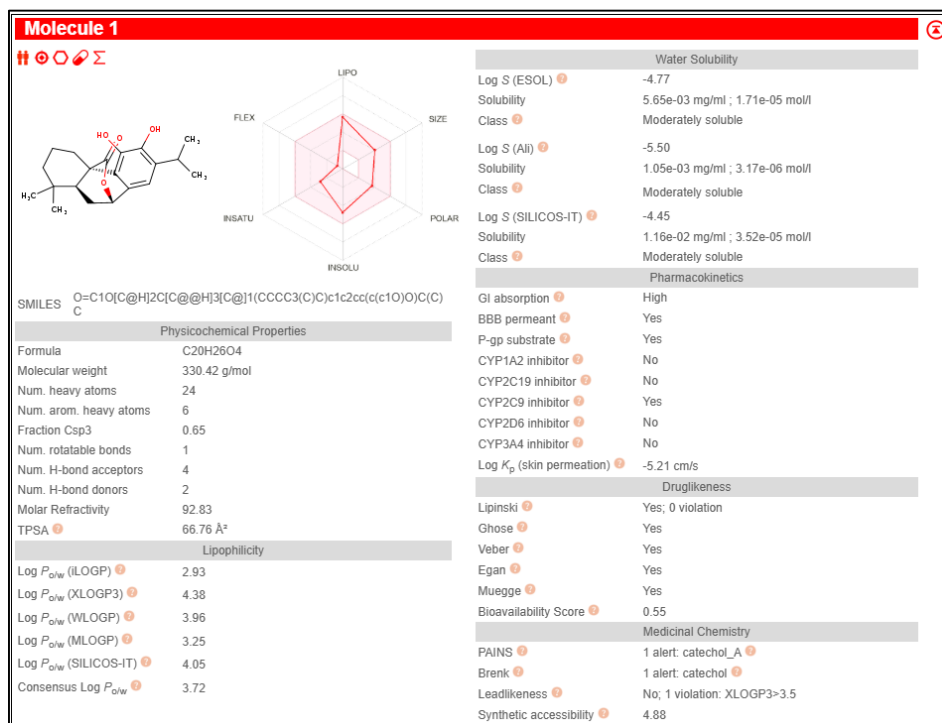


Figure 12: ADME Profile of Carnosol

Table 5: Drug-Likeness Comparison of Primary Ligands (SwissADME Metrics)

Property	1,8-naphthyridine-3-carboxamide	Carnosic Acid	Carnesol
<b>Molecular Weight</b>	173.17 g/mol	332.43 g/mol	330.42 g/mol
<b>Consensus log P</b>	0.68	3.82	3.72
<b>TPSA</b>	68.87 Å <sup>2</sup>	77.76 Å <sup>2</sup>	66.76 Å <sup>2</sup>
<b>Lipinski</b>	Pass	Pass	Pass
<b>Ghose</b>	Pass	Pass	Pass
<b>Veber</b>	Pass	Pass	Pass
<b>Egan</b>	Pass	Pass	Pass

Muegge	Fail (MW < 200)	Pass	Pass
Bioavailability Score	0.55	0.56	0.55
PAINS Alerts	0	1/ (catechol_A)	1 (catechol_A)
Brenk Alerts	0	1 (catechol)	1 (catechol)
Leadlikeness	Pass	Fail (XLOGP3 > 3.5)	Fail (XLOGP3 > 3.5)
Synthetic Accessibility	1.28 (easy)	3.81 (moderate)	4.88 (moderate-hard)
Overall Verdict	Very drug-like	Moderate drug-like	Moderate drug-like

## ADME Analysis of Secondary Ligands

### ADME Analysis of Secondary Ligands for 1,8-naphthyridine-3-carboxamide

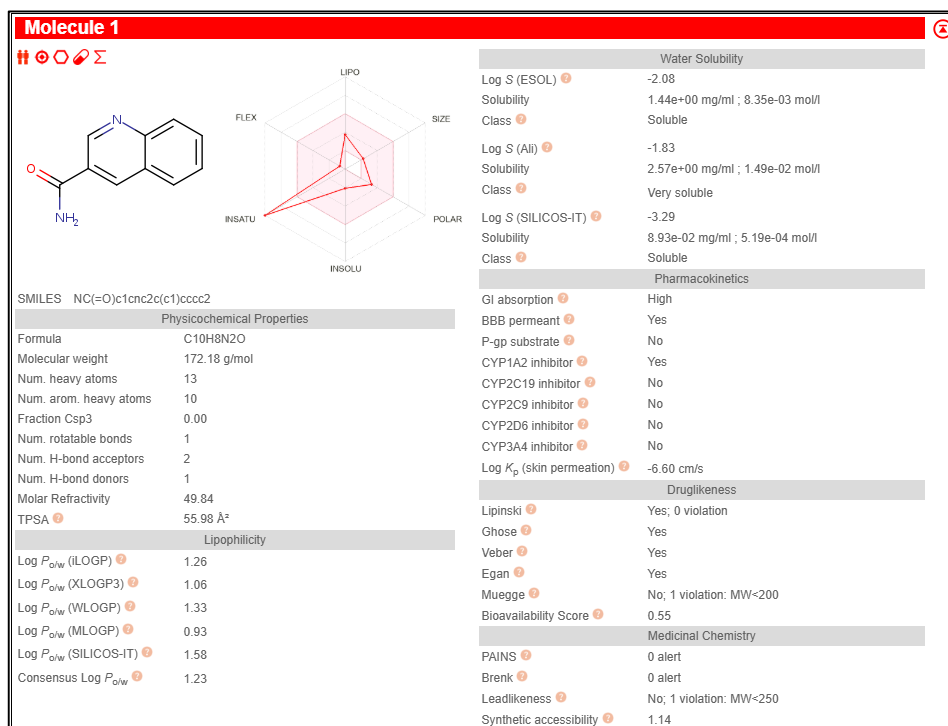


Figure 13: ADME Analysis of Quinoline-3-carboxamide

The molecule ( $C_{10}H_8N_2O$ ) exhibits an excellent ADMET profile, demonstrating strong drug-likeness with minimal medicinal chemistry concerns. With a low molecular weight of 172.18 g/mol and a consensus log P of 1.23, it is likely to possess good oral bioavailability and membrane permeability. Water solubility is favorable across all models, and high gastrointestinal absorption is predicted, supported by positive Caco-2 permeability and absence of P-glycoprotein substrate behavior. It shows potential for central nervous system activity due to its ability to cross the blood-brain barrier. Importantly, it does not inhibit any major cytochrome P450 enzymes, suggesting a low risk of metabolic drug-drug interactions. The molecule passes all key drug-likeness rules except for a single Ghose and Muegge violation, with a bioavailability score of 0.55. It raises no PAINS or Brenk alerts and has an excellent synthetic accessibility score of 1.14, implying it

is easy to synthesize. Overall, this compound is a well-balanced, low-risk lead candidate with strong pharmacokinetic and medicinal chemistry attributes, and is well-suited for further structure-based drug design, including docking and virtual screening studies.

### ADME Analysis of Secondary Ligands of Carnosic Acid

#### CHEMBL4868012:(4aS,10aS)-5-hydroxy-6-methoxy-1,1-dimethyl-7-propan-2-yl-2,3,4,9,10,10a-hexahydrophenanthrene-4a-carboxylic acid

The molecule ( $C_{21}H_{30}O_4$ ) demonstrates a strong pharmacokinetic and drug-likeness profile with a few manageable medicinal chemistry concerns. It has a moderate molecular weight of 346.46 g/mol and a relatively high consensus log P of 4.14, suggesting good lipophilicity and membrane permeability. Although its water solubility is limited (Log S ranging from  $-4.85$  to  $-6.37$  across models), it shows high gastrointestinal absorption and can cross the blood–brain barrier, making it a viable candidate for CNS-targeted applications. It is not a substrate for P-glycoprotein and avoids inhibition of most cytochrome P450 enzymes, except CYP3A4, which may warrant caution in combination therapies. The compound meets all major drug-likeness rules—Lipinski, Ghose, Veber, and Egan—but shows a single Muegge and lead-likeness violation due to its high XLOGP3 value. It raises no PAINS or Brenk alerts and has a favorable bioavailability score of 0.85, with a moderate synthetic accessibility score of 3.92. **Given its favorable ADME properties, strong CNS permeability, and lack of major red flags, this molecule is suitable for further molecular docking and structure-based screening.** However, follow-up optimization may be required to improve solubility and address the CYP3A4 inhibition risk if progression toward lead development is intended.

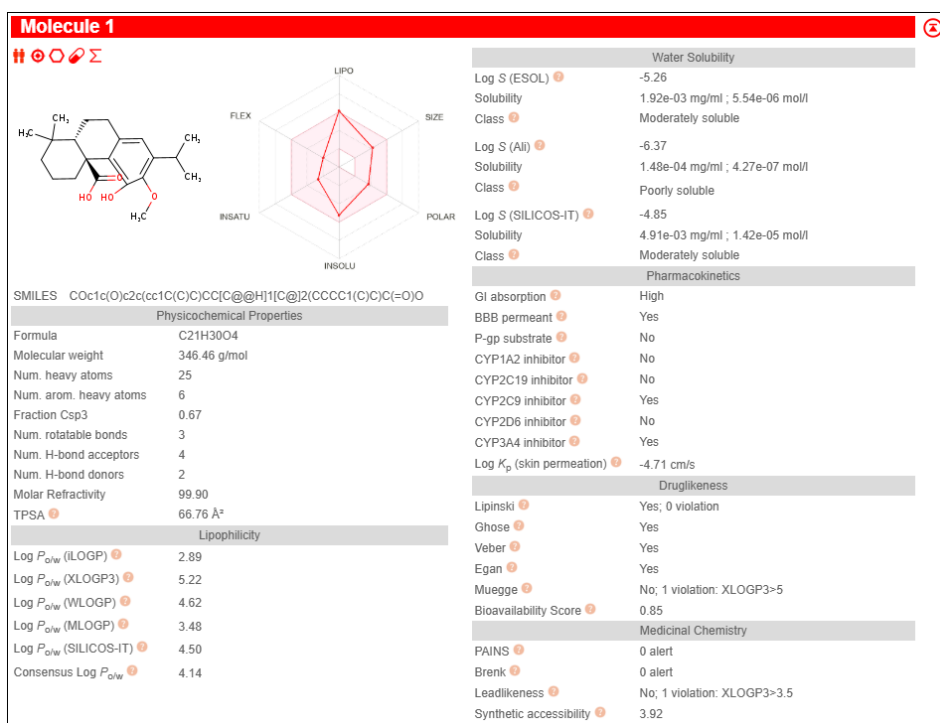


Figure 14: ADME Analysis of CHEMBL4868012

#### CHEMBL1096627: 12-O-Methylcarnosic acid

The molecule ( $C_{21}H_{30}O_4$ ) displays a favorable ADME and drug-likeness profile, indicating good potential as a drug candidate with minor medicinal chemistry flags. It has a moderate molecular weight of 346.46 g/mol and a consensus log P of 4.18, supporting good membrane permeability and passive diffusion. Despite low predicted solubility across all models (Log S ESOL:  $-5.26$  to  $-6.37$ ), it retains high gastrointestinal absorption

and can cross the blood-brain barrier, making it viable for CNS-targeted therapies. It is not a P-gp substrate and does not inhibit major CYP enzymes like CYP1A2, CYP2C19, CYP2C9, or CYP2D6, though it does inhibit CYP3A4, which may affect metabolic stability and raise drug–drug interaction concerns. The compound satisfies all key drug-likeness filters—Lipinski, Ghose, Veber, and Egan—but shows a single Muegge and lead-likeness violation due to its high XLOGP3 value. No PAINS or Brenk alerts are triggered, and the bioavailability score is strong at 0.85. With a synthetic accessibility score of 3.92, the molecule is of moderate complexity to synthesize. **Given its favorable permeability, lack of structural alerts, and robust pharmacokinetic features, this molecule is a strong candidate for further docking-based virtual screening and target interaction studies, although post-docking refinement to improve solubility and address CYP3A4 liability may be necessary.**

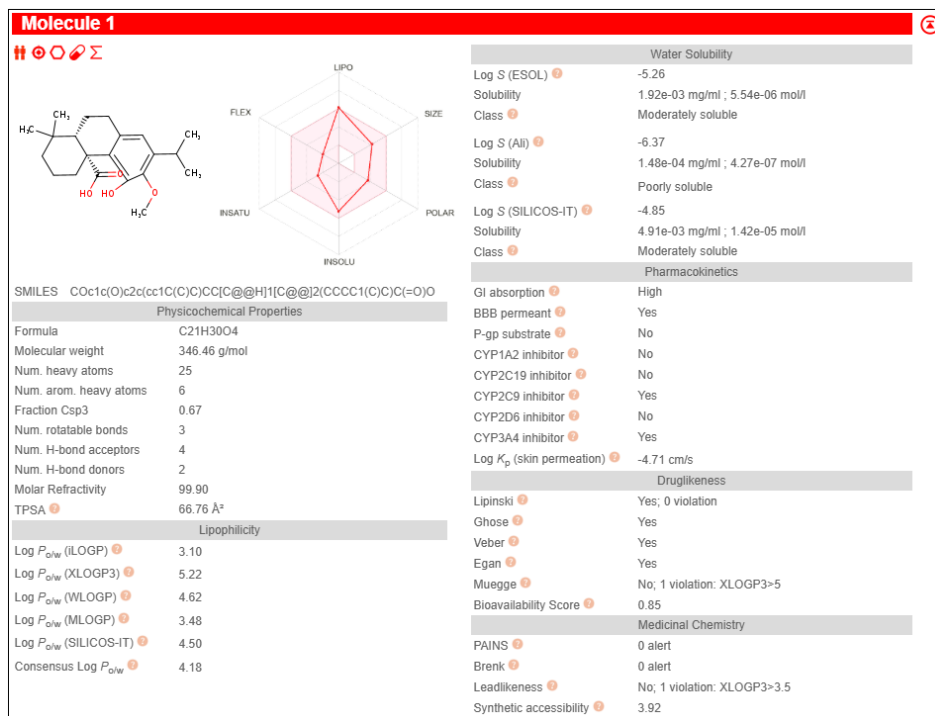


Figure 15: ADME Analysis of 12-O-Methylcarnosic acid

**CHEMBL4471445:** *(4aR,10aS)-5,6-dihydroxy-N,1,1-trimethyl-7-propan-2-yl-2,3,4,9,10,10a-hexahydrophenanthrene-4a-carboxamide*

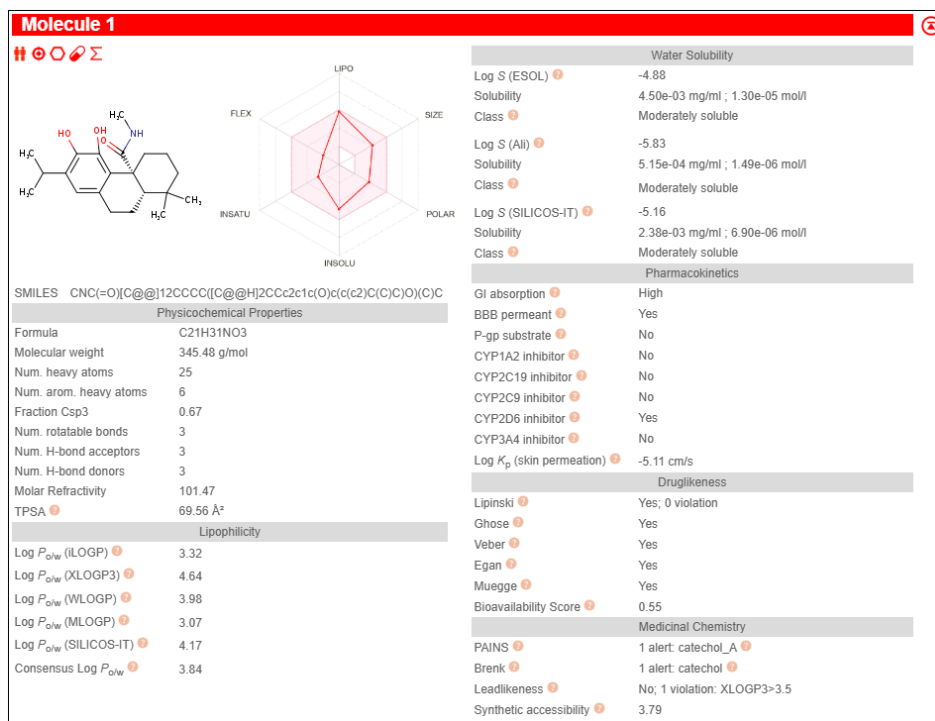


Figure 16: ADME Analysis of CHEMBL4471445

The molecule ( $C_{21}H_{31}NO_3$ ) presents a balanced ADMET and drug-likeness profile with some cautionary flags in medicinal chemistry. It has a molecular weight of 345.48 g/mol and a consensus Log P of 3.84, suggesting favorable lipophilicity and good membrane permeability. Solubility is moderate across all prediction models (Log S from  $-4.88$  to  $-5.83$ ), and it shows high gastrointestinal absorption along with blood–brain barrier permeability, making it suitable for potential CNS activity. It is not a P-glycoprotein substrate and does not inhibit key CYP enzymes except CYP2D6, which could raise concerns for drug–drug interactions in polypharmacy contexts. The molecule satisfies all major drug-likeness rules—Lipinski, Ghose, Veber, Egan, and Muegge—with a decent bioavailability score of 0.55. However, it triggers one PAINS alert (catechol\_A) and one Brenk alert (catechol), which suggest the possibility of non-specific reactivity or redox liability. Its synthetic accessibility score of 3.79 indicates moderate ease of synthesis. **Despite minor medicinal chemistry liabilities, this molecule is well-suited for docking-based studies and virtual screening workflows due to its strong pharmacokinetic profile and absence of major ADMET red flags, though structural refinement to reduce catechol-related alerts may be advisable for downstream development.**

#### CHEMBL2333537: Methyl Carnosate

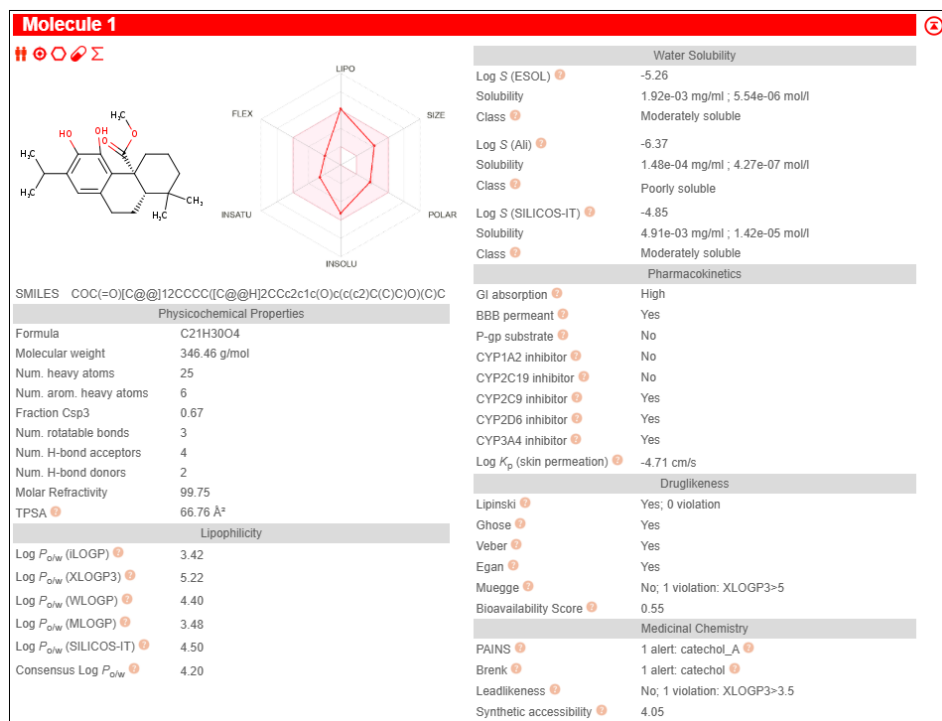


Figure 17: ADME Analysis of Methyl Carnosate

The molecule ( $C_{21}H_{30}O_4$ ) shows a largely favorable ADME and drug-likeness profile, though it presents a few medicinal chemistry flags that may need attention. With a molecular weight of 346.46 g/mol and a consensus Log P of 4.20, it is expected to have good membrane permeability and passive diffusion. Its water solubility is moderate across all models (Log S ESOL:  $-5.26$  to  $-6.37$ ), and it demonstrates high gastrointestinal absorption along with the ability to cross the blood–brain barrier, making it a viable candidate for CNS-targeted applications. It is not a P-glycoprotein substrate and does not inhibit key CYP enzymes like CYP1A2, CYP2C19, or CYP2C9, although it does inhibit CYP2D6 and CYP3A4, which may affect metabolic stability and drug–drug interaction potential. The molecule passes Lipinski, Ghose, Veber, and Egan filters, with a single Muegge and lead-likeness violation due to a high XLOGP3 value. A bioavailability score of 0.55 and a moderate synthetic accessibility score of 4.05 support its practical feasibility. However, the compound triggers both PAINS and Brenk alerts due to the presence of a catechol moiety, which may contribute to non-specific reactivity or oxidative instability. **Despite these structural alerts, the molecule's strong pharmacokinetic properties and lack of major ADMET liabilities make it suitable for further molecular docking studies and virtual screening, though analog development or masking strategies may be needed in downstream lead optimization.**

**CHEMBL4519804: (4aR,10aS)-5,6-dihydroxy-1,1-dimethyl-7-propan-2-yl-2,3,4,9,10,10a-hexahydrophenanthrene-4a-carbohydrazide**

The molecule ( $C_{20}H_{30}N_2O_3$ ) shows a favorable ADME and drug-likeness profile, though it raises some medicinal chemistry concerns. With a molecular weight of 346.46 g/mol and a consensus Log P of 2.99, it is expected to have balanced hydrophilicity and lipophilicity, supporting adequate membrane permeability. The compound demonstrates high gastrointestinal absorption but does not cross the blood–brain barrier, limiting its potential for central nervous system applications. It is not a P-glycoprotein substrate and does not inhibit major cytochrome P450 enzymes (CYP1A2, CYP2C19, CYP2C9, CYP2D6, or CYP3A4), minimizing risks of metabolic interactions. The molecule is moderately soluble in water across all predictive models (Log S:  $-4.41$  to  $-5.61$ ), and shows a relatively low skin permeability (Log K<sub>p</sub>:  $-5.64$  cm/s). It complies with all major drug-likeness filters (Lipinski, Ghose, Veber, Egan, Muegge), and has a bioavailability score of 0.55,

indicating decent oral availability. However, the presence of a catechol group triggers one PAINS alert and three Brenk alerts (catechol, hydrazine, acyl\_hydrazine), which may be associated with assay interference or reactivity issues. The compound also violates lead-likeness criteria due to a high XLOGP3 value (>3.5). Despite these red flags, its overall ADMET profile and synthetic accessibility score of 3.92 suggest that the molecule remains a viable candidate for further structure-based drug design and **can be taken forward for molecular docking to evaluate its target-specific binding potential**, although structural optimization may be needed during lead development.

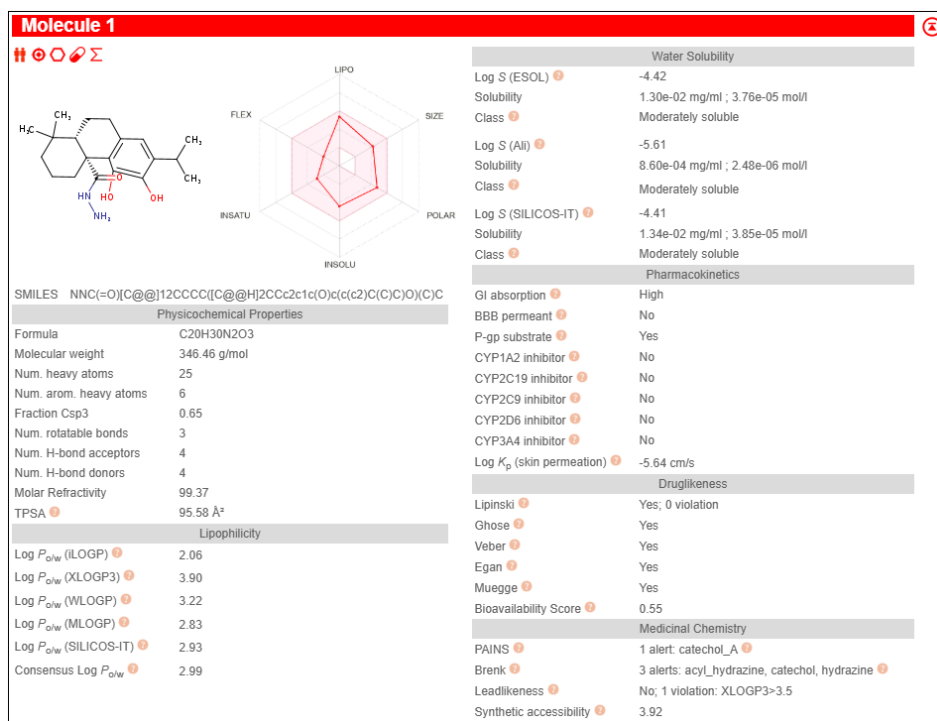


Figure 18: ADME Analysis of CHEMBL4519804

### CHEMBL4515503: (4aR,10aS)-N-acetyl-5,6-dihydroxy-1,1-dimethyl-7-propan-2-yl-2,3,4,9,10,10a-hexahydrophenanthrene-4a-carboxamide

The molecule ( $C_{22}H_{31}N_1O_4$ ) exhibits a generally favorable ADME and drug-likeness profile, with some cautionary medicinal chemistry alerts. With a molecular weight of 373.49 g/mol and a consensus Log P of 3.76, it shows suitable lipophilicity for membrane permeability and passive diffusion. The compound demonstrates high gastrointestinal absorption but is not blood–brain barrier permeant, and it is also a substrate of P-glycoprotein, which could affect its bioavailability through efflux. It does not inhibit major CYP enzymes like CYP1A2, CYP2C19, CYP2C9, or CYP2D6, but it does inhibit CYP3A4, which may raise concerns for drug–drug interactions. Its water solubility is moderate across all models (Log S: -4.85 to -5.97), and it exhibits low skin permeability (Log K<sub>p</sub>: -5.43 cm/s). The molecule passes all major drug-likeness filters (Lipinski, Ghose, Veber, Egan, Muegge) and has a bioavailability score of 0.55, suggesting reasonable oral bioavailability. However, it triggers one PAINS alert (catechol\_A) and one Brenk alert (catechol), which may be associated with assay interference and oxidative liability. Lead-likeness violations include a slightly elevated molecular weight (>350 g/mol) and XLOGP3 > 3.5. Despite these minor flags, its synthetic accessibility score of 3.87 and strong pharmacokinetic properties support its viability, and **the compound**

can be taken forward for molecular docking studies to assess its binding efficacy, keeping in mind the need for potential optimization during lead refinement.

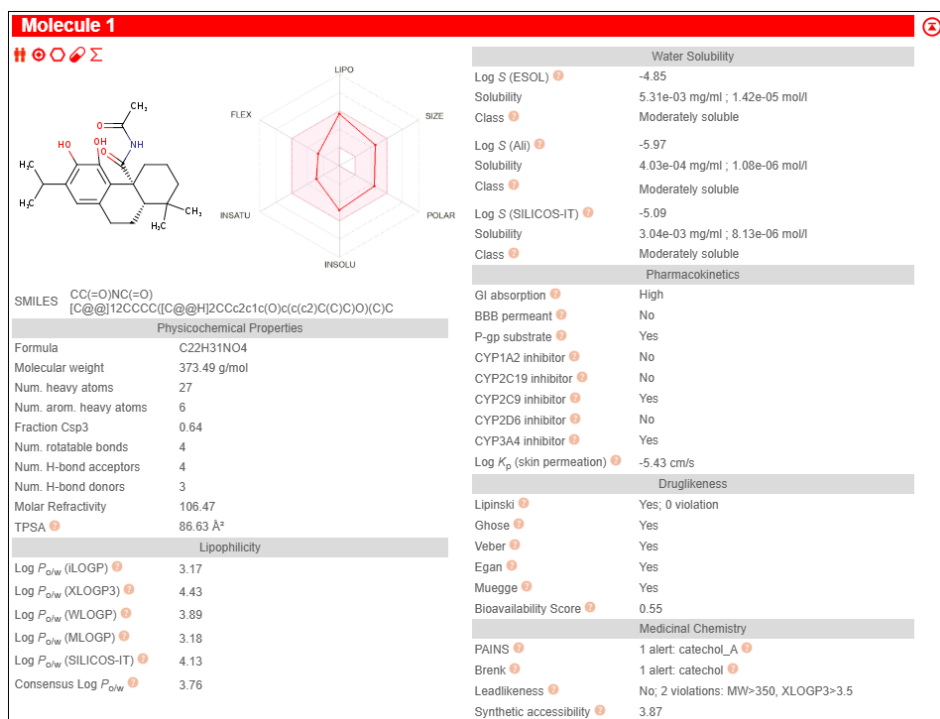


Figure 18: ADME Analysis of CHEMBL4515503

**CHEMBL4574206:** *(4aR,10aS)-N-acetyl-5,6-dihydroxy-1,1-dimethyl-7-propan-2-yl-2,3,4,9,10,10a-hexahydrophenanthrene-4a-carboxamide*

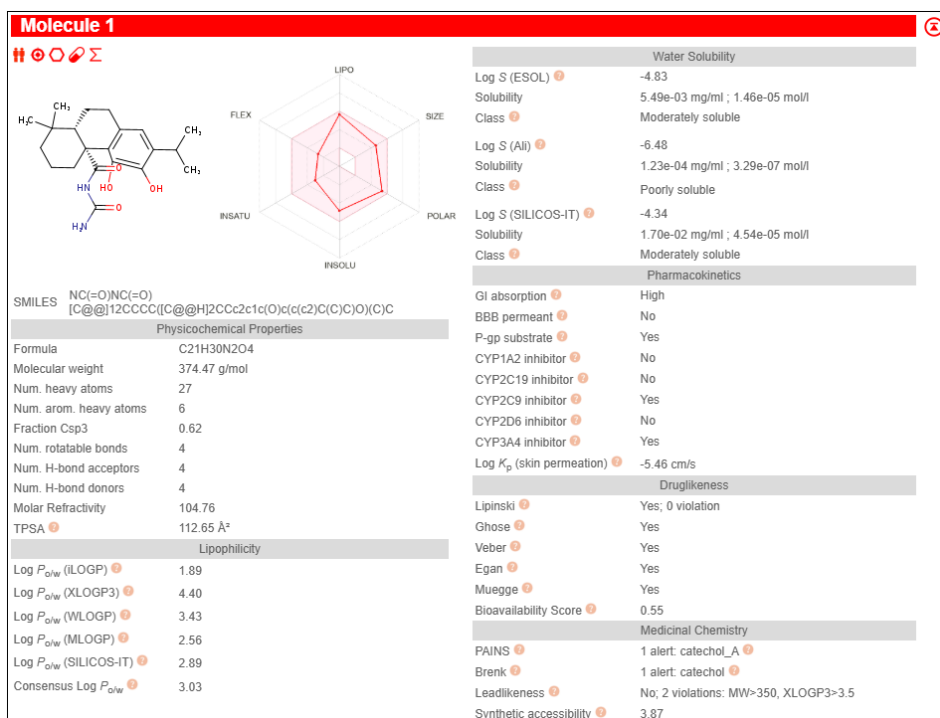


Figure 19: ADME Analysis of CHEMBL4574206

The molecule (C<sub>21</sub>H<sub>30</sub>N<sub>2</sub>O<sub>4</sub>) exhibits a generally favorable ADME and drug-likeness profile, with some cautionary medicinal chemistry alerts. With a molecular weight of 374.47 g/mol and a consensus Log P of 3.03, it shows suitable lipophilicity for membrane permeability and passive diffusion. The compound

demonstrates high gastrointestinal absorption but is not blood-brain barrier permeant, and it is a substrate of P-glycoprotein, which could affect its bioavailability through efflux. It does not inhibit major CYP enzymes like CYP1A2, CYP2C19, CYP2D6, or CYP3A4, but it does inhibit CYP2C9, which may raise concerns for drug-drug interactions. Its water solubility is moderate across all models (Log S: -4.83 to -6.48), and it exhibits low skin permeability (Log K<sub>p</sub>: -5.46 cm/s). The molecule passes all major drug-likeness filters (Lipinski, Ghose, Veber, Egan, Muegge) and has a bioavailability score of 0.55, suggesting reasonable oral bioavailability. However, it triggers one PAINS alert (catechol\_A) and one Brenk alert (catechol), which may be associated with assay interference and oxidative liability. Lead-likeness violations include a slightly elevated molecular weight (>350 g/mol) and XLOGP3 > 3.5. Despite these minor flags, its synthetic accessibility score of 3.87 and strong pharmacokinetic properties support its viability, and **the compound can be taken forward for molecular docking studies to assess its binding efficacy**, keeping in mind the need for potential optimization during lead refinement.

**CHEMBL4451825: (4aR,10aS)-N-cycloheptyl-5,6-dihydroxy-1,1-dimethyl-7-propan-2-yl-2,3,4,9,10,10a-hexahydrophenanthrene-4a-carboxamide**

The molecule (C<sub>27</sub>H<sub>41</sub>N<sub>1</sub>O<sub>3</sub>) exhibits a generally unfavorable ADME and drug-likeness profile, with several cautionary medicinal chemistry alerts. With a molecular weight of 427.62 g/mol and a consensus Log P of 5.34, it shows high lipophilicity, which may be problematic for solubility. The compound demonstrates high gastrointestinal absorption and is not a substrate of P-glycoprotein, but it is not blood-brain barrier permeant. It does not inhibit major CYP enzymes like CYP1A2, CYP2C19, CYP2C9, or CYP2D6, but it does inhibit CYP3A4, which may raise concerns for drug-drug interactions. Its water solubility is poor across all models (Log S: -6.78 to -8.28), and it exhibits low skin permeability (Log K<sub>p</sub>: -3.94 cm/s). The molecule fails several major drug-likeness filters, violating Lipinski's rule (MLOGP > 4.15), Ghose's filter (WLOGP > 5.6 and atoms > 70), Veber's filter (WLOGP > 5.88), and Muegge's filter (XLOGP3 > 5). It has a bioavailability score of 0.55, suggesting reasonable oral bioavailability despite the violations. However, it triggers one PAINS alert (catechol\_A) and one Brenk alert (catechol), which may be associated with assay interference and oxidative liability. Lead-likeness violations include a high molecular weight (>350 g/mol) and XLOGP3 > 3.5. **Despite these flags, its synthetic accessibility score of 4.41 and high gastrointestinal absorption support its viability, but the compound needs significant optimization and lead refinement to address the drug-likeness and solubility issues before moving forward with molecular docking studies.**

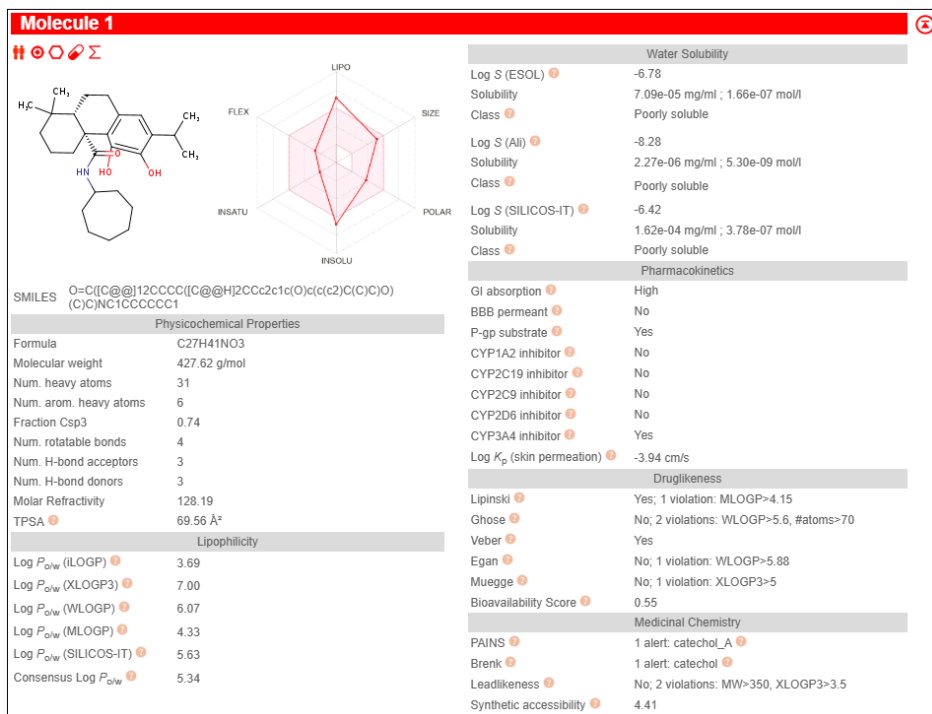


Figure 20: ADME Analysis of CHEMBL4451825

**CHEMBL4471914:** *(4aR,10aS)-5,6-dihydroxy-N-(2-hydroxyethyl)-1,1-dimethyl-7-propan-2-yl-2,3,4,9,10,10a-hexahydrophenanthrene-4a-carboxamide*

The molecule (C<sub>22</sub>H<sub>33</sub>N<sub>1</sub>O<sub>4</sub>) exhibits a generally favorable ADME and drug-likeness profile, with some cautionary medicinal chemistry alerts. With a molecular weight of 375.50 g/mol and a consensus Log P of 3.39, it shows suitable lipophilicity for membrane permeability and passive diffusion. The compound demonstrates high gastrointestinal absorption but is not blood-brain barrier permeant, and it is also a substrate of P-glycoprotein, which could affect its bioavailability through efflux. It does not inhibit major CYP enzymes like CYP1A2, CYP2C19, or CYP2C9, but it does inhibit CYP2D6 and CYP3A4, which may raise concerns for drug-drug interactions. Its water solubility is moderate across all models (Log S: -4.50 to -5.55), and it exhibits low skin permeability (Log K<sub>p</sub>: -5.78 cm/s). The molecule passes all major drug-likeness filters (Lipinski, Ghose, Veber, Egan, Muegge) and has a bioavailability score of 0.55, suggesting reasonable oral bioavailability. However, it triggers one PAINS alert (catechol\_A) and one Brenk alert (catechol), which may be associated with assay interference and oxidative liability. Lead-likeness violations include a slightly elevated molecular weight (>350 g/mol) and XLOGP3 > 3.5. Despite these minor flags, **its synthetic accessibility score of 3.97 and strong pharmacokinetic properties support its viability, and the compound can be taken forward for molecular docking studies to assess its binding efficacy, keeping in mind the need for potential optimization during lead refinement.**

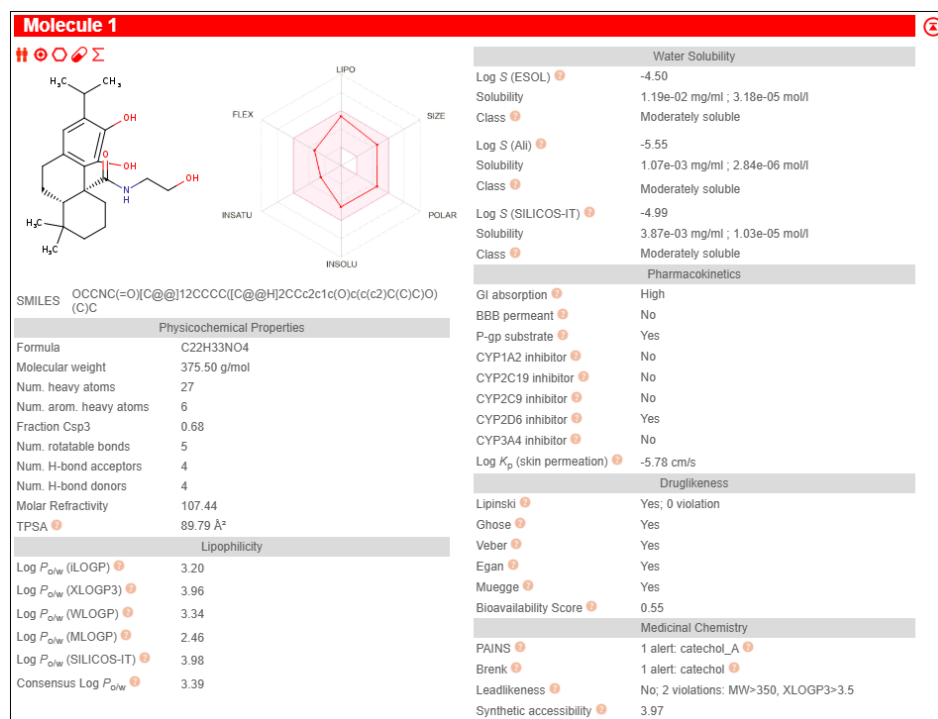


Figure 21: ADME Analysis of CHEMBL4471914

**CHEMBL447764: (4aR,10aS)-N-benzyl-5,6-dihydroxy-1,1-dimethyl-7-propan-2-yl-2,3,4,9,10,10a-hexahydrophenanthrene-4a-carboxamide**

The molecule ( $C_{27}H_{35}N_1O_3$ ) exhibits a generally unfavorable ADME and drug-likeness profile, with some cautionary medicinal chemistry alerts. With a molecular weight of 421.57 g/mol and a consensus Log P of 4.98, it shows high lipophilicity, which may be problematic for solubility. The compound demonstrates high gastrointestinal absorption and is not a P-glycoprotein substrate, but it is not blood-brain barrier permeant. It does not inhibit major CYP enzymes like CYP1A2, CYP2C19, CYP2C9, or CYP2D6, but it does inhibit CYP3A4, which may raise concerns for drug-drug interactions. Its water solubility is poor across all models (Log S: -6.28 to -7.63), and it exhibits low skin permeability (Log K<sub>p</sub>: -4.51 cm/s). The molecule passes most major drug-likeness filters, violating only Muegge's filter (XLOGP3 > 5). It has a bioavailability score of 0.55, suggesting reasonable oral bioavailability despite the violations. However, it triggers one PAINS alert (catechol\_A) and one Brenk alert (catechol), which may be associated with assay interference and oxidative liability. Lead-likeness violations include a high molecular weight (>350 g/mol) and XLOGP3 > 3.5. Despite these flags, its synthetic accessibility score of 4.11 and high gastrointestinal absorption support its viability, **but the compound needs significant optimization and lead refinement to address the drug-likeness and solubility issues before moving forward with molecular docking studies.**

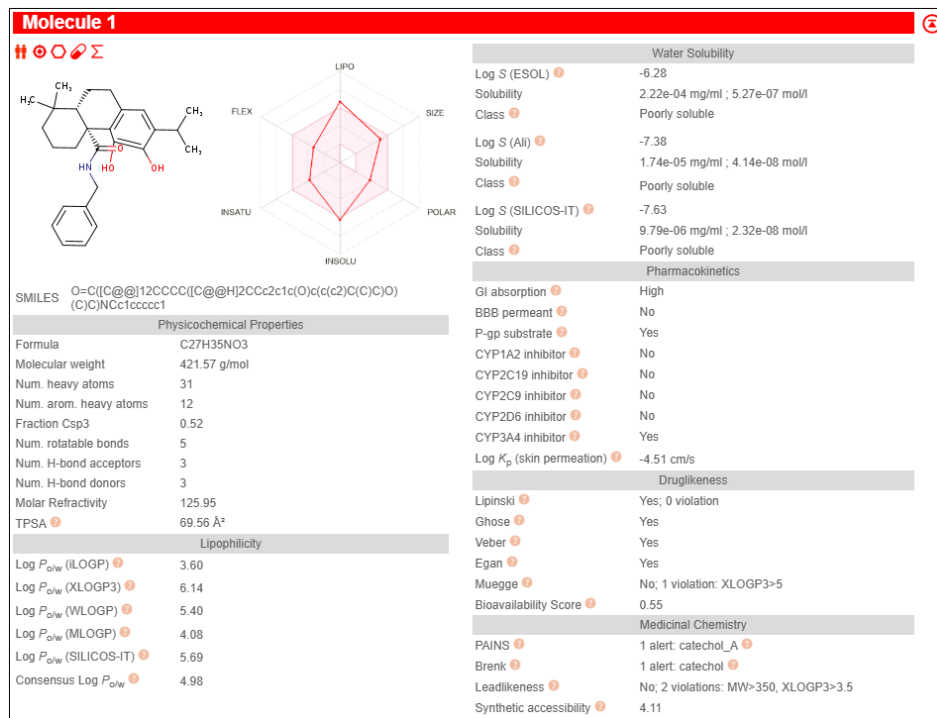


Figure 22: ADME Analysis of CHEMBL4447764

**CHEMBL4468065:** *(4aR,10aS)-N-[2-(dimethylamino)ethyl]-5,6-dihydroxy-1,1-dimethyl-7-propan-2-yl-2,3,4,9,10,10a-hexahydrophenanthrene-4a-carboxamide*

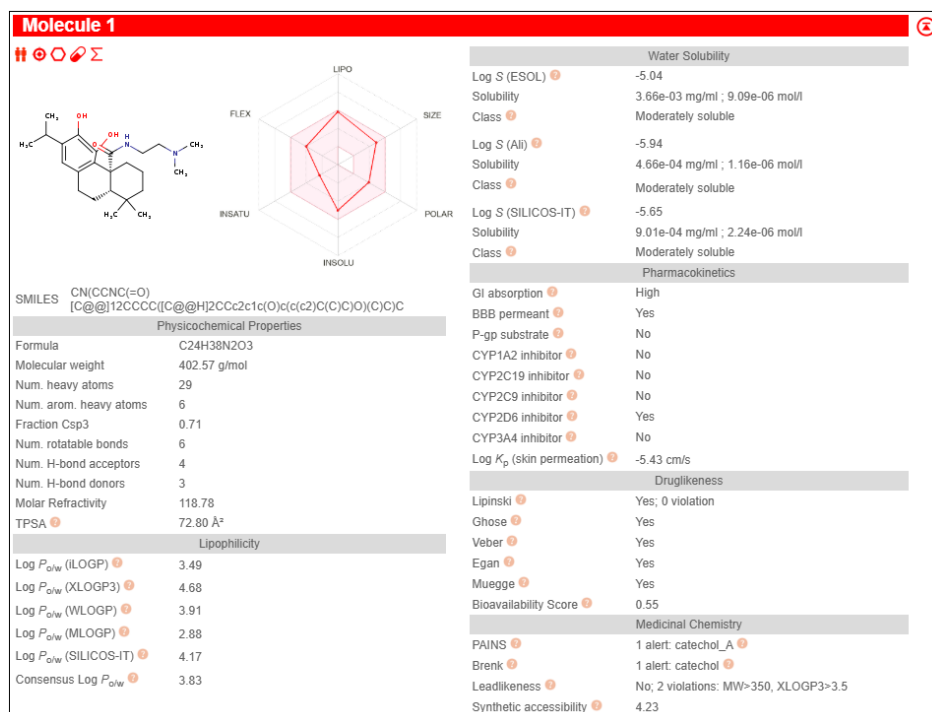


Figure 23: ADME Analysis of CHEMBL4468085

The molecule ( $C_{24}H_{38}N_2O_3$ ) exhibits a generally favorable ADME and drug-likeness profile, with some cautionary medicinal chemistry alerts. With a molecular weight of 402.57 g/mol and a consensus Log P of 3.83, it shows suitable lipophilicity for membrane permeability and passive diffusion. The compound demonstrates high gastrointestinal absorption and is blood-brain barrier permeant, and it is not a P-glycoprotein substrate. It does not inhibit major CYP enzymes like CYP1A2, CYP2C19, CYP2C9, or CYP2D6, but it does inhibit CYP3A4, which may raise concerns for drug-drug interactions. Its water solubility is

moderate across all models (Log S: -5.04 to -5.94), and it exhibits low skin permeability (Log K<sub>p</sub>: -5.43 cm/s). The molecule passes all major drug-likeness filters (Lipinski, Ghose, Veber, Egan, Muegge) and has a bioavailability score of 0.55, suggesting reasonable oral bioavailability. However, it triggers one PAINS alert (catechol\_A) and one Brenk alert (catechol), which may be associated with assay interference and oxidative liability. Lead-likeness violations include a high molecular weight (>350 g/mol) and XLOGP3 > 3.5. Despite these flags, its synthetic accessibility score of 4.23 and strong pharmacokinetic properties support its viability, and **the compound can be taken forward for molecular docking studies to assess its binding efficacy**, keeping in mind the need for potential optimization during lead refinement.

### CHEMBL221380: Methyl 12-O-methylcarnosoate

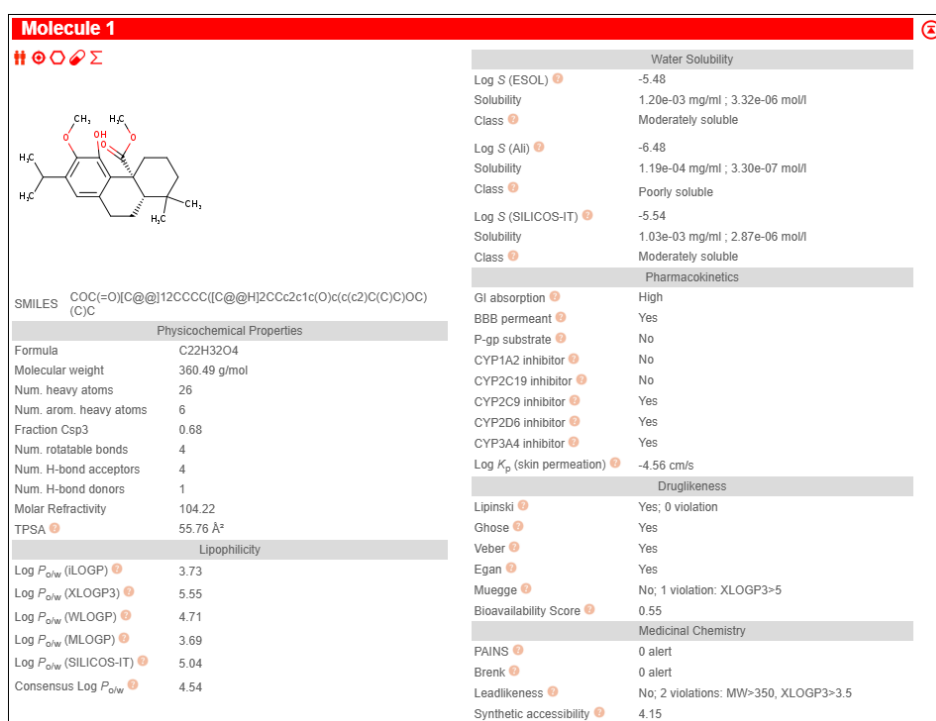


Figure 24: ADME Analysis of methyl 12-O-methylcarnosoate

The molecule ( $C_{22}H_{32}O_4$ ) exhibits a generally favorable ADME and drug-likeness profile, with some cautionary medicinal chemistry alerts. With a molecular weight of 360.49 g/mol and a consensus Log P of 4.54, it shows suitable lipophilicity for membrane permeability and passive diffusion. The compound demonstrates high gastrointestinal absorption and is blood-brain barrier permeant, and it is not a P-glycoprotein substrate. It does not inhibit major CYP enzymes like CYP1A2 or CYP2C19, but it does inhibit CYP2C9, CYP2D6, and CYP3A4, which may raise significant concerns for drug-drug interactions. Its water solubility is moderately soluble across most models (Log S: -5.48 to -6.48), and it exhibits low skin permeability (Log K<sub>p</sub>: -4.56 cm/s). The molecule passes most major drug-likeness filters, violating only Muegge's filter (XLOGP3 > 5). It has a bioavailability score of 0.55, suggesting reasonable oral bioavailability despite the violations. It does not trigger any PAINS or Brenk alerts, indicating a low risk of assay interference and oxidative liability. Lead-likeness violations include a high molecular weight (>350 g/mol) and XLOGP3 > 3.5. Despite these flags, its synthetic accessibility score of 4.15 and strong pharmacokinetic properties support its viability, but the **compound needs significant optimization and lead refinement to address the CYP inhibition issues before moving forward with molecular docking studies.**

### CHEMBL2376099: Carnosaldehyde

The molecule ( $C_{20}H_{28}O_3$ ) exhibits a generally favorable ADME and drug-likeness profile, with some cautionary medicinal chemistry alerts. With a molecular weight of 316.43 g/mol and a consensus Log P of 4.02, it shows suitable lipophilicity for membrane permeability and passive diffusion. The compound demonstrates high gastrointestinal absorption and is blood-brain barrier permeant, and it is not a P-glycoprotein substrate. It does not inhibit major CYP enzymes like CYP1A2, CYP2C19, CYP2D6, or CYP3A4, but it does inhibit CYP2C9, which may raise concerns for drug-drug interactions. Its water solubility is moderate across all models (Log S: -4.74 to -5.77), and it exhibits low skin permeability (Log K<sub>p</sub>: -4.80 cm/s). The molecule passes all major drug-likeness filters (Lipinski, Ghose, Veber, Egan, Muegge) and has a bioavailability score of 0.55, suggesting reasonable oral bioavailability. However, it triggers one PAINS alert (catechol\_A) and two Brenk alerts (aldehyde, catechol), which may be associated with assay interference and oxidative liability. The molecule violates a lead-likeness rule with XLOGP3 > 3.5. Despite these flags, its synthetic accessibility score of 3.66 and strong pharmacokinetic properties support its viability, and **the compound can be taken forward for molecular docking studies to assess its binding efficacy**, keeping in mind the need for potential optimization during lead refinement.

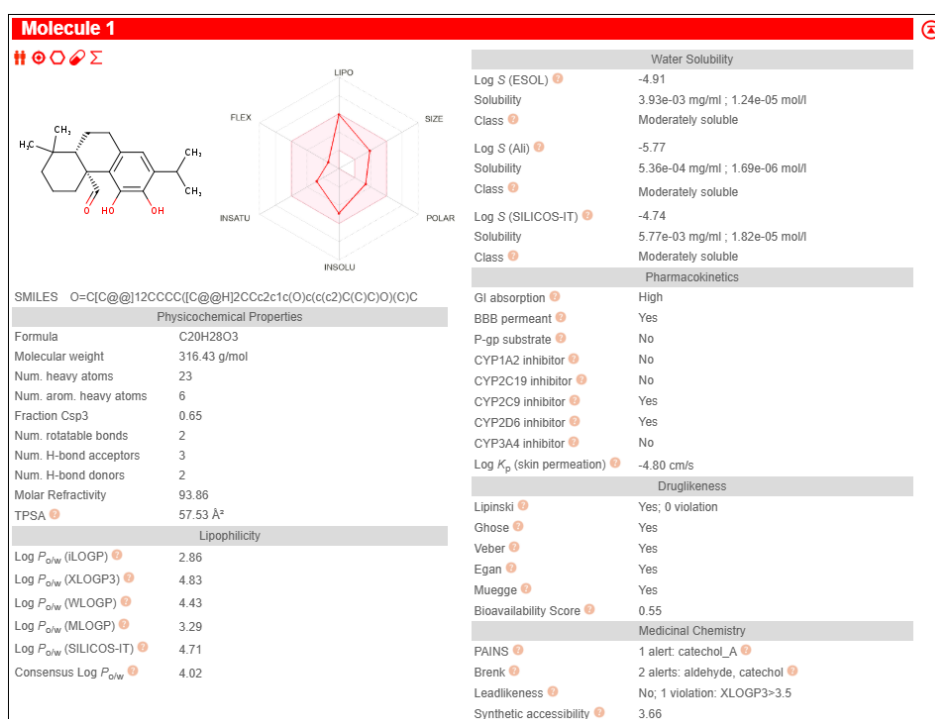


Figure 25: ADME Analysis of Carnosaldehyde

**CHEMBL4447390:** *(4aR,10aS)-N-(4-bromobenzoyl)-5,6-dihydroxy-1,1-dimethyl-7-propan-2-yl-2,3,4,9,10,10a-hexahydrophenanthrene-4a-carboxamide*

The molecule ( $C_{27}H_{32}BrN_1O_4$ ) exhibits a generally unfavorable ADME and drug-likeness profile, with several cautionary medicinal chemistry alerts. With a molecular weight of 514.45 g/mol and a consensus Log P of 5.40, it shows high lipophilicity, which may be problematic for solubility. The compound demonstrates high gastrointestinal absorption and is a P-glycoprotein substrate, but it is not blood-brain barrier permeant. It does not inhibit major CYP enzymes like CYP1A2, CYP2C19, or CYP2D6, but it does inhibit CYP2C9 and CYP3A4, which may raise concerns for drug-drug interactions. Its water solubility is poor across all models (Log S: -7.24 to -8.41), and it exhibits low skin permeability (Log K<sub>p</sub>: -4.62 cm/s). The molecule fails several major drug-likeness filters, violating Lipinski's rule (MW > 500, MLOGP > 4.15), Ghose's filter (MW > 480, WLOGP > 5.6, MR > 130), Veber's filter (WLOGP > 5.88), and Muegge's filter (XLOGP3 > 5). It has a very low bioavailability score of 0.17, suggesting poor oral bioavailability. However, it triggers one PAINS alert

(catechol\_A) and two Brenk alerts (catechol, phthalimide), which may be associated with assay interference and oxidative liability. Lead-likeness violations include a high molecular weight (>350 g/mol) and XLOGP3 > 3.5. Despite these flags, its synthetic accessibility score of 4.13 suggests that it may be synthesizable, but the compound **needs significant optimization and lead refinement to address the multiple drug-likeness, solubility, and CYP inhibition issues before being considered for further studies.**

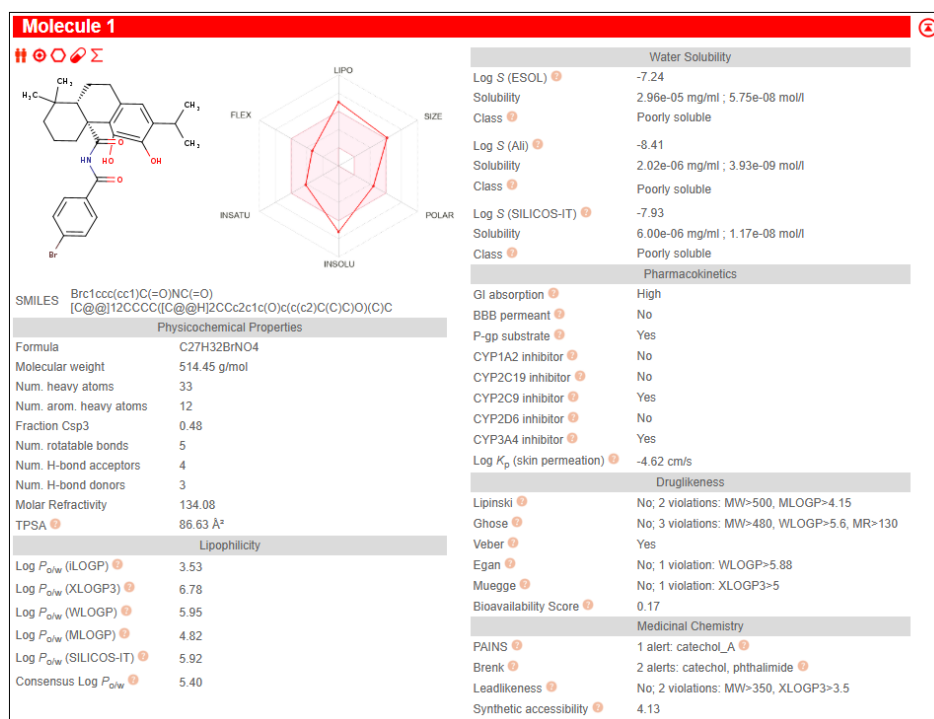


Figure 26: ADME Analysis of CHEMBL4447390

### CHEMBL479111: O-methylpisiferic acid

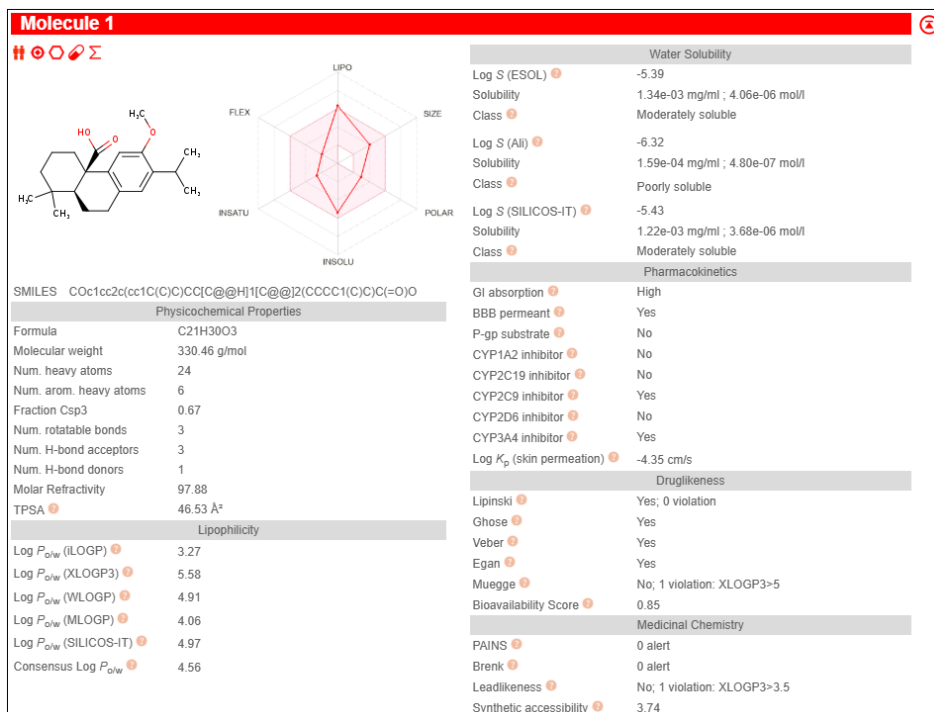


Figure 27: ADME Analysis of O-methylpisiferic acid

The molecule ( $C_{21}H_{30}O_3$ ) exhibits a generally favorable ADME and drug-likeness profile, with some minor cautionary medicinal chemistry alerts. With a molecular weight of 330.46 g/mol and a consensus Log P of 4.56, it shows suitable lipophilicity for membrane permeability and passive diffusion. The compound demonstrates high gastrointestinal absorption and is blood-brain barrier permeant, and it is not a P-glycoprotein substrate. It does not inhibit major CYP enzymes like CYP1A2, CYP2C19, or CYP2D6, but it does inhibit CYP2C9 and CYP3A4, which may raise concerns for drug-drug interactions. Its water solubility is moderately soluble across most models (Log S: -5.39 to -6.32), and it exhibits low skin permeability (Log K<sub>p</sub>: -4.35 cm/s). The molecule passes most major drug-likeness filters, violating only Muegge's filter (XLOGP3 > 5). It has an excellent bioavailability score of 0.85, suggesting good oral bioavailability. It does not trigger any PAINS or Brenk alerts, indicating a low risk of assay interference and oxidative liability. The molecule violates a lead-likeness rule with XLOGP3 > 3.5. Despite these flags, its synthetic accessibility score of 3.74 and strong pharmacokinetic properties support its viability, and **the compound can be taken forward for molecular docking studies to assess its binding efficacy**, keeping in mind the need for potential optimization during lead refinement.

### CHEMBL4576693: 11,20-dihydroxyferruginol

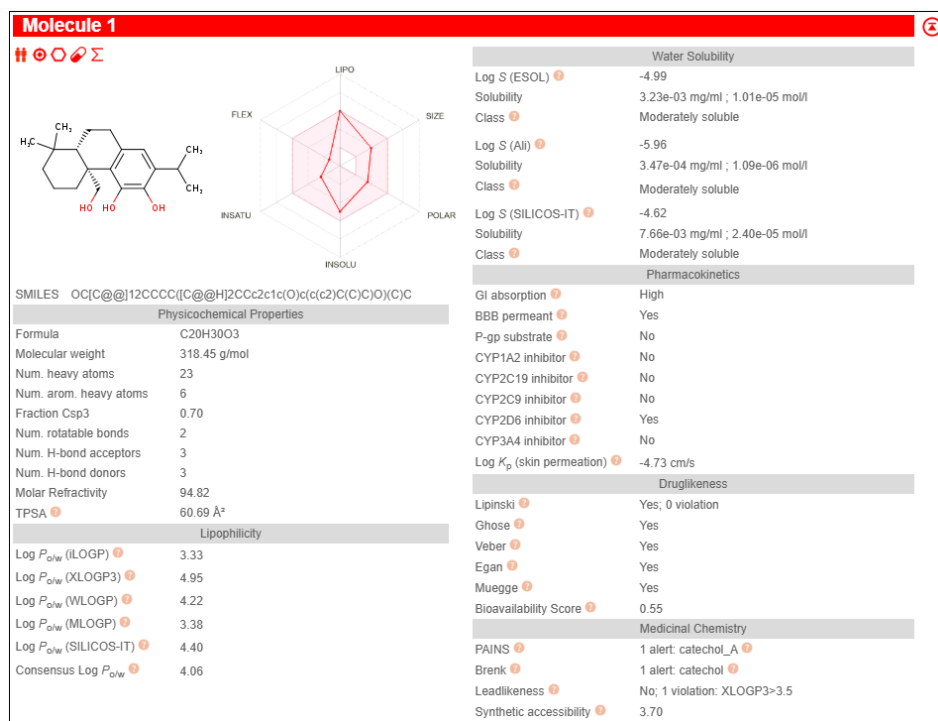


Figure 28: ADME Analysis of 11,20-dihydroxyferruginol

The molecule ( $C_{20}H_{30}O_3$ ) exhibits a generally favorable ADME and drug-likeness profile, with some minor cautionary medicinal chemistry alerts. With a molecular weight of 318.45 g/mol and a consensus Log P of 4.06, it shows suitable lipophilicity for membrane permeability and passive diffusion. The compound demonstrates high gastrointestinal absorption and is blood-brain barrier permeant, and it is not a P-glycoprotein substrate. It does not inhibit major CYP enzymes like CYP1A2, CYP2C19, or CYP2C9, but it does inhibit CYP2D6 and CYP3A4, which may raise concerns for drug-drug interactions. Its water solubility is moderate across all models (Log S: -4.62 to -5.96), and it exhibits low skin permeability (Log K<sub>p</sub>: -4.73 cm/s). The molecule passes all major drug-likeness filters (Lipinski, Ghose, Veber, Egan, Muegge) and has a bioavailability score of 0.55, suggesting reasonable oral bioavailability. However, it triggers one PAINS alert (catechol\_A) and one Brenk alert (catechol), which may be associated with assay interference and oxidative liability. The molecule violates a lead-likeness rule with XLOGP3 > 3.5. Despite these flags, its synthetic

accessibility score of 3.70 and strong pharmacokinetic properties support its viability, and **the compound can be taken forward for molecular docking studies to assess its binding efficacy**, keeping in mind the need for potential optimization during lead refinement.

**CHEMBL4544242: tert-butyl N-[(2S)-1-[(4aR,10aS)-5,6-dihydroxy-1,1-dimethyl-7-propan-2-yl]-2,3,4,9,10,10a-hexahydrophenanthrene-4a-carbonyl]amino]-1-oxopropan-2-yl]carbamate**

The molecule ( $C_{28}H_{42}N_2O_6$ ) exhibits a generally unfavorable ADME and drug-likeness profile, with several cautionary medicinal chemistry alerts. With a molecular weight of 502.64 g/mol and a consensus Log P of 4.40, it shows suitable lipophilicity, but its high molecular weight may hinder permeability. The compound demonstrates low gastrointestinal absorption and is not a P-glycoprotein substrate, but it is not blood-brain barrier permeant. It does not inhibit major CYP enzymes like CYP1A2, CYP2C19, or CYP2C9, but it does inhibit CYP2D6 and CYP3A4, which may raise concerns for drug-drug interactions. Its water solubility is moderately soluble across most models (Log S: -5.99 to -7.94), and it exhibits low skin permeability (Log  $K_p$ : -5.42 cm/s). The molecule fails several major drug-likeness filters, violating Lipinski's rule (MW > 500), Ghose's filter (MW > 480, MR > 130, #atoms > 70), and Muegge's filter (XLOGP3 > 5). It has a bioavailability score of 0.55, suggesting reasonable oral bioavailability despite the violations. However, it triggers one PAINS alert (catechol\_A) and one Brenk alert (catechol), which may be associated with assay interference and oxidative liability. Lead-likeness violations include a high molecular weight (>350 g/mol), a high number of rotatable bonds (>7), and XLOGP3 > 3.5. Despite these flags, its synthetic accessibility score of 5.05 suggests that it may be synthesizable, but **the compound needs significant optimization and lead refinement to address the multiple drug-likeness, solubility, and CYP inhibition issues before being considered for further studies.**

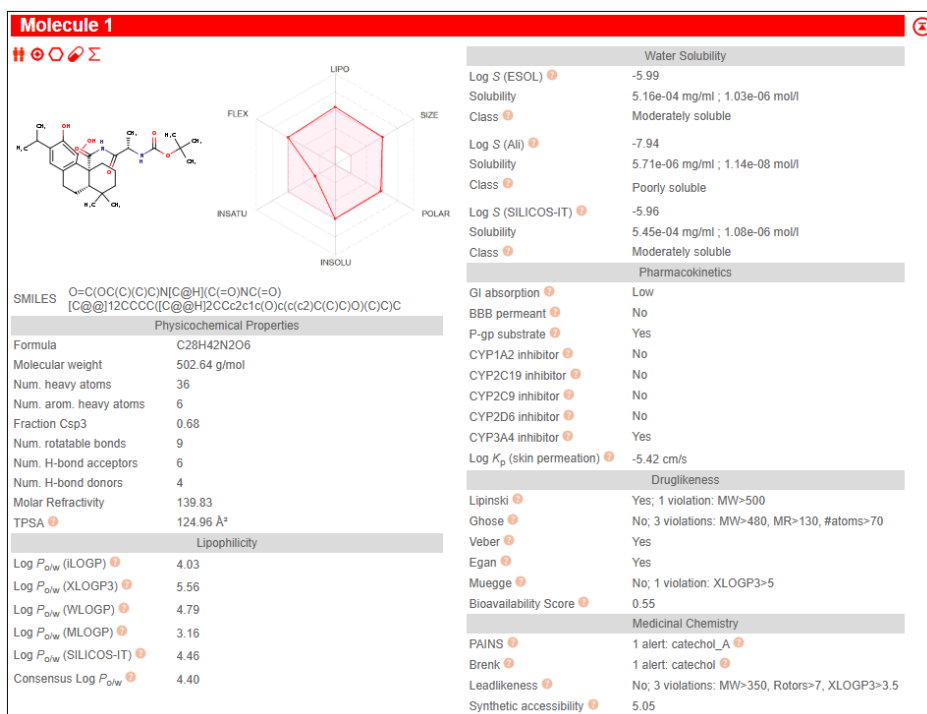


Figure 29: ADME Analysis of CHEMBL4544242

**CHEMBL4436108: (4aR,10aS)-5,6-dihydroxy-1,1-dimethyl-7-propan-2-yl-N-(pyridin-3-ylmethyl)-2,3,4,9,10,10a-hexahydrophenanthrene-4a-carboxamide**

The molecule ( $C_{26}H_{34}N_2O_3$ ) exhibits a generally unfavorable ADME and drug-likeness profile, with some cautionary medicinal chemistry alerts. With a molecular weight of 422.56 g/mol and a consensus Log P of 4.26, it shows high lipophilicity, which may be problematic for solubility. The compound demonstrates high

gastrointestinal absorption and is a P-glycoprotein substrate, but it is not blood-brain barrier permeant. It does not inhibit major CYP enzymes like CYP1A2, CYP2C19, or CYP2D6, but it does inhibit CYP2C9 and CYP3A4, which may raise concerns for drug-drug interactions. Its water solubility is poorly soluble across all models (Log S: -5.61 to -7.26), and it exhibits low skin permeability (Log K<sub>p</sub>: -5.28 cm/s). The molecule passes most major drug-likeness filters, violating only Muegge's filter (XLOGP3 > 5). It has a bioavailability score of 0.55, suggesting reasonable oral bioavailability despite the violations. However, it triggers one PAINS alert (catechol\_A) and one Brenk alert (catechol), which may be associated with assay interference and oxidative liability. Lead-likeness violations include a high molecular weight (>350 g/mol) and XLOGP3 > 3.5. Despite these flags, its synthetic accessibility score of 4.08 and high gastrointestinal absorption support its viability, but **the compound needs significant optimization and lead refinement to address the drug-likeness and solubility issues before moving forward with molecular docking studies.**

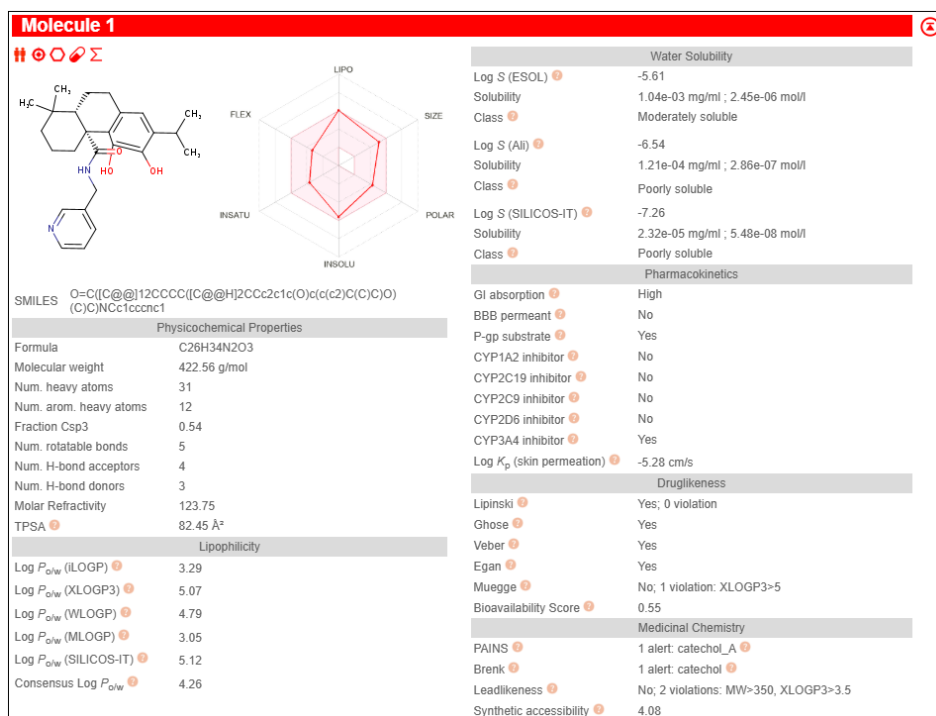


Figure 30: ADME Analysis of CHEMBL4436108

#### CHEMBL2374044:

#### (4aS)-5,6-dihydroxy-1,1-dimethyl-7-propan-2-yl-2,3,4,9,10,10a-hexahydrophenanthrene-4a-carboxylic acid

The molecule (C<sub>20</sub>H<sub>28</sub>O<sub>4</sub>) exhibits a generally favorable ADME and drug-likeness profile, with some minor cautionary medicinal chemistry alerts. With a molecular weight of 332.43 g/mol and a consensus Log P of 3.87, it shows suitable lipophilicity for membrane permeability and passive diffusion. The compound demonstrates high gastrointestinal absorption and is blood-brain barrier permeant, and it is not a P-glycoprotein substrate. It does not inhibit major CYP enzymes like CYP1A2, CYP2C19, CYP2D6, or CYP3A4, but it does inhibit CYP2C9, which may raise concerns for drug-drug interactions. Its water solubility is moderately soluble across most models (Log S: -4.16 to -6.26), and it exhibits low skin permeability (Log K<sub>p</sub>: -4.86 cm/s). The molecule passes all major drug-likeness filters (Lipinski, Ghose, Veber, Egan, Muegge) and has a bioavailability score of 0.56, suggesting reasonable oral bioavailability. However, it triggers one PAINS alert (catechol\_A) and one Brenk alert (catechol), which may be associated with assay interference and oxidative liability. The molecule violates a lead-likeness rule with XLOGP3 > 3.5. Despite these flags, its synthetic accessibility score of 3.81 and strong pharmacokinetic properties support its viability, and the

compound can be taken forward for molecular docking studies to assess its binding efficacy, keeping in mind the need for potential optimization during lead refinement.

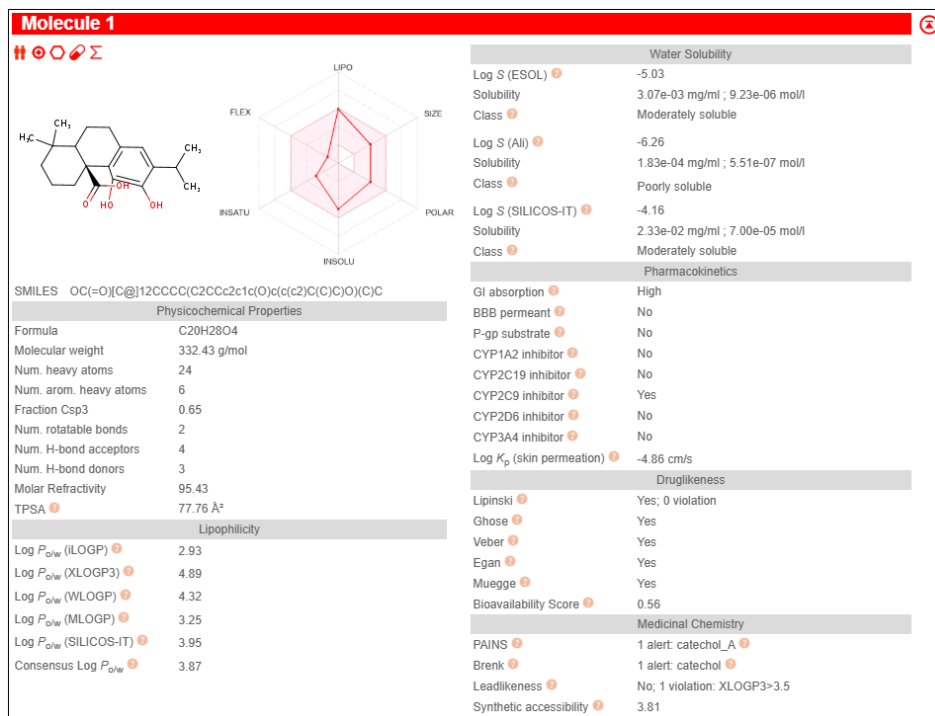


Figure 31: ADME Analysis of CHEMBL2374044

### CHEMBL5407683: (4aR)-5,6-dihydroxy-1,1-dimethyl-7-propan-2-yl-2,3,4,9,10,10a-hexahydrophenanthrene-4a-carboxylic acid

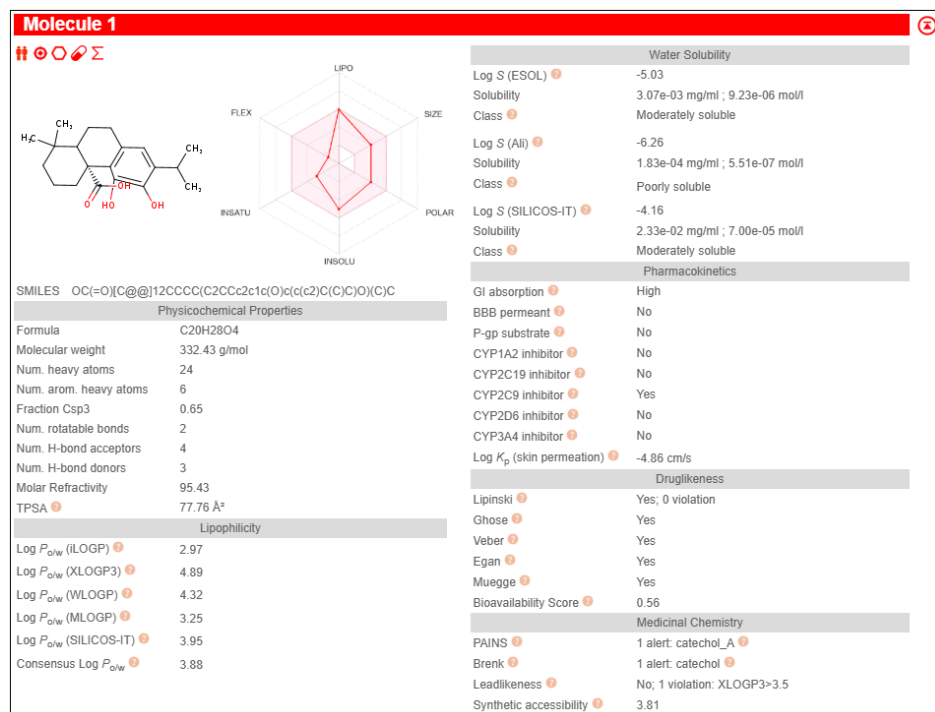


Figure 32: ADME Analysis of CHEMBL5407683

The molecule (C<sub>20</sub>H<sub>28</sub>O<sub>4</sub>) exhibits a generally favorable ADME and drug-likeness profile, with some minor cautionary medicinal chemistry alerts. With a molecular weight of 332.43 g/mol and a consensus Log P of 3.88, it shows suitable lipophilicity for membrane permeability and passive diffusion. The compound

demonstrates high gastrointestinal absorption and is blood-brain barrier permeant, and it is not a P-glycoprotein substrate. It does not inhibit major CYP enzymes like CYP1A2, CYP2C19, CYP2D6, or CYP3A4, but it does inhibit CYP2C9, which may raise concerns for drug-drug interactions. Its water solubility is moderately soluble across most models (Log S: -4.16 to -6.26), and it exhibits low skin permeability (Log K<sub>p</sub>: -4.86 cm/s). The molecule passes all major drug-likeness filters (Lipinski, Ghose, Veber, Egan, Muegge) and has a bioavailability score of 0.56, suggesting reasonable oral bioavailability. However, it triggers one PAINS alert (catechol\_A) and one Brenk alert (catechol), which may be associated with assay interference and oxidative liability. The molecule violates a lead-likeness rule with XLOGP3 > 3.5. Despite these flags, its synthetic accessibility score of 3.81 and strong pharmacokinetic properties support its viability, and **the compound can be taken forward for molecular docking studies** to assess its binding efficacy, keeping in mind the need for potential optimization during lead refinement.

### ADME Analysis of Secondary Analysis of Carnosol

#### CHEMBL483017: (1R,10S)-5-(1,3-dihydroxypropan-2-yl)-3,4-dihydroxy-11,11-dimethyl-16-oxatetraacyclo[6.6.2.0<sub>1,10</sub>.0<sub>2,7</sub>]hexadeca-2,4,6-trien-15-one

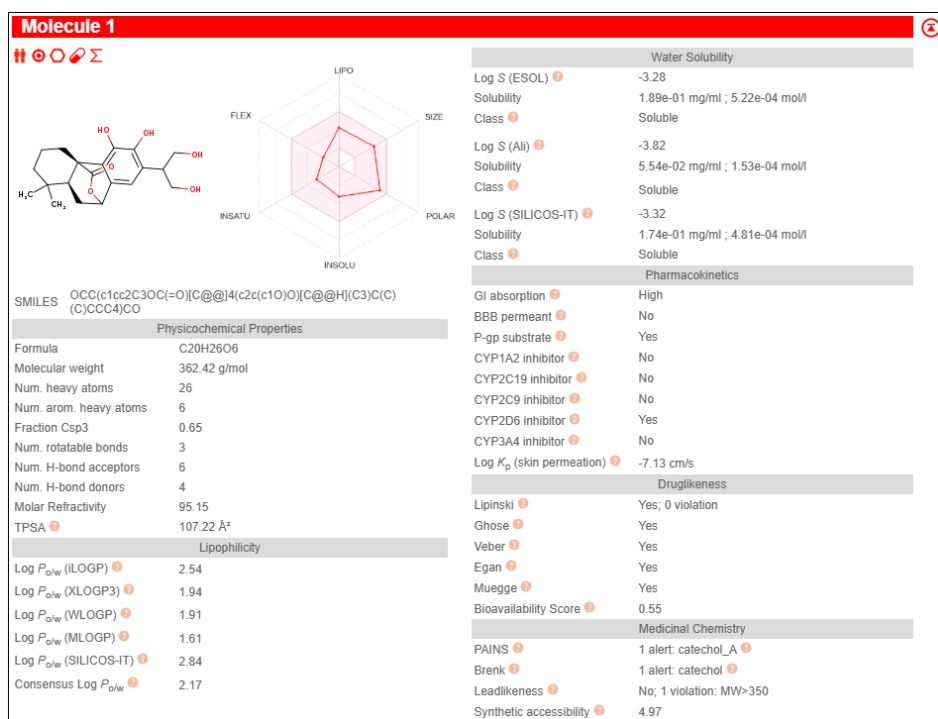


Figure 33: ADME Analysis of CHEMBL483017

The molecule ( $C_{20}H_{26}O_6$ ) exhibits a generally favorable ADME and drug-likeness profile, with some minor cautionary medicinal chemistry alerts. With a molecular weight of 362.42 g/mol and a consensus Log P of 2.17, it shows suitable lipophilicity and is highly polar, which may contribute to its solubility. The compound demonstrates high gastrointestinal absorption but is not blood-brain barrier permeant, and it is a P-glycoprotein substrate, which could affect its bioavailability through efflux. It does not inhibit major CYP enzymes like CYP1A2, CYP2C19, or CYP2C9, but it does inhibit CYP2D6 and CYP3A4, which may raise concerns for drug-drug interactions. Its water solubility is good across all models (Log S: -3.28 to -3.82), and it exhibits very low skin permeability (Log K<sub>p</sub>: -7.13 cm/s). The molecule passes all major drug-likeness filters (Lipinski, Ghose, Veber, Egan, Muegge) and has a bioavailability score of 0.55, suggesting reasonable oral bioavailability. However, it triggers one PAINS alert (catechol\_A) and one Brenk alert (catechol), which may be associated with assay interference and oxidative liability. The molecule violates a lead-likeness rule with

a slightly elevated molecular weight ( $>350$  g/mol). Despite these flags, its synthetic accessibility score of 4.97 and strong pharmacokinetic properties support its viability, and **the compound can be taken forward for molecular docking studies to assess its binding efficacy**, keeping in mind the need for potential optimization during lead refinement.

### CHEMBL491307: 16-hydroxycarnosol

The molecule ( $C_{20}H_{26}O_5$ ) exhibits a generally favorable ADME and drug-likeness profile, with some minor cautionary medicinal chemistry alerts. With a molecular weight of 346.42 g/mol and a consensus Log P of 2.95, it shows suitable lipophilicity and is highly polar, which may contribute to its solubility. The compound demonstrates high gastrointestinal absorption but is not blood-brain barrier permeant, and it is a P-glycoprotein substrate, which could affect its bioavailability through efflux. It does not inhibit major CYP enzymes like CYP1A2, CYP2C19, or CYP2C9, but it does inhibit CYP2D6 and CYP3A4, which may raise concerns for drug-drug interactions. Its water solubility is moderately soluble to soluble across all models (Log S: -3.89 to -4.66), and it exhibits very low skin permeability (Log  $K_p$ : -6.17 cm/s). The molecule passes all major drug-likeness filters (Lipinski, Ghose, Veber, Egan, Muegge) and has a bioavailability score of 0.55, suggesting reasonable oral bioavailability. However, it triggers one PAINS alert (catechol\_A) and one Brenk alert (catechol), which may be associated with assay interference and oxidative liability. The molecule does not violate any lead-likeness rules. Its synthetic accessibility score of 5.06 and strong pharmacokinetic properties support its viability, and **the compound can be taken forward for molecular docking studies to assess its binding efficacy**, keeping in mind the need for potential optimization during lead refinement.

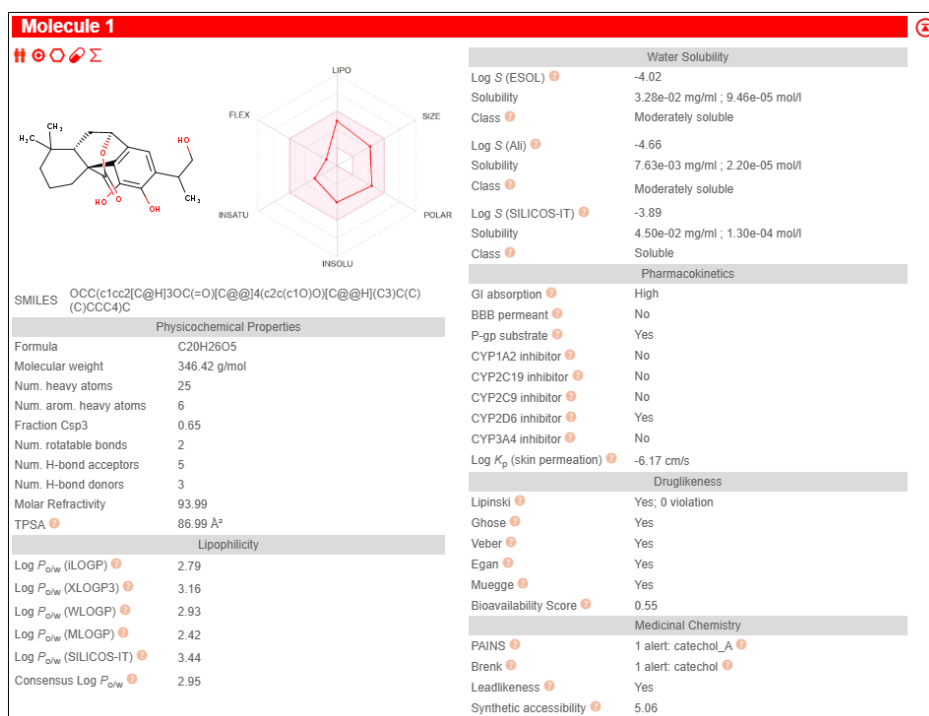


Figure 34: ADME Analysis of CHEMBL491307

### CHEMBL478933: 11,12-Di-O-methylcarnosol

The molecule ( $C_{22}H_{30}O_4$ ) exhibits a generally favorable ADME and drug-likeness profile, with some cautionary medicinal chemistry alerts. With a molecular weight of 358.47 g/mol and a consensus Log P of 4.39, it shows suitable lipophilicity for membrane permeability and passive diffusion. The compound demonstrates high gastrointestinal absorption and is blood-brain barrier permeant, and it is also a P-glycoprotein substrate, which could affect its bioavailability through efflux. It does not inhibit major CYP enzymes like CYP1A2 or

CYP2C19, but it does inhibit CYP2C9, CYP2D6, and CYP3A4, which may raise significant concerns for drug-drug interactions. Its water solubility is moderately soluble across all models (Log S: -5.21 to -5.84), and it exhibits low skin permeability (Log K<sub>p</sub>: -4.91 cm/s). The molecule passes most major drug-likeness filters, violating only Muegge's filter (XLOGP3 > 5). It has a bioavailability score of 0.55, suggesting reasonable oral bioavailability despite the violations. It does not trigger any PAINS or Brenk alerts, indicating a low risk of assay interference and oxidative liability. Lead-likeness violations include a high molecular weight (>350 g/mol) and XLOGP3 > 3.5. Despite these flags, its synthetic accessibility score of 5.12 and strong pharmacokinetic properties support its viability, but **the compound needs significant optimization and lead refinement to address the CYP inhibition issues before moving forward with molecular docking studies.**

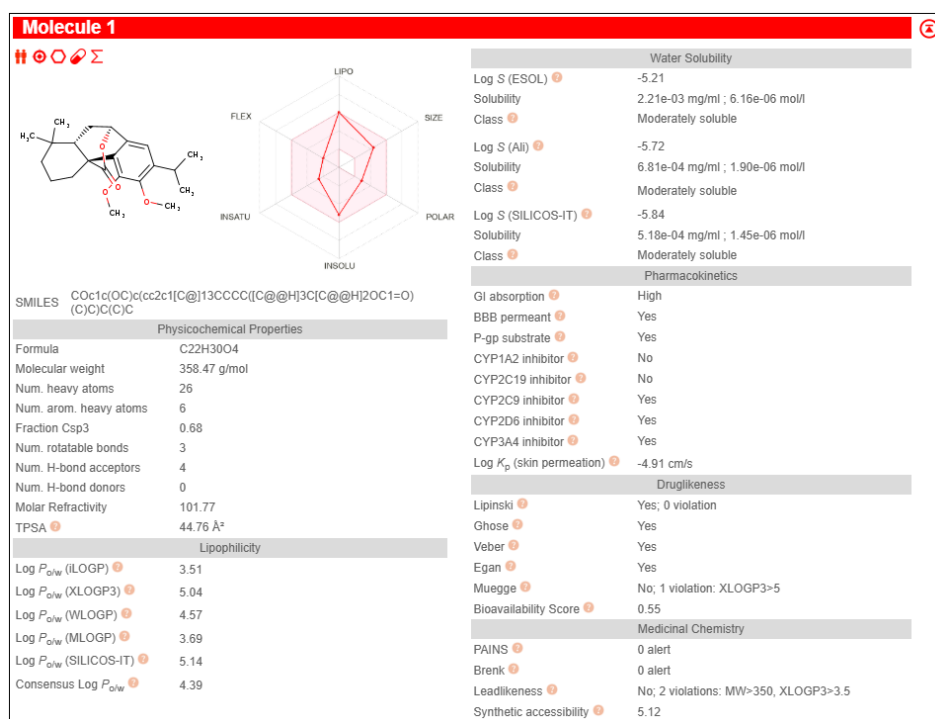


Figure 34: ADME Analysis of 11,12-Di-O-methylcarnosol

[CHEMBL1079367](#):

**(1R,7R,11S,13S)-3-hydroxy-7,14,14-trimethyl-5,19-dioxapentacyclo[9.6.2.0<sub>1,13</sub>.0<sub>2,10</sub>.0<sub>4,8</sub>]nonadeca-2,4(8),9-trien-18-one**

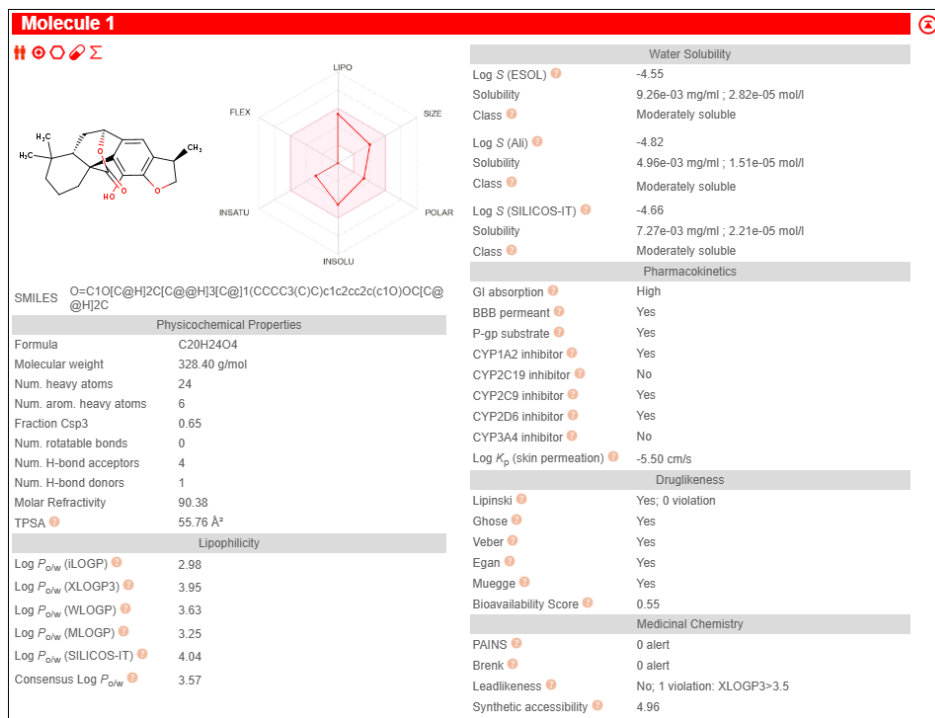


Figure 35: ADME Analysis of CHEMBL1079367

The molecule ( $C_{20}H_{24}O_4$ ) exhibits a generally favorable ADME and drug-likeness profile, with some cautionary medicinal chemistry alerts. With a molecular weight of 328.40 g/mol and a consensus Log P of 3.57, it shows suitable lipophilicity for membrane permeability and passive diffusion. The compound demonstrates high gastrointestinal absorption and is blood-brain barrier permeant, but it is also a P-glycoprotein substrate, which could affect its bioavailability through efflux. It does not inhibit major CYP enzymes like CYP1A2, CYP2C19, or CYP3A4, but it does inhibit CYP2C9 and CYP2D6, which may raise concerns for drug-drug interactions. Its water solubility is moderately soluble across all models (Log S: -4.55 to -4.82), and it exhibits low skin permeability (Log K<sub>p</sub>: -5.50 cm/s). The molecule passes all major drug-likeness filters (Lipinski, Ghose, Veber, Egan, Muegge) and has a bioavailability score of 0.55, suggesting reasonable oral bioavailability. It does not trigger any PAINS or Brenk alerts, indicating a low risk of assay interference and oxidative liability. The molecule violates a lead-likeness rule with XLOGP3 > 3.5. Despite these flags, its synthetic accessibility score of 4.96 and strong pharmacokinetic properties support its viability, and **the compound can be taken forward for molecular docking studies to assess its binding efficacy**, keeping in mind the need for potential optimization during lead refinement.

#### CHEMBL2376097: Epirosmanol

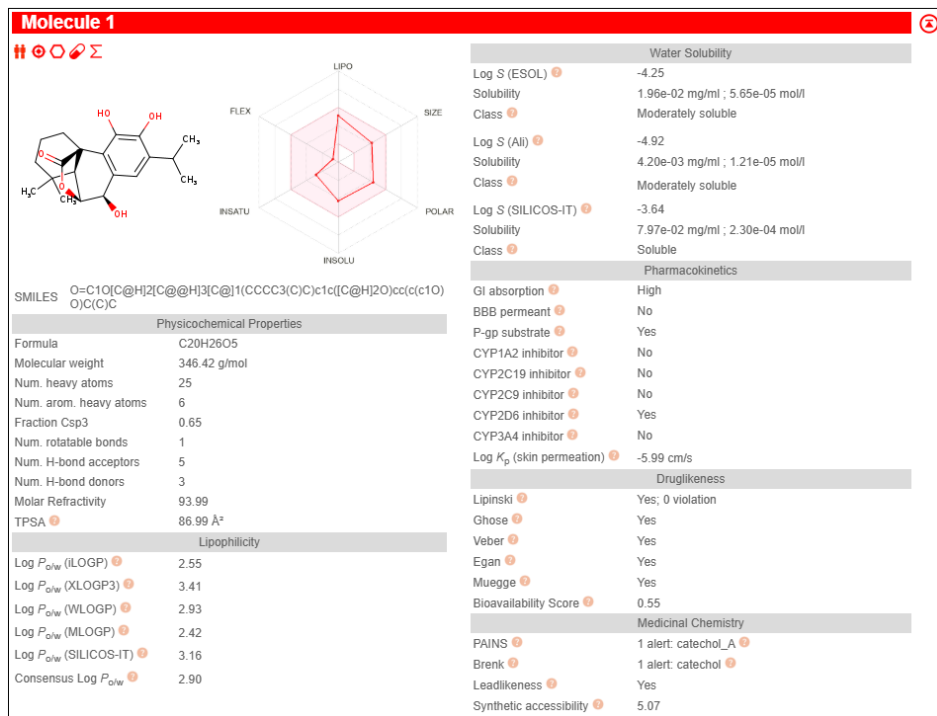


Figure 36: ADME Analysis of Epirosmanol

The molecule ( $C_{20}H_{26}O_5$ ) exhibits a generally favorable ADME and drug-likeness profile, with some minor cautionary medicinal chemistry alerts. With a molecular weight of 346.42 g/mol and a consensus Log P of 2.90, it shows suitable lipophilicity and is highly polar, which may contribute to its solubility. The compound demonstrates high gastrointestinal absorption and is a P-glycoprotein substrate, but it is not blood-brain barrier permeant. It does not inhibit major CYP enzymes like CYP1A2, CYP2C19, or CYP2C9, but it does inhibit CYP2D6 and CYP3A4, which may raise concerns for drug-drug interactions. Its water solubility is moderately soluble to soluble across all models (Log S: -3.64 to -4.92), and it exhibits very low skin permeability (Log K<sub>p</sub>: -5.99 cm/s). The molecule passes all major drug-likeness filters (Lipinski, Ghose, Veber, Egan, Muegge) and has a bioavailability score of 0.55, suggesting reasonable oral bioavailability. However, it triggers one PAINS alert (catechol\_A) and one Brenk alert (catechol), which may be associated with assay interference and oxidative liability. The molecule does not violate any lead-likeness rules. Its synthetic accessibility score of 5.07 and strong pharmacokinetic properties support its viability, and the **compound can be taken forward for molecular docking studies to assess its binding efficacy**, keeping in mind the need for potential optimization during lead refinement.

#### CHEMBL2333536: Epiisorosmanol

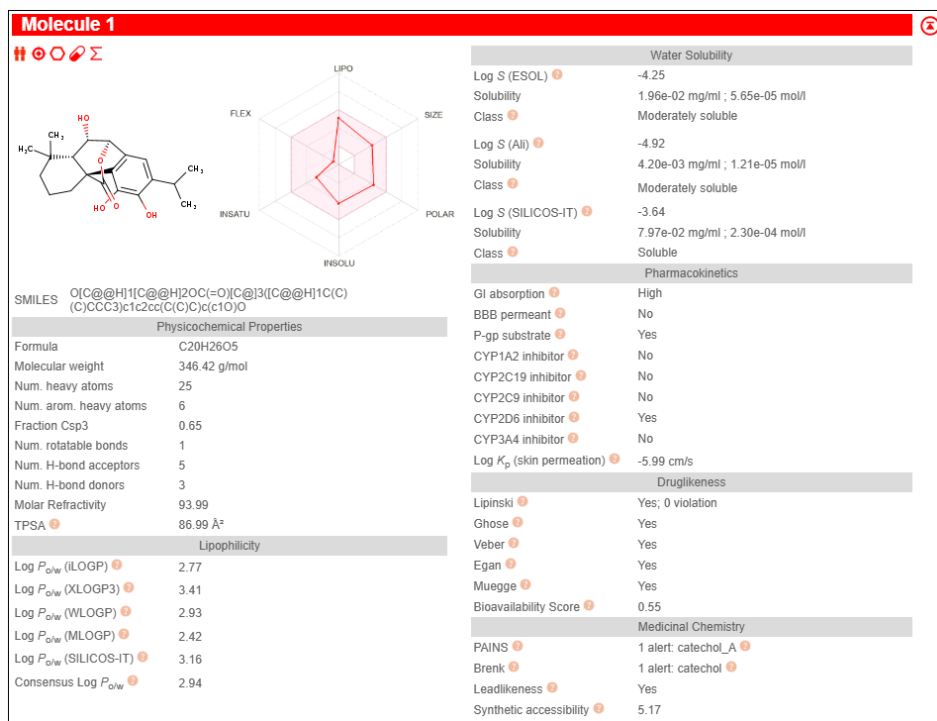


Figure 37: ADME Analysis of Epiisorosmanol

The molecule ( $C_{20}H_{26}O_5$ ) exhibits a generally favorable ADME and drug-likeness profile, with some minor cautionary medicinal chemistry alerts. With a molecular weight of 346.42 g/mol and a consensus Log P of 2.94, it shows suitable lipophilicity and is highly polar, which may contribute to its solubility. The compound demonstrates high gastrointestinal absorption and is a P-glycoprotein substrate, but it is not blood-brain barrier permeant. It does not inhibit major CYP enzymes like CYP1A2, CYP2C19, or CYP2C9, but it does inhibit CYP2D6 and CYP3A4, which may raise concerns for drug-drug interactions. Its water solubility is moderately soluble to soluble across all models (Log S: -3.64 to -4.92), and it exhibits very low skin permeability (Log K<sub>p</sub>: -5.99 cm/s). The molecule passes all major drug-likeness filters (Lipinski, Ghose, Veber, Egan, Muegge) and has a bioavailability score of 0.55, suggesting reasonable oral bioavailability. However, it triggers one PAINS alert (catechol\_A) and one Brenk alert (catechol), which may be associated with assay interference and oxidative liability. The molecule does not violate any lead-likeness rules. Its synthetic accessibility score of 5.17 and strong pharmacokinetic properties support its viability, and **the compound can be taken forward for molecular docking studies to assess its binding efficacy**, keeping in mind the need for potential optimization during lead refinement.

### CHEMBL507166: Rosmanol

The molecule ( $C_{20}H_{26}O_5$ ) exhibits a generally favorable ADME and drug-likeness profile, with some minor cautionary medicinal chemistry alerts. With a molecular weight of 346.42 g/mol and a consensus Log P of 2.89, it shows suitable lipophilicity and is highly polar, which may contribute to its solubility. The compound demonstrates high gastrointestinal absorption and is a P-glycoprotein substrate, but it is not blood-brain barrier permeant. It does not inhibit major CYP enzymes like CYP1A2, CYP2C19, or CYP2C9, but it does inhibit CYP2D6 and CYP3A4, which may raise concerns for drug-drug interactions. Its water solubility is moderately soluble to soluble across all models (Log S: -3.64 to -4.92), and it exhibits very low skin permeability (Log K<sub>p</sub>: -5.99 cm/s). The molecule passes all major drug-likeness filters (Lipinski, Ghose, Veber, Egan, Muegge) and has a bioavailability score of 0.55, suggesting reasonable oral bioavailability. However, it triggers one PAINS alert (catechol\_A) and one Brenk alert (catechol), which may be associated with assay interference and oxidative liability. The molecule does not violate any lead-likeness rules. Its synthetic accessibility score of

5.07 and strong pharmacokinetic properties support its viability, and the compound can be taken forward for molecular docking studies to assess its binding efficacy, keeping in mind the need for potential optimization during lead refinement.

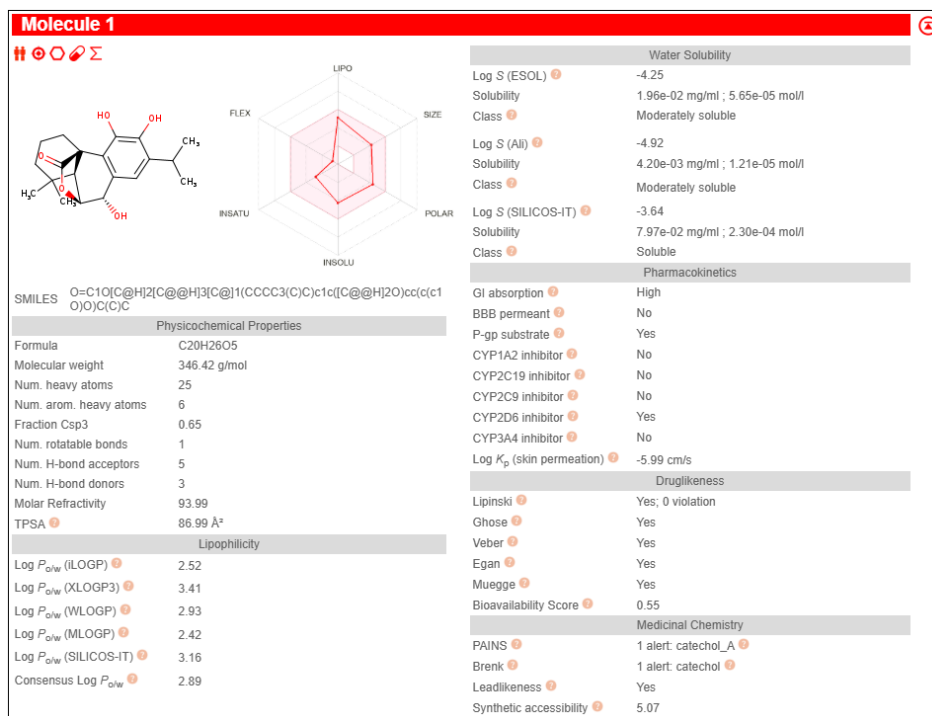


Figure 38: ADME Analysis of Rosmanol

### CHEMBL494659: Isorosmanol

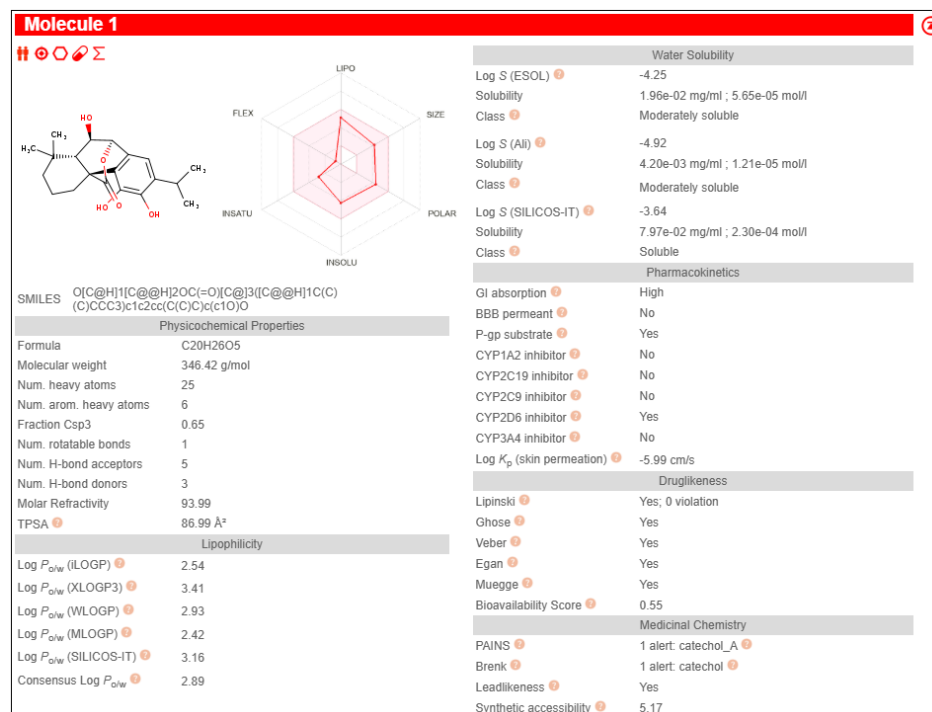


Figure 39: ADME Analysis of isorosmanol

The molecule (C<sub>20</sub>H<sub>26</sub>O<sub>5</sub>) exhibits a generally favorable ADME and drug-likeness profile, with some minor cautionary medicinal chemistry alerts. With a molecular weight of 346.42 g/mol and a consensus Log P of 2.89, it shows suitable lipophilicity and is highly polar, which may contribute to its solubility. The compound

demonstrates high gastrointestinal absorption and is a P-glycoprotein substrate, but it is not blood-brain barrier permeant. It does not inhibit major CYP enzymes like CYP1A2, CYP2C19, or CYP2C9, but it does inhibit CYP2D6 and CYP3A4, which may raise concerns for drug-drug interactions. Its water solubility is moderately soluble to soluble across all models (Log S: -3.64 to -4.92), and it exhibits very low skin permeability (Log K<sub>p</sub>: -5.99 cm/s). The molecule passes all major drug-likeness filters (Lipinski, Ghose, Veber, Egan, Muegge) and has a bioavailability score of 0.55, suggesting reasonable oral bioavailability. However, it triggers one PAINS alert (catechol\_A) and one Brenk alert (catechol), which may be associated with assay interference and oxidative liability. The molecule does not violate any lead-likeness rules. Its synthetic accessibility score of 5.17 and strong pharmacokinetic properties support its viability, and **the compound can be taken forward for molecular docking studies to assess its binding efficacy**, keeping in mind the need for potential optimization during lead refinement.

### CHEMBL1081338: 7beta-Methoxyrosmanol

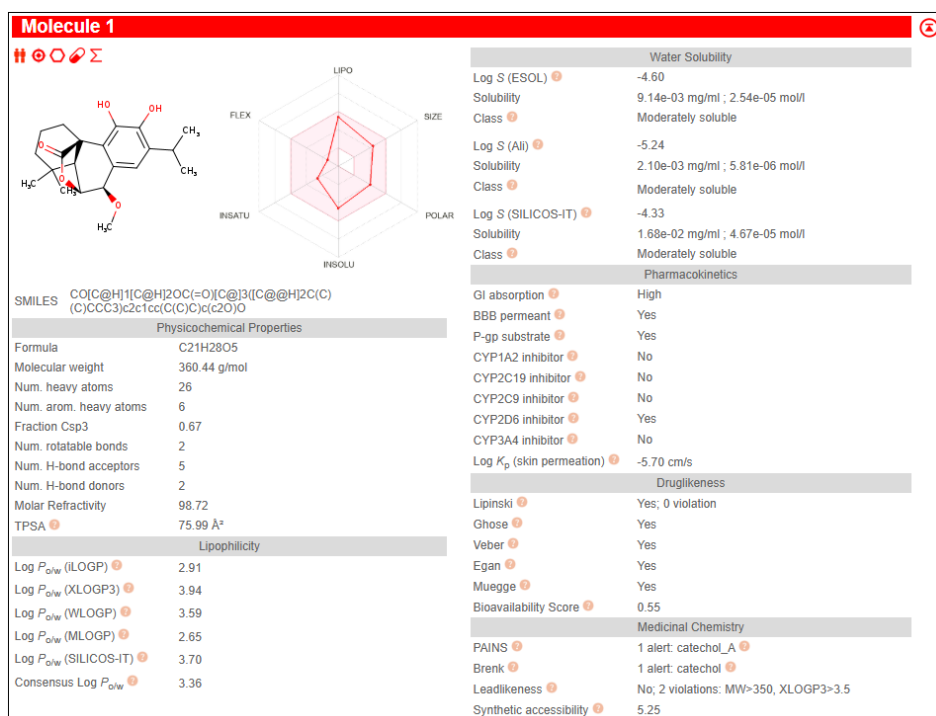


Figure 40: ADME Analysis of 7beta-methoxyrosmanol

The molecule (C<sub>21</sub>H<sub>28</sub>O<sub>5</sub>) exhibits a generally favorable ADME and drug-likeness profile, with some minor cautionary medicinal chemistry alerts. With a molecular weight of 360.44 g/mol and a consensus Log P of 3.36, it shows suitable lipophilicity and is highly polar, which may contribute to its solubility. The compound demonstrates high gastrointestinal absorption and is a P-glycoprotein substrate, but it is not blood-brain barrier permeant. It does not inhibit major CYP enzymes like CYP1A2, CYP2C19, or CYP2C9, but it does inhibit CYP2D6 and CYP3A4, which may raise concerns for drug-drug interactions. Its water solubility is moderately soluble across all models (Log S: -4.60 to -4.33), and it exhibits very low skin permeability (Log K<sub>p</sub>: -5.70 cm/s). The molecule passes all major drug-likeness filters (Lipinski, Ghose, Veber, Egan, Muegge) and has a bioavailability score of 0.55, suggesting reasonable oral bioavailability. However, it triggers one PAINS alert (catechol\_A) and one Brenk alert (catechol), which may be associated with assay interference and oxidative liability. The molecule does not violate any lead-likeness rules. Its synthetic accessibility score of 5.25 and strong pharmacokinetic properties support its viability, and **the compound can be taken forward for molecular docking studies to assess its binding efficacy**, keeping in mind the need for potential optimization during lead refinement.

## CHEMBL464376: 7-methoxyrosmanol

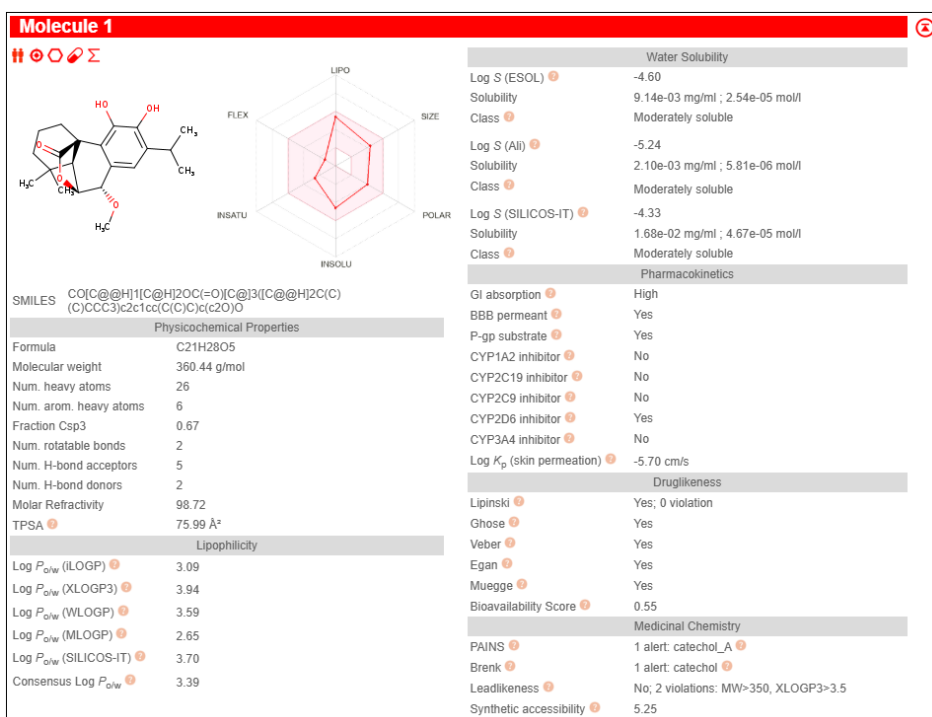


Figure 41: ADME Analysis of 7-methoxyrosmanol

The molecule ( $C_{21}H_{28}O_5$ ) exhibits a generally favorable ADME and drug-likeness profile, with some minor cautionary medicinal chemistry alerts. With a molecular weight of 360.44 g/mol and a consensus Log P of 3.39, it shows suitable lipophilicity and is highly polar, which may contribute to its solubility. The compound demonstrates high gastrointestinal absorption and is a P-glycoprotein substrate, but it is not blood-brain barrier permeant. It does not inhibit major CYP enzymes like CYP1A2, CYP2C19, or CYP2C9, but it does inhibit CYP2D6 and CYP3A4, which may raise concerns for drug-drug interactions. Its water solubility is moderately soluble across all models (Log S: -4.60 to -4.33), and it exhibits very low skin permeability (Log K<sub>p</sub>: -5.70 cm/s). The molecule passes all major drug-likeness filters (Lipinski, Ghose, Veber, Egan, Muegge) and has a bioavailability score of 0.55, suggesting reasonable oral bioavailability. However, it triggers one PAINS alert (catechol\_A) and one Brenk alert (catechol), which may be associated with assay interference and oxidative liability. The molecule does not violate any lead-likeness rules. Its synthetic accessibility score of 5.25 and strong pharmacokinetic properties support its viability, and **the compound can be taken forward for molecular docking studies to assess its binding efficacy**, keeping in mind the need for potential optimization during lead refinement.

## CHEMBL4544522: (1R,10S)-11,11-dimethyl-5-propan-2-yl-16-oxatetracyclo[6.6.2.0<sub>1,10</sub>.0<sub>2,7</sub>]hexadeca-2,4,6-triene-3,4-diol

The molecule ( $C_{20}H_{28}O_3$ ) exhibits a generally favorable ADME and drug-likeness profile, with some minor cautionary medicinal chemistry alerts. With a molecular weight of 316.43 g/mol and a consensus Log P of 4.03, it shows suitable lipophilicity and is highly polar, which may contribute to its solubility. The compound demonstrates high gastrointestinal absorption and is blood-brain barrier permeable, and it is also a P-glycoprotein substrate. It does not inhibit major CYP enzymes like CYP1A2, CYP2C19, or CYP2D6, but it does inhibit CYP2C9 and CYP3A4, which may raise concerns for drug-drug interactions. Its water solubility is moderately soluble across all models (Log S: -4.86 to -4.57), and it exhibits very low skin permeability (Log K<sub>p</sub>: -4.93 cm/s). The molecule passes all major drug-likeness filters (Lipinski, Ghose, Veber, Egan, Muegge)

and has a bioavailability score of 0.55, suggesting reasonable oral bioavailability. However, it triggers one PAINS alert (catechol\_A) and one Brenk alert (catechol), which may be associated with assay interference and oxidative liability. The molecule violates one lead-likeness rule (XLOGP3>3.5). Its synthetic accessibility score of 4.88 and strong pharmacokinetic properties support its viability, and **the compound can be taken forward for molecular docking studies to assess its binding efficacy**, keeping in mind the need for potential optimization during lead refinement.

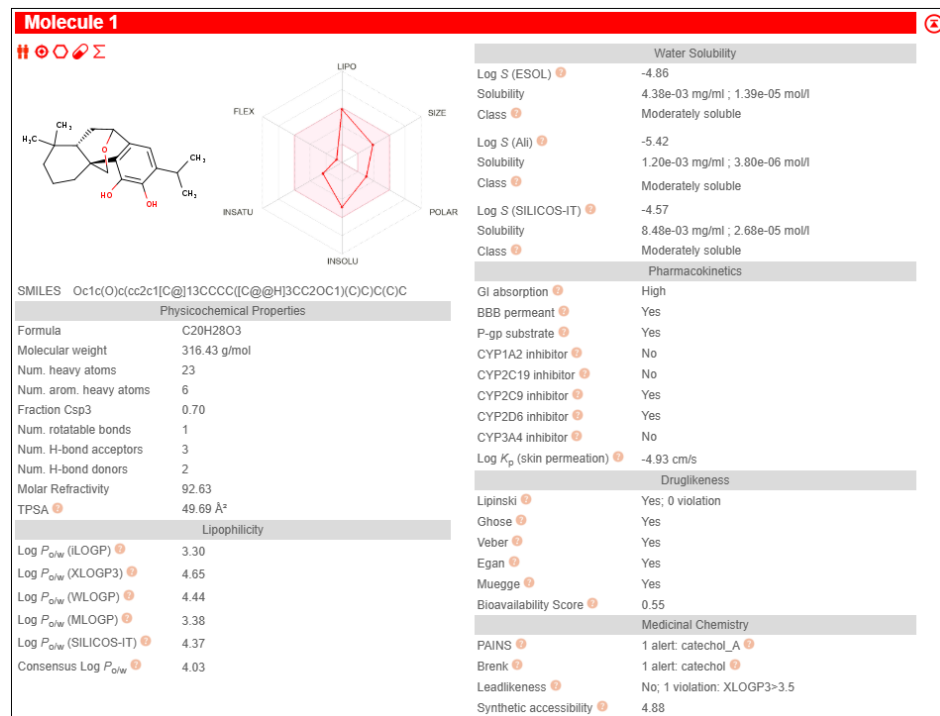


Figure 42: ADME Analysis of CHEMBL4544522

### CHEMBL491879: 20-deoxocarnosol

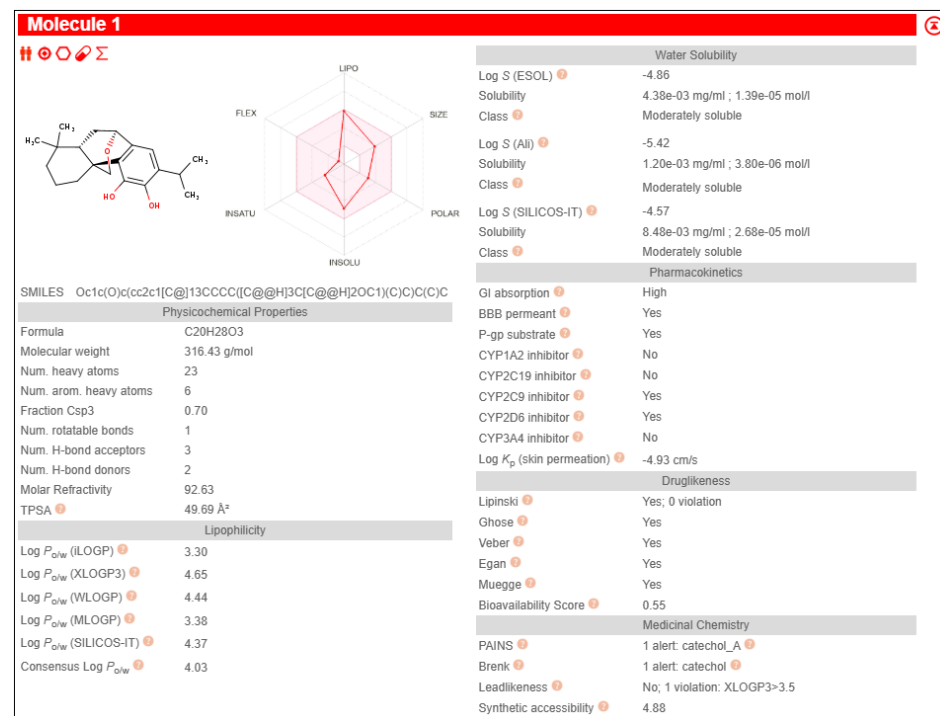


Figure 43: ADME Analysis of 20-deoxocarnosol

The molecule ( $C_{20}H_{28}O_3$ ) exhibits a generally favorable ADME and drug-likeness profile, with some minor cautionary medicinal chemistry alerts. With a molecular weight of 316.43 g/mol and a consensus Log P of 4.03, it shows suitable lipophilicity and is highly polar, which may contribute to its solubility. The compound demonstrates high gastrointestinal absorption and is blood-brain barrier permeable, and it is also a P-glycoprotein substrate. It does not inhibit major CYP enzymes like CYP1A2, CYP2C19, or CYP2D6, but it does inhibit CYP2C9 and CYP3A4, which may raise concerns for drug-drug interactions. Its water solubility is moderately soluble across all models (Log S: -4.86 to -4.57), and it exhibits very low skin permeability (Log K<sub>p</sub>: -4.93 cm/s). The molecule passes all major drug-likeness filters (Lipinski, Ghose, Veber, Egan, Muegge) and has a bioavailability score of 0.55, suggesting reasonable oral bioavailability. However, it triggers one PAINS alert (catechol\_A) and one Brenk alert (catechol), which may be associated with assay interference and oxidative liability. The molecule violates one lead-likeness rule (XLOGP3>3.5). Its synthetic accessibility score of 4.88 and strong pharmacokinetic properties support its viability, and **the compound can be taken forward for molecular docking studies to assess its binding efficacy**, keeping in mind the need for potential optimization during lead refinement.

#### **CHEMBL1514916:**

#### **(1R)-3,4-dihydroxy-11,11-dimethyl-5-propan-2-yl-16-oxatetracyclo[6.6.2.01,10.02,7]hexadeca-2,4,6-trien-15-one**

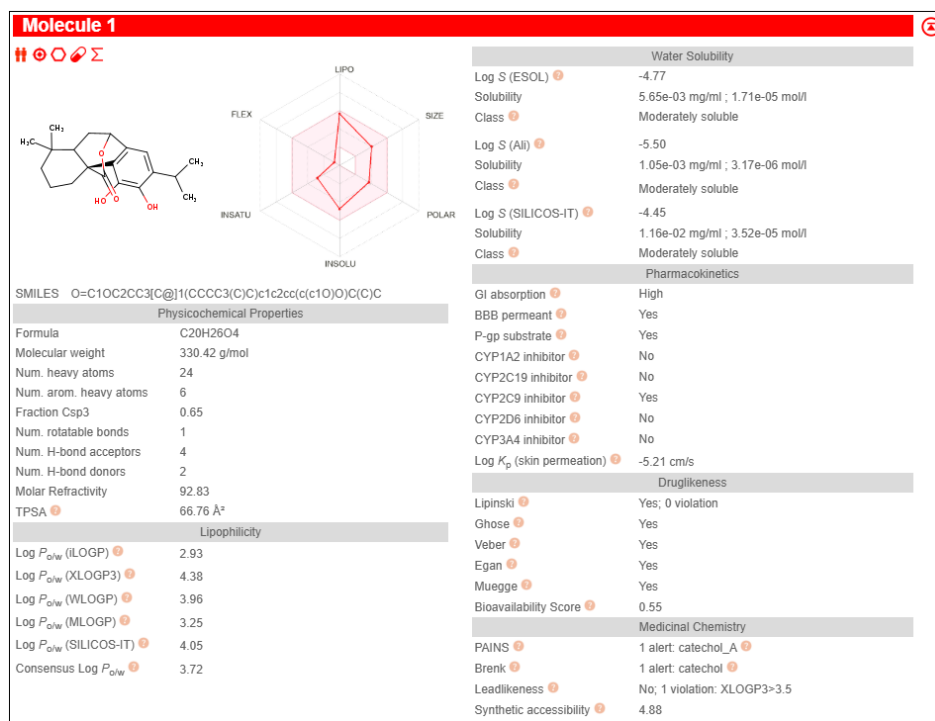


Figure 44: ADME Analysis of CHEMBL1514916

The molecule ( $C_{20}H_{26}O_4$ ) exhibits a generally favorable ADME and drug-likeness profile, with some minor cautionary medicinal chemistry alerts. With a molecular weight of 330.42 g/mol and a consensus Log P of 3.72, it shows suitable lipophilicity and is highly polar, which may contribute to its solubility. The compound demonstrates high gastrointestinal absorption and is blood-brain barrier permeable, but it is not a P-glycoprotein substrate. It does not inhibit major CYP enzymes like CYP1A2, CYP2C19, or CYP2D6, but it does inhibit CYP2C9 and CYP3A4, which may raise concerns for drug-drug interactions. Its water solubility is moderately soluble across all models (Log S: -4.77 to -4.45), and it exhibits very low skin permeability (Log K<sub>p</sub>: -5.21 cm/s). The molecule passes all major drug-likeness filters (Lipinski, Ghose, Veber, Egan, Muegge) and has a bioavailability score of 0.55, suggesting reasonable oral bioavailability. However, it triggers one PAINS alert (catechol\_A) and one Brenk alert (catechol), which may be associated with assay interference and oxidative liability. The molecule violates one lead-likeness rule (XLOGP3>3.5). Its synthetic accessibility score of 4.88 and strong pharmacokinetic properties support its viability, and **the compound can be taken forward for molecular docking studies to assess its binding efficacy**, keeping in mind the need for potential optimization during lead refinement.

and oxidative liability. The molecule violates one lead-likeness rule (XLOGP3>3.5). Its synthetic accessibility score of 4.88 and strong pharmacokinetic properties support its viability, and **the compound can be taken forward for molecular docking studies to assess its binding efficacy**, keeping in mind the need for potential optimization during lead refinement.

### CHEMBL519970:

### (1R,10S)-3,4-dihydroxy-11,11-dimethyl-5-propan-2-yl-16-

### oxatetracyclo[6.6.2.01,10.02,7]hexadeca-2,4,6-trien-15-one

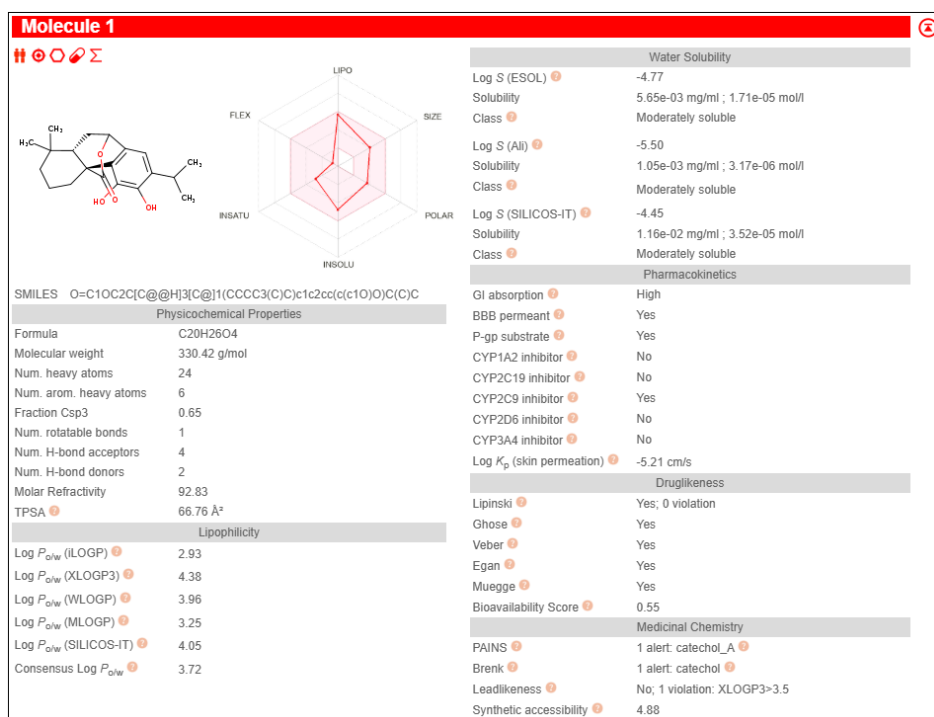


Figure 45: ADME Analysis from CHEMBL519970

The molecule ( $C_{20}H_{26}O_4$ ) exhibits a generally favorable ADME and drug-likeness profile, with some minor cautionary medicinal chemistry alerts. With a molecular weight of 330.42 g/mol and a consensus Log P of 3.72, it shows suitable lipophilicity and is highly polar, which may contribute to its solubility. The compound demonstrates high gastrointestinal absorption and is blood-brain barrier permeable, and it is also a P-glycoprotein substrate. It does not inhibit major CYP enzymes like CYP1A2, CYP2C19, or CYP2D6, but it does inhibit CYP2C9 and CYP3A4, which may raise concerns for drug-drug interactions. Its water solubility is moderately soluble across all models (Log S: -4.77 to -4.45), and it exhibits very low skin permeability (Log K<sub>p</sub>: -5.21 cm/s). The molecule passes all major drug-likeness filters (Lipinski, Ghose, Veber, Egan, Muegge) and has a bioavailability score of 0.55, suggesting reasonable oral bioavailability. However, it triggers one PAINS alert (catechol\_A) and one Brenk alert (catechol), which may be associated with assay interference and oxidative liability. The molecule violates one lead-likeness rule (XLOGP3>3.5). Its synthetic accessibility score of 4.88 and strong pharmacokinetic properties support its viability, and **the compound can be taken forward for molecular docking studies to assess its binding efficacy**, keeping in mind the need for potential optimization during lead refinement.

Table 6: Compounds selected for further analysis by docking

Primary Ligands		
Ligand	PubChem CID	Docking Consideration
1,8-naphthyridine-3-carboxamide	23435869	Considered for further docking

Carnosic Acid	65126	Considered for further docking
Carnosol	442009	Considered for further docking
Secondary Ligands: 1,8-naphthyridine-3-carboxamide		
Quinoline-3-carboxamide	15561101	Considered for further docking
Secondary Ligands: Carnosic Acid		
CHEMBL4868012	101371515	Considered for further docking
CHEMBL1096627	9974918	Considered for further docking
CHEMBL4471445	155535100	Considered for further docking
CHEMBL2333537	11336941	Considered for further docking
CHEMBL4519804	155542101	Considered for further docking
CHEMBL4515503	155539703	Considered for further docking
CHEMBL4574206	155563682	Considered for further docking
CHEMBL4451825	155521642	Considered for further docking
CHEMBL4471914	155535609	Considered for further docking
CHEMBL4447764	155519974	Cannot be considered for further docking
CHEMBL4468065	155532943	Considered for further docking
CHEMBL221380	16663298	Cannot be considered for further docking
CHEMBL2376099	71712255	Considered for further docking
CHEMBL4447390	155518823	Cannot be considered for further docking
CHEMBL479111	13654835	Considered for further docking
CHEMBL4576693	15602222	Considered for further docking
CHEMBL4544242	155552286	Cannot be considered for further docking
CHEMBL4436108	155511438	Cannot be considered for further docking
CHEMBL2374044	16758167	Considered for further docking
CHEMBL5407683	455260	Considered for further docking
Secondary Ligands: Carnosol		
CHEMBL483017	10215621	Consider for further docking
CHEMBL491307	44566424	Consider for further docking
CHEMBL478933		Cannot be considered for further docking
CHEMBL1079367	636675	Consider for further docking
CHEMBL2376097	23243694	Consider for further docking
CHEMBL2333536	13820510	Consider for further docking
CHEMBL507166	13966122	Consider for further docking
CHEMBL494659	13820511	Consider for further docking
CHEMBL1081338	46883406	Consider for further docking

CHEMBL464376	23243692	Consider for further docking
CHEMBL4544522	13855852	Consider for further docking
CHEMBL491879	13855851	Consider for further docking
CHEMBL1514916	455264	Consider for further docking
CHEMBL519970	65158	Consider for further docking

## Protein Preparation and Active Site Preparation

The goal of protein preparation is to generate protein models that accurately represent the bioactive conformations of the protein when ligands are bound. This ensures that computational studies, such as molecular docking or virtual screening, are based on realistic and biologically relevant structures, increasing the reliability of predictions.

The crystal structure of the QacA protein was obtained from the Protein Data Bank, under the ID **7Y58**. This structure was selected as the target model for molecular docking research because it accurately represents the active conformation of QacA, an antibacterial efflux protein involved in multidrug resistance. The structure provides a reliable framework for assessing ligand binding interactions within the active site, facilitating structure-based drug design approaches to identify potential inhibitors in the context of antibacterial resistance.

As there were no ligands or water molecules in association with the structure, no cleaning was required.

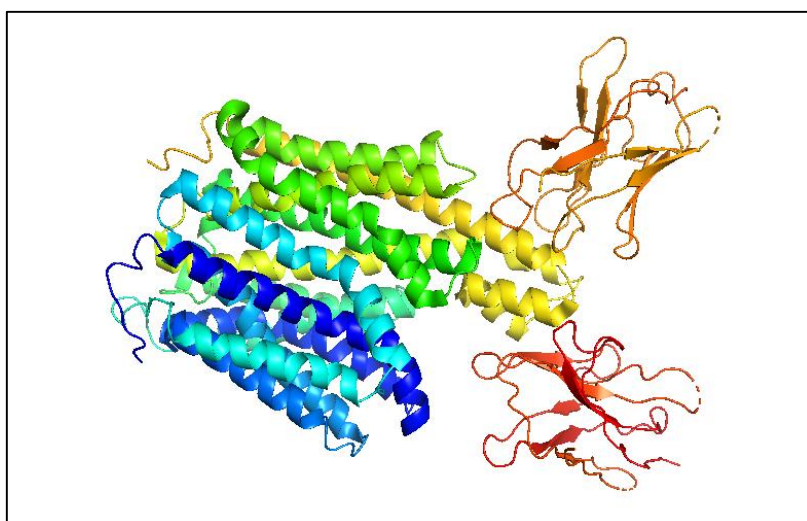


Figure 46: 3-Dimensional Structure of the QacA Protein

### Active Site Prediction

Active site prediction is the process of determining the regions of a protein or enzyme where ligands (such as substrates, inhibitors, or medicines) are most likely to interact. This stage is critical in drug discovery and structure-based drug design because it allows researchers to concentrate on biologically important locations for molecular docking, virtual screening, and rational drug design.

Active site prediction was done using DogSiteScorer (<https://proteins.plus/help/dogsites>) and the following binding sites were obtained:

Name	Volume Å³	Surface Å²
P_0	1069.68	1123.84
P_1	878.45	1339.77
P_10	229.81	378.98
P_11	207.82	352.05
P_12	207.41	420.03
P_13	197.87	390.17
P_14	197.32	199.51

P_15	192.75	359.68
P_16	187.36	283.51
P_17	157.22	200.65
P_18	150.03	249.11
P_19	141.18	332.34
P_2	813.88	1125.52
P_20	130.12	214.00
P_21	129.98	183.92
P_22	118.78	291.48
P_23	111.72	143.20
P_24	106.75	273.46
P_25	102.74	267.52
P_26	100.39	348.81
P_3	386.34	687.40
P_4	378.32	626.95
P_5	354.67	408.86
P_6	345.13	478.03
P_7	290.10	415.79
P_8	274.75	258.72
P_9	238.94	438.96

Table 7: Active Sites Predicted in QacA Efflux Protein



Figure 47: Binding Site with the Highest Surface Area (P\_0)

The residues included in the binding site: LEU28A, VAL31A, THR32A, MET33A, ASP34A, MET35A, THR36A, ILE39A, MET40A, TYR63A, SER64A, LEU67A, ALA68A, PHE94A, LEU117A, GLY118A, ALA120A, ILE124A, MET125A, PRO126A, THR128A, LEU129A, TRP149A, SER153A, ALA157A, PRO161A, VAL224A, LYS228A, MET278A, MET290A, ALA291A, LEU294A, LEU295A, SER298A, GLN302A, PRO309A, ALA312A, GLY313A, LEU316A, GLU407A, TYR410A, ASN411A, ASN414A, VAL415A and VAL418A.

## Grid Box Setting and Molecular Docking

### Grid Box Setting

Molecular docking is a computational technique used to predict the preferred orientation and binding affinity of one molecule (typically a small molecule ligand) when it interacts with a target molecule (often a protein or nucleic acid), forming a stable complex. This process is fundamental in structural molecular biology and plays a pivotal role in computer-assisted drug design.

The grid box setting process in molecular docking defines the three-dimensional region of the protein where the docking simulation will search for potential ligand binding poses. This involves specifying the center coordinates (x, y, z) and the size (number of points or length in each dimension) of the box, typically using graphical tools like AutoDock Tools or Chimera. The grid box should be large enough to encompass the entire active site or binding pocket, allowing the ligand to explore all relevant conformations, but not so large that it includes irrelevant regions, which could decrease docking accuracy and efficiency.

The docking process was conducted using PyRx 0.8. The grid box was set around the complete protein, to allow for multiple binding sites.

Figure 48: Grid Box Setting

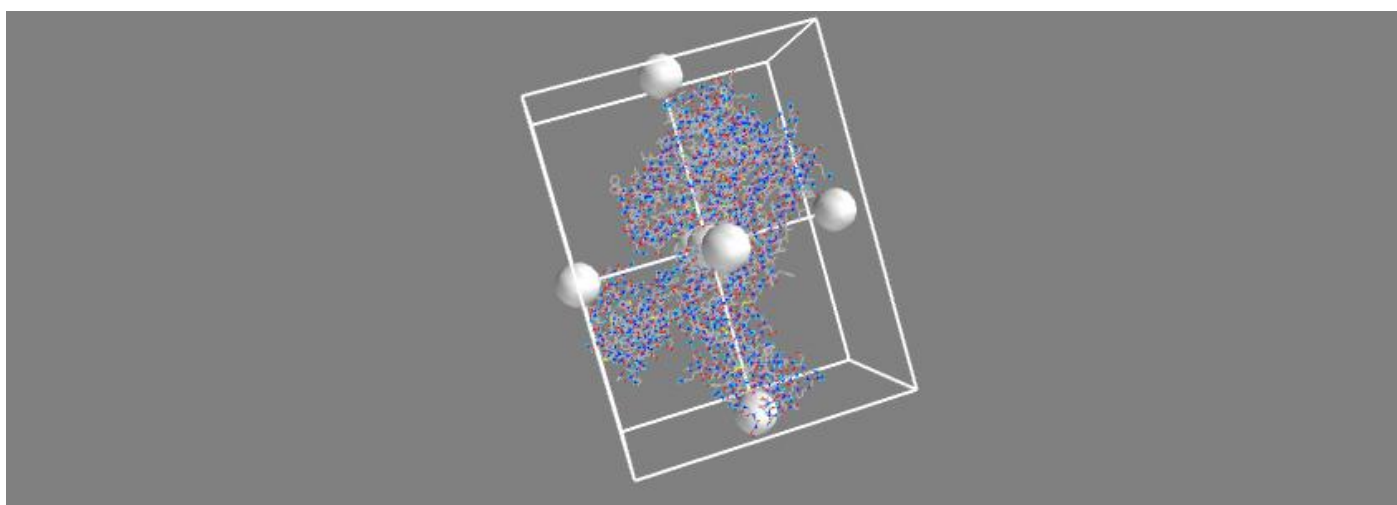


Table 8: Grid Box Conformations

Parameter	Value
center_x	148.907
center_y	153.4343
center_z	155.899
size_x	62.7674791718
size_y	80.825794754
size_z	104.400856247

## Docking Results

### Primary Ligands Docking Results

Table 9: Docking Results – 1,8-Naphthyridine-3-Carboxamide

Ligand	Binding Affinity	rmsd/ub	rmsd/lb
qac_a_23435869_uff_E=119.30_uff_E=119.21	-6.7	0	0
qac_a_23435869_uff_E=119.30_uff_E=119.21	-6.3	5.048	3.162
qac_a_23435869_uff_E=119.30_uff_E=119.21	-5.9	33.789	31.645
qac_a_23435869_uff_E=119.30_uff_E=119.21	-5.8	28.45	26.408
qac_a_23435869_uff_E=119.30_uff_E=119.21	-5.8	36.575	34.096
qac_a_23435869_uff_E=119.30_uff_E=119.21	-5.7	39.151	36.536
qac_a_23435869_uff_E=119.30_uff_E=119.21	-5.7	62.203	60.001
qac_a_23435869_uff_E=119.30_uff_E=119.21	-5.6	31.859	29.915
qac_a_23435869_uff_E=119.30_uff_E=119.21	-5.5	63.468	61.359

Naphthyridine-3-carboxamide exhibits a top-ranked binding pose with a strong affinity of -6.7 kcal/mol and an RMSD of 0, indicating a stable and well-aligned interaction with the target site. The second pose, with a slightly weaker affinity (-6.3 kcal/mol) and moderate RMSD (~5 Å), may represent an alternate binding mode worth evaluating for flexibility or induced-fit effects. However, subsequent poses show very high RMSD values (>25 Å) and diminished affinities, suggesting non-specific or irrelevant binding modes unlikely to contribute to therapeutic activity. For lead optimization or hit selection, only the top one or two poses should be prioritized for further structural refinement and validation.

Table 10: Docking Results of Carnosic Acid

Ligand	Binding Affinity	rmsd/ub	rmsd/lb
qac_a_65126_uff_E=468.40	-7.4	0	0
qac_a_65126_uff_E=468.40	-6.8	33.762	30.631
qac_a_65126_uff_E=468.40	-6.7	29.148	27.728
qac_a_65126_uff_E=468.40	-6.6	8.106	3.953
qac_a_65126_uff_E=468.40	-6.4	41.995	38.583
qac_a_65126_uff_E=468.40	-6.4	35.59	32.736
qac_a_65126_uff_E=468.40	-6.3	2.856	2.002
qac_a_65126_uff_E=468.40	-6.2	40.582	37.823
qac_a_65126_uff_E=468.40	-6.1	31.113	28.719

Carnosic acid shows a promising top binding pose with a strong affinity of -7.4 kcal/mol and an RMSD of 0, making it the reference conformation. Two other poses, with affinities of -6.6 and -6.3 kcal/mol and RMSDs of ~4 Å and ~2 Å respectively, may represent biologically relevant alternate binding modes, potentially useful for understanding conformational flexibility. The remaining poses exhibit much higher RMSD values (above 27 Å) and weaker affinities, indicating likely non-specific or unstable interactions. For downstream lead development, only the top three poses merit consideration for detailed structural and pharmacophore analysis.

Table 11: Docking Results – Carnosol

Ligand	Binding Affinity	rmsd/ub	rmsd/lb
qac_a_442009_uff_E=653.04	-8.5	0	0
qac_a_442009_uff_E=653.04	-7.3	21.247	18.94
qac_a_442009_uff_E=653.04	-6.8	11.371	7.702
qac_a_442009_uff_E=653.04	-6.7	11.621	8.388
qac_a_442009_uff_E=653.04	-6.6	13.406	10.373
qac_a_442009_uff_E=653.04	-6.5	22.421	19.73
qac_a_442009_uff_E=653.04	-6.5	45.396	42.923
qac_a_442009_uff_E=653.04	-6.5	44.457	41.546
qac_a_442009_uff_E=653.04	-6.5	22.449	20.362

Carnosol displays a highly favorable top binding pose with a strong affinity of -8.5 kcal/mol and an RMSD of 0, marking it as the most stable and relevant conformation. A few alternate poses with moderately lower affinities (-6.8 to -6.5 kcal/mol) and RMSDs in the 7–13 Å range may indicate flexible binding but are generally considered too divergent to be biologically meaningful. Several other poses exhibit very high RMSD values (over 20 Å), suggesting they represent non-specific or artifactual interactions. Therefore, only the top pose should be prioritized for further validation, while the rest are likely not relevant for hit optimization.

### Secondary Ligands of Carnosic Acid

Table 12 – Docking Results: CHEMBL479111: O-methylpisiferic acid

Ligand	Binding Affinity	rmsd/ub	rmsd/lb
qac_a_13654835_uff_E=506.73	-7.2	0	0
qac_a_13654835_uff_E=506.73	-7.1	28.447	24.857
qac_a_13654835_uff_E=506.73	-7	35.254	30.696
qac_a_13654835_uff_E=506.73	-7	7.868	3.67
qac_a_13654835_uff_E=506.73	-6.9	28.444	26.808
qac_a_13654835_uff_E=506.73	-6.8	26.06	21.468
qac_a_13654835_uff_E=506.73	-6.8	22.77	19.251
qac_a_13654835_uff_E=506.73	-6.7	39.522	36.653
qac_a_13654835_uff_E=506.73	-6.6	35.213	31.729

O-methylpisiferic acid displays a highly favorable top binding pose with a strong affinity of -8.5 kcal/mol and an RMSD of 0, marking it as the most stable and relevant conformation. A few alternate poses with moderately lower affinities (-6.8 to -6.5 kcal/mol) and RMSDs in the 7–13 Å range may indicate flexible binding but are generally considered too divergent to be biologically meaningful. Several other poses exhibit very high RMSD values (over 20 Å), suggesting they represent non-specific or artifactual interactions. Therefore, only the top pose should be prioritized for further validation, while the rest are likely not relevant for hit optimization.

Table 13: Docking Results: CHEMBL1096627 – 12-O-Methylcarnosic Acid

Ligand	Binding Affinity	rmsd/ub	rmsd/lb
qac_a_9974918_uff_E=529.05	-6.9	0	0
qac_a_9974918_uff_E=529.05	-6.7	29.417	27.179

qac_a_9974918_uff_E=529.05	-6.7	8.311	4.308
qac_a_9974918_uff_E=529.05	-6.7	23.44	20.86
qac_a_9974918_uff_E=529.05	-6.6	33.681	29.785
qac_a_9974918_uff_E=529.05	-6.5	23.729	18.937
qac_a_9974918_uff_E=529.05	-6.3	26.877	22.033
qac_a_9974918_uff_E=529.05	-6.2	12.625	8.984
qac_a_9974918_uff_E=529.05	-6.2	29.29	27.135

12-O-methylcarnosic acid demonstrates a best binding pose with an affinity of -6.9 kcal/mol and RMSD of 0, establishing it as the most stable and reliable docking conformation. One alternate pose with -6.7 kcal/mol affinity and a moderate RMSD (~4–8 Å) could reflect some degree of flexibility, though still slightly outside the ideal threshold for reliable binding modes. Most other poses show high RMSD values (above 20 Å), indicating substantial deviations from the reference pose and suggesting non-specific or energetically unfavorable interactions. Therefore, only the top pose—and possibly the moderately deviated one—are of interest for further structural and pharmacological evaluation.

Table 14: Docking Results – CHEMBL2333537: Methyl carnosate

Ligand	Binding Affinity	rmsd/ub	rmsd/lb
qac_a_11336941_uff_E=689.97	-8.6	0	0
qac_a_11336941_uff_E=689.97	-7.9	19.56	18.074
qac_a_11336941_uff_E=689.97	-7.8	28.538	24.027
qac_a_11336941_uff_E=689.97	-7.8	17.348	15.478
qac_a_11336941_uff_E=689.97	-7.7	14.009	9.723
qac_a_11336941_uff_E=689.97	-7.7	42.338	38.883
qac_a_11336941_uff_E=689.97	-7.6	14.842	10.226
qac_a_11336941_uff_E=689.97	-7.6	18.221	17.193
qac_a_11336941_uff_E=689.97	-7.4	24.649	21.801

Methyl carnosate exhibits a highly favorable top binding pose with an affinity of -8.6 kcal/mol and RMSD of 0, indicating a strong and well-defined interaction with the target site. Several alternate poses show moderately high binding affinities (-7.9 to -7.4 kcal/mol) but have RMSDs ranging from ~10 Å to over 28 Å, suggesting significant structural deviations from the reference. While these poses may reflect some degree of conformational flexibility, their high RMSDs reduce their biological relevance. As a result, only the top pose should be considered reliable for downstream structure-based optimization and hit validation.

Table 15: Docking Results – CHEMBL2374044

Ligand	Binding Affinity	rmsd/ub	rmsd/lb
qac_a_16758167_uff_E=329.45	-7.3	0	0
qac_a_16758167_uff_E=329.45	-6.8	21.484	18.978
qac_a_16758167_uff_E=329.45	-6.8	24.344	22.426
qac_a_16758167_uff_E=329.45	-6.8	23.677	21.135
qac_a_16758167_uff_E=329.45	-6.7	18.585	16.51
qac_a_16758167_uff_E=329.45	-6.7	38.327	34.654
qac_a_16758167_uff_E=329.45	-6.5	40.085	37.092
qac_a_16758167_uff_E=329.45	-6.5	8.479	4.493
qac_a_16758167_uff_E=329.45	-6.4	4.123	2.437

CHEMBL2374044 shows a strong top binding pose with an affinity of -7.3 kcal/mol and RMSD of 0, making it the most stable and relevant conformation. Two other poses with affinities of -6.4 and -6.5 kcal/mol and low RMSDs (~2–4 Å) may represent alternate but biologically plausible binding modes, useful for understanding flexibility or induced-fit effects. The remaining poses, despite having similar binding energies, exhibit high RMSDs (16–40 Å), suggesting non-specific or unstable interactions. Therefore, only the top three poses should be considered for further structure-based analysis and lead optimization.

Table 16: Docking Results – CHEMBL2376099 – Carnosaldehyde

Ligand	Binding Affinity	rmsd/ub	rmsd/lb
qac_a_71712255_uff_E=471.71	-7.3	0	0
qac_a_71712255_uff_E=471.71	-7.1	29.006	27.587
qac_a_71712255_uff_E=471.71	-7	7.821	5.136
qac_a_71712255_uff_E=471.71	-6.8	33.767	30.367
qac_a_71712255_uff_E=471.71	-6.7	8.281	4.099
qac_a_71712255_uff_E=471.71	-6.7	35.229	32.263
qac_a_71712255_uff_E=471.71	-6.4	34.887	32.158
qac_a_71712255_uff_E=471.71	-6.2	18.384	16.103
qac_a_71712255_uff_E=471.71	-6.2	23.539	20.365

CHEMBL2376099 exhibits a favorable top binding pose with an affinity of -7.3 kcal/mol and RMSD of 0, making it the most stable and relevant conformation. Two alternate poses with slightly lower affinities (-7.0 and -6.7 kcal/mol) and moderate RMSDs (~4–8 Å) may indicate some conformational flexibility, though they border on the threshold of structural reliability. The remaining poses, despite similar binding energies, show high RMSD values (>16 Å), suggesting non-specific or energetically unfavorable interactions. Overall, only the top pose and possibly two moderately deviated poses are worth considering for further structural evaluation and lead refinement.

Table 17: Docking Results: CHEMBL4436108

Ligand	Binding Affinity	rmsd/ub	rmsd/lb
qac_a_155511438_uff_E=428.22	-7.2	0	0
qac_a_155511438_uff_E=428.22	-7.1	50.894	48.422
qac_a_155511438_uff_E=428.22	-7.1	56.156	54.554
qac_a_155511438_uff_E=428.22	-7	56.938	55.419
qac_a_155511438_uff_E=428.22	-7	44.964	41.646
qac_a_155511438_uff_E=428.22	-6.9	56.271	54.677
qac_a_155511438_uff_E=428.22	-6.9	39.119	36.207
qac_a_155511438_uff_E=428.22	-6.9	45.859	43.171
qac_a_155511438_uff_E=428.22	-6.8	31.294	28.837

CHEMBL4436108 demonstrates a strong top binding pose with an affinity of -7.2 kcal/mol and RMSD of 0, making it the most reliable and structurally stable conformation. Although other poses have similar binding affinities (-7.1 to -6.8 kcal/mol), they exhibit extremely high RMSD values (>28 Å), indicating large deviations and likely non-specific or irrelevant binding. These alternative poses are not structurally consistent with the

top pose and are unlikely to represent biologically meaningful interactions. As such, only the top-ranked pose is suitable for further consideration in structure-based drug design.

Table 18: Docking Results: CHEMBL4451825

Ligand	Binding Affinity	rmsd/ub	rmsd/lb
qac_a_155521642_uff_E=557.43	-8	0	0
qac_a_155521642_uff_E=557.43	-8	59.84	55.74
qac_a_155521642_uff_E=557.43	-7.8	55.298	53.368
qac_a_155521642_uff_E=557.43	-7.5	44.232	41.359
qac_a_155521642_uff_E=557.43	-7.4	32.37	29.151
qac_a_155521642_uff_E=557.43	-7.3	30.045	26.798
qac_a_155521642_uff_E=557.43	-7.1	50.655	46.885
qac_a_155521642_uff_E=557.43	-7.1	45.722	43.294
qac_a_155521642_uff_E=557.43	-7	30.047	26.362

CHEMBL4451825 shows a highly favorable top binding pose with a binding affinity of -8.0 kcal/mol and an RMSD of 0, indicating a stable and well-aligned interaction with the target. Although several other poses exhibit comparable binding affinities (-7.8 to -7.0 kcal/mol), they all show extremely high RMSD values (>26 Å), suggesting major conformational differences and likely non-specific or irrelevant binding. These high deviations diminish their biological relevance and reliability for structure-based optimization. Thus, only the top-ranked pose is suitable for further consideration in lead development or pharmacophore modeling.

Table 19: Docking Results: CHEMBL4468065

Ligand	Binding Affinity	rmsd/ub	rmsd/lb
qac_a_155532943_uff_E=441.09	-6.8	0	0
qac_a_155532943_uff_E=441.09	-6.8	60.387	57.026
qac_a_155532943_uff_E=441.09	-6.7	45.994	44.04
qac_a_155532943_uff_E=441.09	-6.7	38.385	35.222
qac_a_155532943_uff_E=441.09	-6.5	61.613	58.281
qac_a_155532943_uff_E=441.09	-6.4	46.154	44.121
qac_a_155532943_uff_E=441.09	-6.2	46.464	43.757
qac_a_155532943_uff_E=441.09	-6.1	53.682	51.653
qac_a_155532943_uff_E=441.09	-6.1	38.424	35.309

CHEMBL4468065 displays a top binding pose with an affinity of -6.8 kcal/mol and RMSD of 0, indicating a stable and structurally reliable interaction with the target. While several other poses have similar binding affinities (-6.8 to -6.1 kcal/mol), all of them show very high RMSD values (35–61 Å), reflecting substantial conformational divergence from the top pose. These large deviations suggest non-specific or energetically unfavorable binding modes that are unlikely to be biologically meaningful. Therefore, only the top-ranked pose should be considered valid for downstream optimization and structure-based design.

Table 20: Docking Results – CHEMBL4471445

Ligand	Binding Affinity	rmsd/ub	rmsd/lb
qac_a_155535100_uff_E=518.38	-7	0	0
qac_a_155535100_uff_E=518.38	-7	16.855	14.298
qac_a_155535100_uff_E=518.38	-6.8	46.494	44.681

qac_a_155535100_uff_E=518.38	-6.7	57.283	55.42
qac_a_155535100_uff_E=518.38	-6.7	37.22	34.207
qac_a_155535100_uff_E=518.38	-6.5	15.787	13.977
qac_a_155535100_uff_E=518.38	-6.4	45.038	42.849
qac_a_155535100_uff_E=518.38	-6.4	14.627	12.984
qac_a_155535100_uff_E=518.38	-6.3	36.706	33.531

CHEMBL4471445 exhibits a stable top binding pose with a binding affinity of -7.0 kcal/mol and an RMSD of 0, marking it as the most reliable conformation. A few alternate poses with slightly lower affinities (-6.4 to -6.8 kcal/mol) and moderate RMSDs (~13–17 Å) suggest potential conformational flexibility but are on the upper edge of what's typically considered biologically relevant. Several other poses show very high RMSD values (>30 Å), indicating likely non-specific or unstable interactions. Therefore, only the top pose, along with one or two moderately deviated poses, may be useful for further structural analysis or refinement.

Table 21: Docking Results – CHEMBL4471914

Ligand	Binding Affinity	rmsd/ub	rmsd/lb
qac_a_155535609_uff_E=406.55	-6.5	0	0
qac_a_155535609_uff_E=406.55	-6.5	61.925	58.487
qac_a_155535609_uff_E=406.55	-6.4	45.846	43.804
qac_a_155535609_uff_E=406.55	-6.3	61.724	58.549
qac_a_155535609_uff_E=406.55	-6	75.123	71.852
qac_a_155535609_uff_E=406.55	-5.9	46.103	44.021
qac_a_155535609_uff_E=406.55	-5.9	61.287	57.988
qac_a_155535609_uff_E=406.55	-5.9	36.676	34.746
qac_a_155535609_uff_E=406.55	-5.8	30.591	28.679

CHEMBL4471914 shows a best binding pose with an affinity of -6.5 kcal/mol and an RMSD of 0, making it the most stable and relevant conformation. Although some alternate poses have comparable binding affinities (-6.4 to -5.8 kcal/mol), they all exhibit very high RMSD values (29–75 Å), indicating large deviations from the reference pose and suggesting non-specific or artifactual binding. These alternative conformations are unlikely to be biologically meaningful due to their poor structural alignment. Consequently, only the top pose should be considered for downstream structure-based drug design or lead optimization efforts.

Table 22: Docking Results - CHEMBL4515503

Ligand	Binding Affinity	rmsd/ub	rmsd/lb
qac_a_155539703_uff_E=413.03	-7.2	0	0
qac_a_155539703_uff_E=413.03	-7.2	29.374	25.569
qac_a_155539703_uff_E=413.03	-7.1	16.496	13.735
qac_a_155539703_uff_E=413.03	-7.1	44.034	42.574
qac_a_155539703_uff_E=413.03	-7.1	26.841	23.278
qac_a_155539703_uff_E=413.03	-7	50.187	48.218
qac_a_155539703_uff_E=413.03	-7	23.542	21.323
qac_a_155539703_uff_E=413.03	-6.9	27.864	25.629
qac_a_155539703_uff_E=413.03	-6.9	29.395	25.852

CHEMBL4515503 presents a strong top binding pose with an affinity of -7.2 kcal/mol and RMSD of 0, indicating a stable and specific interaction with the target. A few alternate poses with similar binding affinities (-7.2 to -7.0 kcal/mol) and moderate RMSDs (~13–16 Å) suggest some degree of flexibility, though their biological relevance is limited due to structural deviation. The remaining poses exhibit higher RMSDs (>20 Å), indicating significant conformational drift and likely non-specific binding modes. Thus, only the top pose—and at most one moderately deviated pose—should be considered for further structure-based drug design.

Table 23: Docking Results - CHEMBL4519804

Ligand	Binding Affinity	rmsd/ub	rmsd/lb
qac_a_155542101_uff_E=518.72	-7	0	0
qac_a_155542101_uff_E=518.72	-7	30.949	28.393
qac_a_155542101_uff_E=518.72	-6.9	56.801	54.911
qac_a_155542101_uff_E=518.72	-6.9	27.522	24.272
qac_a_155542101_uff_E=518.72	-6.8	43.399	41.154
qac_a_155542101_uff_E=518.72	-6.8	36.278	34.12
qac_a_155542101_uff_E=518.72	-6.7	42.377	38.303
qac_a_155542101_uff_E=518.72	-6.7	69.746	66.679
qac_a_155542101_uff_E=518.72	-6.7	39.721	36.181

CHEMBL4519804 shows a top binding pose with an affinity of -7.0 kcal/mol and RMSD of 0, indicating a stable and well-aligned conformation suitable for further evaluation. Although other poses have similar binding affinities (-6.9 to -6.7 kcal/mol), they exhibit high RMSD values (24–69 Å), reflecting substantial conformational deviations from the reference pose. These deviations suggest non-specific binding or unstable alternative orientations that are unlikely to be biologically relevant. Therefore, only the top pose should be considered for structure-based lead development and downstream optimization.

Table 24: Docking Results - CHEMBL4574206

Ligand	Binding Affinity	rmsd/ub	rmsd/lb
qac_a_155563682_uff_E=423.90	-7.1	0	0
qac_a_155563682_uff_E=423.90	-7.1	38.291	35.21
qac_a_155563682_uff_E=423.90	-7.1	60.347	56.925
qac_a_155563682_uff_E=423.90	-7	38.567	35.324
qac_a_155563682_uff_E=423.90	-6.9	61.783	58.32
qac_a_155563682_uff_E=423.90	-6.9	46.004	43.939
qac_a_155563682_uff_E=423.90	-6.9	51.751	50.255
qac_a_155563682_uff_E=423.90	-6.9	61.861	58.458
qac_a_155563682_uff_E=423.90	-6.8	45.277	42.423

CHEMBL4574206 demonstrates a top-ranked binding pose with a docking score of -7.1 kcal/mol and RMSD of 0, indicating a well-aligned and stable interaction with the target binding site. This pose serves as the reference conformation for further structure-based analysis. Although multiple other poses share the same binding affinity (up to -7.1 kcal/mol), they exhibit high RMSD values (35–60 Å), indicating substantial structural divergence from the reference pose. These alternative poses likely represent non-specific or less relevant interactions and should not be prioritized for lead optimization.

Table 25: Docking Results - CHEMBL4868012

Ligand	Binding Affinity	rmsd/ub	rmsd/lb
qac_a_101371515_uff_E=452.36	-7.2	0	0
qac_a_101371515_uff_E=452.36	-7.1	31.923	29.667
qac_a_101371515_uff_E=452.36	-6.8	10.584	7.376
qac_a_101371515_uff_E=452.36	-6.6	29.371	26.116
qac_a_101371515_uff_E=452.36	-6.5	27.322	24.655
qac_a_101371515_uff_E=452.36	-6.5	38.686	35.527
qac_a_101371515_uff_E=452.36	-6.5	42.36	39.389
qac_a_101371515_uff_E=452.36	-6.3	32.915	30.253
qac_a_101371515_uff_E=452.36	-6.3	21.879	17.872

CHEMBL4868012 presents a best binding pose with a docking score of -7.2 kcal/mol and RMSD of 0, indicating a highly stable and specific interaction with the target site. A slightly weaker pose at -6.8 kcal/mol shows moderate deviation (RMSD ~7.4 Å), which may still hold relevance depending on the binding pocket's flexibility. However, the remaining poses—with scores from -7.1 to -6.3 kcal/mol—exhibit very high RMSD values (17–39 Å), suggesting they deviate substantially from the optimal conformation and are likely non-specific. Therefore, only the top pose should be retained for detailed interaction analysis, hit-to-lead progression, and potential experimental validation.

Table 26: Docking Results - CHEMBL5407683

Ligand	Binding Affinity	rmsd/ub	rmsd/lb
qac_a_455260_uff_E=337.63	-6.9	0	0
qac_a_455260_uff_E=337.63	-6.4	50.837	49.341
qac_a_455260_uff_E=337.63	-6.4	49.18	46.884
qac_a_455260_uff_E=337.63	-6.3	45.585	42.845
qac_a_455260_uff_E=337.63	-6.3	55.653	53.399
qac_a_455260_uff_E=337.63	-6.3	30.075	28.373
qac_a_455260_uff_E=337.63	-6.2	21.603	18.982
qac_a_455260_uff_E=337.63	-6.2	26.585	24.29
qac_a_455260_uff_E=337.63	-6.2	53.582	51.168

CHEMBL5407683 demonstrates a most favorable binding pose with a docking score of -6.9 kcal/mol and an RMSD of 0, indicating a highly stable and well-aligned interaction with the target. All other poses show weaker affinities ranging from -6.4 to -6.2 kcal/mol, but more importantly, they exhibit extremely high RMSD values (19–53 Å), suggesting significant structural deviation and likely non-specific or unstable binding. These large RMSD values imply a loss of binding precision, reducing the reliability of these alternative poses. Thus, only the top-scoring pose should be considered for further in silico or experimental validation in the lead identification process.

#### Secondary Ligands: 1,8-Naphthyridine-3-Carboxamide

Table 27: Docking Results – Quinoline-3-Carboxamide

Ligand	Binding Affinity	rmsd/ub	rmsd/lb
qac_a_15561101_uff_E=120.29	-7	0	0
qac_a_15561101_uff_E=120.29	-6.3	5.302	3.043

qac_a_15561101_uff_E=120.29	-6.2	33.025	30.671
qac_a_15561101_uff_E=120.29	-6.2	36.797	34.555
qac_a_15561101_uff_E=120.29	-6	33.464	31.926
qac_a_15561101_uff_E=120.29	-5.9	33.159	31.579
qac_a_15561101_uff_E=120.29	-5.8	39.129	36.753
qac_a_15561101_uff_E=120.29	-5.8	34.86	34.063
qac_a_15561101_uff_E=120.29	-5.8	28.242	25.611

Quinoline-3-Carboxamide exhibits a strong and specific binding profile, with the top docking pose scoring -7.0 kcal/mol and showing no deviation (RMSD = 0), indicating a well-aligned and energetically favorable conformation. Subsequent poses display less favorable docking scores between -6.3 and -5.8 kcal/mol, with significantly higher RMSDs—most exceeding 30 Å—suggesting poor structural overlap and non-specific binding. Only one alternate pose at -6.3 kcal/mol has a moderately low RMSD (5.3 Å / 3.0 Å), possibly representing a minor conformational variant worth further inspection. Overall, the ligand demonstrates a clear preference for a single, specific binding mode, supporting its candidacy for further optimization in structure-based drug discovery.

### Secondary Ligands – Carnosol

Table 28: Docking Results - CHEMBL464376

Ligand	Binding Affinity	rmsd/ub	rmsd/lb
qac_a_23243692_uff_E=545.61	-7	0	0
qac_a_23243692_uff_E=545.61	-6.9	35.364	32.03
qac_a_23243692_uff_E=545.61	-6.8	33.744	30.304
qac_a_23243692_uff_E=545.61	-6.7	69.253	66.987
qac_a_23243692_uff_E=545.61	-6.7	38.561	35.181
qac_a_23243692_uff_E=545.61	-6.7	46.484	43.753
qac_a_23243692_uff_E=545.61	-6.6	62.2	60.248
qac_a_23243692_uff_E=545.61	-6.5	46.147	44.142
qac_a_23243692_uff_E=545.61	-6.5	38.95	35.367

The ligand CHEMBL464576 displays a distinct and energetically favorable top docking pose with a score of -7.0 kcal/mol and no structural deviation (RMSD = 0), signifying a highly specific and stable binding conformation. All subsequent poses show lower binding affinities ranging from -6.9 to -6.5 kcal/mol, with notably high RMSD values (30–70 Å), indicating divergent and likely non-relevant binding orientations. The absence of low-RMSD alternatives suggests that the ligand adopts a singular, preferred pose when engaging with the target. This level of specificity makes it a promising candidate for structure-guided drug design, particularly for hit-to-lead optimization stages.

Table 29: Docking Results - CHEMBL483017

Ligand	Binding Affinity	rmsd/ub	rmsd/lb
qac_a_10215621_uff_E=647.14	-8	0	0
qac_a_10215621_uff_E=647.14	-7.5	2.336	1.837
qac_a_10215621_uff_E=647.14	-7	4.065	2.092
qac_a_10215621_uff_E=647.14	-6.8	41.772	38.533
qac_a_10215621_uff_E=647.14	-6.8	42.598	38.058

qac_a_10215621_uff_E=647.14	-6.8	29.954	27.35
qac_a_10215621_uff_E=647.14	-6.6	43.643	41.35
qac_a_10215621_uff_E=647.14	-6.6	11.381	8.068
qac_a_10215621_uff_E=647.14	-6.4	15.974	13.015

CHEMBL483017 exhibits a strong top-ranked docking pose with a score of -8.0 kcal/mol and an RMSD of 0, indicating a highly stable and definitive binding orientation. Its next two poses, at -7.5 and -7.0 kcal/mol, show minimal RMSD values (under 4 Å), suggesting that the ligand can adopt a consistent binding mode with slight flexibility. However, lower-ranked poses beyond -6.8 kcal/mol demonstrate a dramatic increase in RMSD (up to 43 Å), highlighting spatial divergence and reduced biological plausibility. This clear energy–conformation clustering pattern supports the ligand’s potential as a structurally stable and potent binder in rational drug design.

Table 30: Docking Results – CHEMBL491307

Ligand	Binding Affinity	rmsd/ub	rmsd/lb
qac_a_44566424_uff_E=484.58	-8	0	0
qac_a_44566424_uff_E=484.58	-7.5	2.562	1.844
qac_a_44566424_uff_E=484.58	-7.1	43.969	40.532
qac_a_44566424_uff_E=484.58	-6.8	41.676	38.386
qac_a_44566424_uff_E=484.58	-6.7	45.065	42.648
qac_a_44566424_uff_E=484.58	-6.6	35.059	31.478
qac_a_44566424_uff_E=484.58	-6.6	39.029	35.971
qac_a_44566424_uff_E=484.58	-6.5	43.671	39.819
qac_a_44566424_uff_E=484.58	-6.5	12.873	9.591

CHEMBL491307 presents a strong and unambiguous top docking pose at -8.0 kcal/mol with 0 Å RMSD, indicating a well-defined and stable binding mode. The second-best pose at -7.5 kcal/mol remains closely aligned with minimal RMSD deviation, reinforcing conformational stability. However, subsequent poses from -7.1 kcal/mol onward show a sharp increase in RMSD values (up to ~45 Å), suggesting spatially distinct and less probable conformations. This clustering behavior supports the ligand’s candidacy in drug discovery, emphasizing a dominant binding conformation with high confidence.

Table 31: Docking Results – CHEMBL491879

Ligand	Binding Affinity	rmsd/ub	rmsd/lb
qac_a_13855851_uff_E=512.74	-6.9	0	0
qac_a_13855851_uff_E=512.74	-6.8	58.362	55.775
qac_a_13855851_uff_E=512.74	-6.6	35.04	33.163
qac_a_13855851_uff_E=512.74	-6.6	29.812	27.653
qac_a_13855851_uff_E=512.74	-6.6	32.463	30.163
qac_a_13855851_uff_E=512.74	-6.6	5.884	2.155
qac_a_13855851_uff_E=512.74	-6.6	61.46	59.855
qac_a_13855851_uff_E=512.74	-6.5	74.807	72.747
qac_a_13855851_uff_E=512.74	-6.5	57.411	55.572

CHEMBL491879 exhibits a best docking score of -6.9 kcal/mol with an RMSD of 0 Å, indicating a unique and well-defined top pose. However, all subsequent poses—even those with similar binding energies—display

significantly high RMSD values (ranging from ~5 to 75 Å), suggesting a lack of convergence in spatial orientation. The clustering is weak and diffuse, indicating poor conformational consistency despite modest binding affinities. From a drug discovery perspective, this undermines the reliability of the binding mode and reduces confidence in this ligand as a strong binder.

Table 32 – Docking Results: CHEMBL494659

Ligand	Binding Affinity	rmsd/ub	rmsd/lb
qac_a_13820511_uff_E=526.64	-7.9	0	0
qac_a_13820511_uff_E=526.64	-7.7	42.054	38.512
qac_a_13820511_uff_E=526.64	-6.9	27.645	24.11
qac_a_13820511_uff_E=526.64	-6.8	41.695	39.305
qac_a_13820511_uff_E=526.64	-6.7	12.628	9.395
qac_a_13820511_uff_E=526.64	-6.6	42.023	40.055
qac_a_13820511_uff_E=526.64	-6.6	35.608	31.582
qac_a_13820511_uff_E=526.64	-6.6	15.781	11.564
qac_a_13820511_uff_E=526.64	-6.6	14.011	10.129

CHEMBL494659 demonstrates a strong top docking score of -7.9 kcal/mol with a 0 Å RMSD, indicating a well-defined and energetically favorable binding pose. However, the spread of subsequent poses—characterized by high RMSD values (up to ~42 Å) and varied clustering—suggests a lack of consistent pose convergence. Even poses with similar docking scores (e.g., -6.6 to -6.9) show poor spatial agreement, pointing to conformational ambiguity. From a drug discovery standpoint, despite a promising binding energy, the weak clustering and inconsistent geometry lower the reliability of this compound's predicted binding mode.

Table 33 – Docking Results: CHEMBL507166

Ligand	Binding Affinity	rmsd/ub	rmsd/lb
qac_a_13966122_uff_E=514.97	-7.6	0	0
qac_a_13966122_uff_E=514.97	-7.4	20.068	18.016
qac_a_13966122_uff_E=514.97	-7.3	7.044	3.224
qac_a_13966122_uff_E=514.97	-7.1	27.863	24.552
qac_a_13966122_uff_E=514.97	-7.1	2.652	1.732
qac_a_13966122_uff_E=514.97	-7	16.598	12.847
qac_a_13966122_uff_E=514.97	-6.9	8.578	5.596
qac_a_13966122_uff_E=514.97	-6.9	14.84	11.039
qac_a_13966122_uff_E=514.97	-6.8	6.576	3.333

CHEMBL507166 exhibits a strong top docking score of -7.6 kcal/mol with an RMSD of 0 Å, indicating a distinct and energetically favorable pose. Moderate clustering is observed, with multiple near-optimal poses within 2–7 Å RMSD and similar binding energies (-7.4 to -6.8), suggesting some convergence in pose geometry. However, a few high-RMSD poses (up to ~28 Å) introduce uncertainty regarding binding consistency. In drug discovery terms, this ligand shows moderate reliability due to the presence of a clear top binder and a subset of geometrically similar alternatives, although broader pose variability may warrant further structural refinement.

Table 34 – Docking Results: CHEMBL519970

Ligand	Binding Affinity	rmsd/ub	rmsd/lb

qac_a_65158_uff_E=609.95	-8.4	0	0
qac_a_65158_uff_E=609.95	-7.5	2.964	2.121
qac_a_65158_uff_E=609.95	-7.3	21.102	18.794
qac_a_65158_uff_E=609.95	-7	22.567	20.249
qac_a_65158_uff_E=609.95	-6.9	41.801	38.475
qac_a_65158_uff_E=609.95	-6.9	12.62	9.549
qac_a_65158_uff_E=609.95	-6.9	43.482	40.292
qac_a_65158_uff_E=609.95	-6.9	32.036	30.261
qac_a_65158_uff_E=609.95	-6.8	11.464	7.772

CHEMBL519970 demonstrates a highly favorable top docking score of -8.4 kcal/mol with 0 Å RMSD, indicating a clear and distinct binding pose. A secondary pose at -7.5 kcal/mol shows minimal deviation (~2 Å), supporting pose reproducibility and potential stability. However, other poses deviate substantially (up to ~43 Å) with less favorable energies, suggesting conformational flexibility or alternate, less stable binding modes. In the context of drug discovery, this ligand is promising due to its strong and well-defined top pose, but further analysis may be needed to confirm binding site specificity and reduce off-target conformations.

Table 35: Docking Results – CHEMBL1079367

Ligand	Binding Affinity	rmsd/ub	rmsd/lb
qac_a_636675_uff_E=605.58	-8.5	0	0
qac_a_636675_uff_E=605.58	-7.6	25.559	23.61
qac_a_636675_uff_E=605.58	-7.6	43.704	40.363
qac_a_636675_uff_E=605.58	-7.5	25.937	23.749
qac_a_636675_uff_E=605.58	-7.5	31.604	30.183
qac_a_636675_uff_E=605.58	-7.4	14.198	10.65
qac_a_636675_uff_E=605.58	-7.4	7.189	4.687
qac_a_636675_uff_E=605.58	-7.3	12.966	9.283
qac_a_636675_uff_E=605.58	-7.2	26.935	23

CHEMBL1079367 shows a top docking score of -8.5 kcal/mol at 0 Å RMSD, indicating a highly favorable and unambiguous binding pose. While this primary pose suggests strong binding affinity, several alternative poses appear at higher energies (-7.6 to -7.2 kcal/mol) with large RMSDs (>20 Å), pointing to conformational flexibility and potentially nonspecific binding. A few intermediate RMSD values (e.g., 7–14 Å) exist, but are still significantly distant from the top pose, lacking tight clustering around a single mode. In a drug discovery context, this ligand presents an excellent lead candidate with strong affinity, though the wide pose spread warrants further validation for binding site selectivity.

Table 36 – Docking Results: CHEMBL1081338

Ligand	Binding Affinity	rmsd/ub	rmsd/lb
qac_a_46883406_uff_E=550.72	-7.1	0	0
qac_a_46883406_uff_E=550.72	-7.1	32.183	29.876
qac_a_46883406_uff_E=550.72	-7	22.685	19.702
qac_a_46883406_uff_E=550.72	-6.8	24.864	21.117
qac_a_46883406_uff_E=550.72	-6.7	39.611	38.014
qac_a_46883406_uff_E=550.72	-6.7	36.664	34.068
qac_a_46883406_uff_E=550.72	-6.6	30.05	27.763

qac_a_46883406_uff_E=550.72	-6.6	37.459	35.013
qac_a_46883406_uff_E=550.72	-6.5	30.412	28.444

CHEMBL1081338 exhibits a top docking score of -7.1 kcal/mol with an RMSD of 0 Å, indicating a single dominant binding pose. However, all alternate poses are spread widely (19–38 Å RMSD) with similar or slightly lower binding affinities (-7.0 to -6.5 kcal/mol), suggesting significant conformational dispersion and lack of a stable binding cluster. The absence of tightly packed alternative poses near the global minimum may indicate nonspecific binding or high flexibility. In a drug discovery context, while the affinity is moderate, the poor clustering raises concerns about pose reproducibility and target engagement reliability.

Table 37: Docking Results – CHEMBL1514916

Ligand	Binding Affinity	rmsd/ub	rmsd/lb
qac_a_455264_uff_E=464.37	-7.8	0	0
qac_a_455264_uff_E=464.37	-6.9	3.189	2.105
qac_a_455264_uff_E=464.37	-6.8	4.412	2.839
qac_a_455264_uff_E=464.37	-6.8	33.997	29.48
qac_a_455264_uff_E=464.37	-6.8	32.985	30.568
qac_a_455264_uff_E=464.37	-6.7	41.848	38.962
qac_a_455264_uff_E=464.37	-6.7	34.244	31.853
qac_a_455264_uff_E=464.37	-6.6	4.083	3.03
qac_a_455264_uff_E=464.37	-6.5	13.392	11.088

CHEMBL1514916 shows a strong primary docking score of -7.8 kcal/mol with 0 Å RMSD, indicating a well-defined top pose. Several alternative poses cluster reasonably close (RMSD 3–4 Å) with slightly lower affinities (-6.9 to -6.6 kcal/mol), supporting pose consistency and a relatively stable binding conformation. However, additional poses appear widely scattered (RMSD >30 Å), suggesting some flexibility or non-specific peripheral interactions. From a drug discovery standpoint, the combination of a clear global minimum and nearby clustered alternatives makes this ligand a promising candidate, pending further structural validation.

Table 38: Docking Results – CHEMBL2333536

Ligand	Binding Affinity	rmsd/ub	rmsd/lb
qac_a_13820510_uff_E=641.77	-6.8	0	0
qac_a_13820510_uff_E=641.77	-6.6	12.646	10.178
qac_a_13820510_uff_E=641.77	-6.6	4.004	2.669
qac_a_13820510_uff_E=641.77	-6.6	34.027	31.982
qac_a_13820510_uff_E=641.77	-6.5	34.794	32.555
qac_a_13820510_uff_E=641.77	-6.5	37.261	35.465
qac_a_13820510_uff_E=641.77	-6.3	26.894	24.605
qac_a_13820510_uff_E=641.77	-6.2	35.035	33.007
qac_a_13820510_uff_E=641.77	-6.2	32.165	30.066

CHEMBL2333536 exhibited a top binding affinity of -6.8 kcal/mol with 0 Å RMSD, suggesting a distinct primary pose. Several additional poses fall within moderate RMSD ranges (2–12 Å) and retain comparable docking scores, indicating some pose flexibility but still plausible binding stability. However, many alternative conformations show high RMSD values (>30 Å), which may reflect nonspecific interactions or peripheral

binding possibilities. While the primary pose is clearly defined, the moderate affinity and conformational spread suggest this compound is a weaker binder and would require further optimization to improve binding consistency and specificity.

Table 39: Docking Results – CHEMBL2376097

Ligand	Binding Affinity	rmsd/ub	rmsd/lb
qac_a_23243694_uff_E=513.07	-8.7	0	0
qac_a_23243694_uff_E=513.07	-7.5	1.35	1.167
qac_a_23243694_uff_E=513.07	-7.4	21.666	19.383
qac_a_23243694_uff_E=513.07	-7.2	29.051	25.339
qac_a_23243694_uff_E=513.07	-7.1	15.845	12.445
qac_a_23243694_uff_E=513.07	-7	9.905	5.476
qac_a_23243694_uff_E=513.07	-6.9	6.813	4.24
qac_a_23243694_uff_E=513.07	-6.9	14.095	10.703
qac_a_23243694_uff_E=513.07	-6.8	11.348	7.669

CHEMBL2376097 demonstrated a strong top binding affinity of -8.7 kcal/mol with 0 Å RMSD, indicating a highly stable and well-defined binding pose. A secondary pose with slightly reduced affinity (-7.5 kcal/mol) and low RMSD (1.35 Å) reinforces this binding site's reliability. Other conformations, despite maintaining moderate binding energies, show significantly higher RMSD values, suggesting less favorable or non-specific interactions. Overall, this ligand appears to be a promising candidate due to its strong and consistent binding profile, with only minimal structural deviation among top-ranked poses.

Table 40: Docking Results – CHEMBL4544522

Ligand	Binding Affinity	rmsd/ub	rmsd/lb
qac_a_13855852_uff_E=512.74	-7.5	0	0
qac_a_13855852_uff_E=512.74	-7.4	37.088	34.007
qac_a_13855852_uff_E=512.74	-7.1	58.584	54.763
qac_a_13855852_uff_E=512.74	-7.1	57.939	55.512
qac_a_13855852_uff_E=512.74	-7	34.975	32.319
qac_a_13855852_uff_E=512.74	-6.8	59.807	57.479
qac_a_13855852_uff_E=512.74	-6.8	6.268	2.736
qac_a_13855852_uff_E=512.74	-6.7	36.244	32.904
qac_a_13855852_uff_E=512.74	-6.7	42.343	38.458

CHEMBL4544522 shows a top binding affinity of -7.5 kcal/mol with 0 Å RMSD, indicating a highly stable and reproducible binding pose. While additional conformers display similar binding energies (-7.4 to -6.7 kcal/mol), their elevated RMSD values—some exceeding 50 Å—suggest alternative, less favorable orientations within the binding pocket. One pose at -6.8 kcal/mol with an RMSD of 6.268/2.736 Å stands out as a secondary stable pose, though less optimal than the top-ranked one. From a drug discovery perspective, this ligand demonstrates a strong and reliable binding mode, meriting further evaluation for lead optimization.

## Post-Docking Analysis

Post-docking analysis refers to the critical evaluation and interpretation of results obtained after molecular docking, a computational method used to predict how small molecules (ligands) bind to a target protein (receptor). This analysis is essential for identifying promising drug candidates, understanding binding mechanisms, and guiding further experimental or computational studies.

Post-docking analysis is crucial for:

- Identifying the most promising ligand candidates for experimental validation.
- Understanding the molecular interactions driving ligand binding.
- Reducing false positives and improving the reliability of virtual screening results.
- Guiding rational drug design and lead optimization efforts

LigPlots are schematic 2D diagrams that visually represent the interactions between a protein and a ligand within a complex, based on structural data (typically from PDB files). These diagrams are generated by the LigPlot program, which automatically analyzes protein–ligand complexes and produces clear illustrations of the key interactions at the binding interface.

LigPlots are widely used in molecular docking and structure-based drug design to:

- Summarize and visualize critical protein–ligand interactions.
- Aid in the interpretation of docking results.
- Facilitate comparison of binding modes across different ligands or protein variants

Post-docking analysis was performed using VinaLigGen, a tool to produce LigPlots in bulk from docked complexes generated using AutoDock Vina.

Table 41: Post-Docking Analysis Results of Primary Ligands – Hydrogen Bond Data

LIGAND_NAME	Hydrogen_bonds	Hydrogen_bond_distance
1,8-Naphthyridine-3-carboxamide		
23435869_uff_E=119.30_uff_E=119.21_out		
23435869_uff_E=119.30_uff_E=119.21_out_1	SER75	2.7
23435869_uff_E=119.30_uff_E=119.21_out_2	LYS398   SER397	2.92   3.00
23435869_uff_E=119.30_uff_E=119.21_out_3	SER345   SER345	3.13   3.16
23435869_uff_E=119.30_uff_E=119.21_out_4	THR32   THR36	2.93   3.01
23435869_uff_E=119.30_uff_E=119.21_out_5	GLN302   SER298	3.10   3.10
23435869_uff_E=119.30_uff_E=119.21_out_6	SER425	2.86
23435869_uff_E=119.30_uff_E=119.21_out_7	VAL444   LYS67	2.95   3.20
23435869_uff_E=119.30_uff_E=119.21_out_8	SER423	3.23
23435869_uff_E=119.30_uff_E=119.21_out_9	ILE60   LYS67	2.99   3.11
Carnosol		
442009_uff_E=653.04_out		
442009_uff_E=653.04_out_1	THR32	3.12
442009_uff_E=653.04_out_2		
442009_uff_E=653.04_out_3		
442009_uff_E=653.04_out_4	SER298	2.94
442009_uff_E=653.04_out_5		
442009_uff_E=653.04_out_6		
442009_uff_E=653.04_out_7	TRP59	2.97

442009_uff_E=653.04_out_8	GLN72   TYR52   SER74   SER74	2.96   3.01   3.16   2.97
442009_uff_E=653.04_out_9	PHE183   PRO182	2.84   3.02
Carnosic Acid		
65126_uff_E=468.40_out		
65126_uff_E=468.40_out_1	ALA157   SER298	3.23   2.99
65126_uff_E=468.40_out_2	SER497	2.86
65126_uff_E=468.40_out_3		
65126_uff_E=468.40_out_4		
65126_uff_E=468.40_out_5	GLN117   LEU5   LEU5	3.01   3.02   2.70
65126_uff_E=468.40_out_6	GLY442	3.11
65126_uff_E=468.40_out_7	SER298	3.28
65126_uff_E=468.40_out_8	TRP59   ARG46	3.35   3.06
65126_uff_E=468.40_out_9	SER497	2.85

Table 42: Post-Docking Analysis Results of Primary Ligands – Hydrophobic Interactions

LIGAND_NAME	Hydrophobic_bonds	Hydrophobic_bond_distance
<b>1,8-naphthyridine-3-carboxamide</b>		
23435869_uff_E=119.30_uff_E=119.21_out		
23435869_uff_E=119.30_uff_E=119.21_out_1	ASN401   ASN401   ALA76   SER75   LYS80   ASN401   ASN401   LYS80   ASN401   ALA76	3.86   3.63   3.67   3.84   3.80   3.34   3.88   3.49   3.89   3.83
23435869_uff_E=119.30_uff_E=119.21_out_2	ALA76   ALA76   ALA76   ALA76   LYS398   SER397   SER397   LEU200   LEU200	3.87   3.69   3.77   3.87   3.74   3.63   3.70   3.58   3.83
23435869_uff_E=119.30_uff_E=119.21_out_3	SER382   SER382   GLY346   SER382   ALA330   ALA330   PHE326	3.75   3.80   3.80   3.74   3.88   3.82   3.87
23435869_uff_E=119.30_uff_E=119.21_out_4	ALA291   LEU295   LEU294   LEU294   LEU294   ALA157   ALA157	3.63   3.57   3.55   3.67   3.88   3.74   3.74
23435869_uff_E=119.30_uff_E=119.21_out_5	SER298   ILE39   THR36   LEU294   PRO161   PRO161	3.76   3.60   3.59   3.79   3.62   3.74
23435869_uff_E=119.30_uff_E=119.21_out_6	SER426   GLY422   LEU295   SER426   LEU296   LEU296   GLY422   SER425   LEU296   GLY422	3.56   3.77   3.77   3.64   3.73   3.53   3.71   3.73   3.89   3.88
23435869_uff_E=119.30_uff_E=119.21_out_7	THR465   THR465   LEU61   LEU61	3.60   3.85   3.67   3.69
23435869_uff_E=119.30_uff_E=119.21_out_8	SER231   PHE230   PHE416   PHE416   ILE227   PHE230   ILE227   ILE227   PHE230   PHE230   PHE230   PHE230	3.77   3.86   3.51   3.75   3.79   3.89   3.76   3.70   3.74   3.47   3.55   3.53
23435869_uff_E=119.30_uff_E=119.21_out_9	LEU61   LEU61   LEU61   THR465   LEU61   LEU61   LEU61	3.78   3.74   3.72   3.73   3.77   3.76   3.79
<b>Carnosol</b>		
442009_uff_E=653.04_out		
442009_uff_E=653.04_out_1	LEU294   LEU295   LEU295   ALA157   ALA157   ALA157   ALA157   ASN414   ASN414   TYR410   MET287   ALA157   TYR410   TYR410	3.67   3.64   3.72   3.89   3.79   3.74   3.72   3.43   3.53   3.61   3.82   3.65   3.62   3.73

442009_uff_E=653.04_out_2	ILE244   ILE244   PHE230   PHE230   PHE230   LEU235   LEU235   PHE230   PHE230   PHE230   PHE230   PHE230   PHE230   VAL420   LEU235   PHE230   PHE230   PHE230	3.61   3.89   3.80   3.67   3.69   3.79   3.81   3.80   3.89   3.86   3.72   3.69   3.61   3.57   3.58   3.27   3.52   3.86   3.57   3.90
442009_uff_E=653.04_out_3	ILE39   LEU295   ILE39   LEU295   LEU295   LEU295   ILE39   ILE39   GLY313   SER298   PRO161   PRO161   PRO309   MET40   ILE39   ILE39   SER298   PRO161	3.76   3.59   3.65   3.65   3.84   3.61   3.53   3.70   3.86   3.80   3.62   3.65   3.88   3.76   3.90   3.67   3.60   3.70
442009_uff_E=653.04_out_4	PRO309   PRO309   PRO309   MET40   ILE39   ILE39   THR36   THR36   THR36   PRO161   MET40   LEU295   MET40   MET40   LEU295   MET40	3.60   3.71   3.78   3.61   3.30   3.68   3.31   3.82   3.69   3.76   3.90   3.66   3.44   3.62   3.51   3.74
442009_uff_E=653.04_out_5	PRO43   PRO309   PRO309   PRO309   PRO309   MET40   GLN302   LEU295   SER298   GLN299   SER298   MET40   SER298   SER298	3.56   3.74   3.88   3.63   3.76   3.87   3.79   3.87   3.65   3.69   3.74   3.74   3.80   3.28
442009_uff_E=653.04_out_6	VAL405   LEU266   ILE72   LEU266   MET409   PHE271   VAL255   PHE271   PHE271   PHE271   PHE271   MET409   PHE271   PHE271   PHE271	3.83   3.75   3.84   3.85   3.56   3.74   3.84   3.67   3.69   3.63   3.74   3.63   3.79   3.82   3.63   3.51
442009_uff_E=653.04_out_7	TRP59   TRP59   ALA48   ALA48   ALA48   ALA48   TRP115   TRP115   PHE38   PHE38   PHE38   PHE38   PHE38   PHE38   ASP111   PHE38   ASP111   PHE38   GLU47   GLU47   ARG46	3.60   3.71   3.70   3.75   3.86   3.80   3.64   3.87   3.89   3.82   3.88   3.73   3.79   3.72   3.73   3.73   3.77   3.35   3.60   3.78   3.59   3.83
442009_uff_E=653.04_out_8	SER71   GLN469   LYS468   ASP32   ASP32	3.65   3.78   3.78   3.90   3.87
442009_uff_E=653.04_out_9	ILE186   PHE183   PHE183   ILE186   ILE186   PHE183   PHE183   PHE183   PHE183   VAL23   VAL26   VAL22   ILE186   VAL23   PHE183   VAL26   ILE186	3.79   3.85   3.75   3.69   3.76   3.85   3.78   3.82   3.46   3.64   3.86   3.52   3.81   3.77   3.61   3.86
<b>Carnosic Acid</b>		
65126_uff_E=468.40_out		
65126_uff_E=468.40_out_1	MET35   MET35   LEU295   ILE39   THR36   LEU295   ILE39   LEU295   ILE39   ILE39   MET40   MET40   PRO161   THR36	3.84   3.78   3.56   3.60   3.77   3.54   3.73   3.85   3.65   3.80   3.72   3.81   3.47   3.67
65126_uff_E=468.40_out_2	SER345   ILE341   PRO344   PRO344   TYR501   TYR501   TYR501   TYR501   TYR501   TYR501   TYR501   TYR501   ILE498   TYR501   TYR501   TYR501   ILE498   TYR501   TYR501   TYR501   ILE498   TYR501   TYR501	3.74   3.86   3.66   3.89   3.89   3.69   3.67   3.89   3.69   3.73   3.64   3.83   3.77   3.67   3.61   3.48   3.32   3.75   3.87   3.50   3.65   3.86
65126_uff_E=468.40_out_3	PHE355   PHE355   ILE352   PHE359   PHE355   PHE359   PHE359   PHE355   PHE359   PHE359   PHE355   PHE355   PHE355   PHE355   PHE355   PHE355   LEU487   PHE359	3.76   3.82   3.68   3.56   3.90   3.86   3.85   3.70   3.80   3.51   3.52   3.15   3.60   3.66   3.45   3.70   3.75   3.44   3.67   3.76   3.70

	PHE355   PHE355   PHE355   PHE359   PHE359   LEU487   LEU487   LEU487   PHE359   PHE359	3.90   3.71   3.86   3.68   3.67   3.50   3.80   3.60   3.88   3.33
65126_uff_E=468.40_out_4	VAL456   GLN302   GLN302   GLN299   GLN299   GLN302   GLN302   GLN302   GLN302   GLN302   GLN302   GLN302   GLN299   PRO161   SER298   PRO161   PRO161   PRO309	3.76   3.64   3.57   3.66   3.82   3.59   3.56   3.88   3.81   3.70   3.65   3.85   3.68   3.88   3.78   3.77
65126_uff_E=468.40_out_5	GLN4   GLN4   GLN4   GLN4   GLN4   GLN4   TYR114   GLN4   TYR114   TYR114   TYR114	3.90   3.76   3.47   3.74   3.60   3.90   3.73   3.78   3.36   3.78   3.89
65126_uff_E=468.40_out_6	LEU107   GLY442   LEU107   LEU61   LEU61   LEU61   LEU61   LEU61   LEU61	3.67   3.86   3.54   3.73   3.53   3.55   3.67   3.83
65126_uff_E=468.40_out_7	LEU295   ILE39   LEU295   ILE39   LEU295   ILE39   LEU295   ILE39   LEU295   MET40   THR36   PRO161   PRO161   MET40   THR36	3.69   3.73   3.43   3.40   3.69   3.70   3.54   3.61   3.87   3.89   3.80   3.74   3.80   3.79   3.84   3.58
65126_uff_E=468.40_out_8	PHE112   GLU47   ALA48   ALA48   PHE38   ARG46   ASP111   PHE38   ASP111   PHE38	3.79   3.83   3.54   3.57   3.83   3.45   3.61   3.36   3.85   3.75
65126_uff_E=468.40_out_9	ILE494   ILE352   ILE494   SER497   TYR501   TYR501   TYR501   ILE498   ILE498   TYR501   TYR501	3.52   3.68   3.69   3.81   3.71   3.68   3.66   3.77   3.74   3.60   3.73

Table 43: Post-Docking Analysis Results – Secondary Ligands of Naphthyridine-3-Carboxamide – Hydrogen Bond Data

LIGAND_NAME	Hydrogen_bonds	Hydrogen_bond_distance
15561101_uff_E=120.29_out		
15561101_uff_E=120.29_out_1	SER75	2.95
15561101_uff_E=120.29_out_2	LYS398   SER397	2.95   2.94
15561101_uff_E=120.29_out_3	SER423	2.92
15561101_uff_E=120.29_out_4	GLN302   SER298	3.09   3.10
15561101_uff_E=120.29_out_5	SER345	3.26
15561101_uff_E=120.29_out_6		
15561101_uff_E=120.29_out_7	GLN299	3.17
15561101_uff_E=120.29_out_8	ILE341	2.93
15561101_uff_E=120.29_out_9	THR32   THR32	3.04   3.06

Table 44: Post-Docking Analysis Results – Secondary Ligands of Naphthyridine-3-Carboxamide – Hydrophobic Interaction Data

LIGAND_NAME	Hydrophobic_bonds	Hydrophobic_bond_distance
15561101_uff_E=120.29_out		
15561101_uff_E=120.29_out_1	ASN401   ASN401   ALA76   SER397   LEU200   SER397   SER397   ASN401   ASN401	3.80   3.72   3.73   3.78   3.71   3.70   3.81   3.89   3.37

15561101_uff_E=120.29_out_2	ALA76   ALA76   ALA76   ALA76   LYS398   SER397   SER397   ASN401   ASN401   LEU200   LEU200	3.82   3.67   3.78   3.87   3.70   3.76   3.76   3.89   3.55   3.56   3.84
15561101_uff_E=120.29_out_3	VAL420   PHE416   PHE416   ILE227   PHE416   SER231   PHE230   VAL420   ALA419   ILE227   PHE230   PHE230   VAL420   PHE230   PHE230	3.88   3.60   3.80   3.62   3.87   3.58   3.81   3.51   3.80   3.34   3.58   3.82   3.80   3.81   3.86
15561101_uff_E=120.29_out_4	SER298   ILE39   THR36   ILE39   ILE39   THR36   LEU294   SER298   PRO161   PRO161	3.75   3.59   3.61   3.73   3.79   3.69   3.78   3.90   3.62   3.74
15561101_uff_E=120.29_out_5	LEU333   SER382   SER382   ALA381   ALA330   PHE326   PHE326   LEU333	3.55   3.83   3.55   3.74   3.75   3.75   3.71   3.82
15561101_uff_E=120.29_out_6	ALA381   ALA330   SER382   ALA330   PHE326   PHE326   VAL342   VAL342	3.67   3.68   3.56   3.55   3.63   3.66   3.83   3.70
15561101_uff_E=120.29_out_7	PHE478   GLY422   LEU295   GLY422   LEU295   LEU295   GLY422   GLY422   LEU296   LEU296   GLY422   GLY422	3.83   3.66   3.86   3.78   3.86   3.77   3.66   3.89   3.59   3.61   3.77   3.89
15561101_uff_E=120.29_out_8	SER345   TYR501   TYR501   TYR501   PRO344   TYR501   ILE498   ILE498   TYR501   TYR501   TYR501   TYR501   TYR501   TYR501   PRO344   TYR501   TYR501   TYR501   TYR501   TYR501   TYR501	3.83   3.82   3.72   3.60   3.41   3.81   3.71   3.49   3.83   3.78   3.88   3.78   3.88   3.84   3.79   3.77   3.82   3.74   3.67   3.73
15561101_uff_E=120.29_out_9	LEU295   LEU294   LEU294   LEU295   LEU294   ALA291   MET290   ALA157   ALA157   ALA157   ALA157	3.71   3.77   3.71   3.58   3.75   3.83   3.57   3.81   3.62   3.55

Table 45: Post-Docking Analysis of Secondary Ligands of Carnosic Acid – Hydrogen Bond Interactions

LIGAND_NAME	Hydrogen_bonds	Hydrogen_bond_distance
<b>CHEMBL4868012</b>		
101371515_uff_E=452.36_out		
101371515_uff_E=452.36_out_1	SER298	2.72
101371515_uff_E=452.36_out_2	ALA63	3.1
101371515_uff_E=452.36_out_3	MET40   GLU44	2.75   3.01
101371515_uff_E=452.36_out_4	LYS468   LYS468   ASP32	3.16   3.29   2.77
101371515_uff_E=452.36_out_5	THR280	2.92
101371515_uff_E=452.36_out_6	TRP115   VAL3   GLY116   LEU5	2.85   2.94   3.15   3.17
101371515_uff_E=452.36_out_7	SER14   THR13   MET12	2.91   3.23   2.81
101371515_uff_E=452.36_out_8	SER497	3.01
101371515_uff_E=452.36_out_9		
<b>CHEMBL2333537</b>		
11336941_uff_E=689.97_out		
11336941_uff_E=689.97_out_1		
11336941_uff_E=689.97_out_2		
11336941_uff_E=689.97_out_3		
11336941_uff_E=689.97_out_4		
11336941_uff_E=689.97_out_5		
11336941_uff_E=689.97_out_6		
11336941_uff_E=689.97_out_7		
11336941_uff_E=689.97_out_8		

11336941_uff_E=689.97_out_9		
<b>CHEMBL479111</b>		
13654835_uff_E=506.73_out		
13654835_uff_E=506.73_out_1	THR36   SER298   SER298	3.24   3.15   3.06
13654835_uff_E=506.73_out_2	SER345   SER345	3.03   2.75
13654835_uff_E=506.73_out_3		
13654835_uff_E=506.73_out_4		
13654835_uff_E=506.73_out_5	ILE352	2.89
13654835_uff_E=506.73_out_6		
13654835_uff_E=506.73_out_7		
13654835_uff_E=506.73_out_8		
13654835_uff_E=506.73_out_9	GLY442	3.01
<b>CHEMBL4436108</b>		
155511438_uff_E=428.22_out		
155511438_uff_E=428.22_out_1		
155511438_uff_E=428.22_out_2	SER277	3.18
155511438_uff_E=428.22_out_3	SER497	2.89
155511438_uff_E=428.22_out_4		
155511438_uff_E=428.22_out_5		
155511438_uff_E=428.22_out_6	SER497	2.82
155511438_uff_E=428.22_out_7		
155511438_uff_E=428.22_out_8		
155511438_uff_E=428.22_out_9		
<b>CHEMBL4451825</b>		
155521642_uff_E=557.43_out		
155521642_uff_E=557.43_out_1	GLY442	2.7
155521642_uff_E=557.43_out_2	THR213	3.32
155521642_uff_E=557.43_out_3		
155521642_uff_E=557.43_out_4		
155521642_uff_E=557.43_out_5		
155521642_uff_E=557.43_out_6		
155521642_uff_E=557.43_out_7		
155521642_uff_E=557.43_out_8		
155521642_uff_E=557.43_out_9	GLN302	3.02
<b>CHEMBL4468065</b>		
155532943_uff_E=441.09_out		
155532943_uff_E=441.09_out_1	THR213	3.31
155532943_uff_E=441.09_out_2	GLY442	2.71
155532943_uff_E=441.09_out_3	SER497	2.83
155532943_uff_E=441.09_out_4		
155532943_uff_E=441.09_out_5		
155532943_uff_E=441.09_out_6	SER497   SER497   SER497	3.18   3.27   2.91
155532943_uff_E=441.09_out_7		
155532943_uff_E=441.09_out_8		
155532943_uff_E=441.09_out_9	GLN302	2.91
<b>CHEMBL4471445</b>		
155535100_uff_E=518.38_out		
155535100_uff_E=518.38_out_1	SER497	2.79
155535100_uff_E=518.38_out_2		

155535100_uff_E=518.38_out_3		
155535100_uff_E=518.38_out_4		
155535100_uff_E=518.38_out_5		
155535100_uff_E=518.38_out_6	SER345	2.69
155535100_uff_E=518.38_out_7		
155535100_uff_E=518.38_out_8		
155535100_uff_E=518.38_out_9		
155535609_uff_E=406.55_out		
<b>CHEMBL4471914</b>		
155535609_uff_E=406.55_out_1		
155535609_uff_E=406.55_out_2	GLY442   SER439	3.06   2.70
155535609_uff_E=406.55_out_3	SER497	2.83
155535609_uff_E=406.55_out_4	ASP64	3.11
155535609_uff_E=406.55_out_5	GLY116	2.99
155535609_uff_E=406.55_out_6	SER497   SER497	3.17   3.29
155535609_uff_E=406.55_out_7	TYR62	2.89
155535609_uff_E=406.55_out_8		
155535609_uff_E=406.55_out_9	THR394   LEU392   ARG142   THR396   ARG133	2.83   3.02   3.03   3.10   3.23
<b>CHEMBL4515503</b>		
155539703_uff_E=413.03_out		
155539703_uff_E=413.03_out_1		
155539703_uff_E=413.03_out_2		
155539703_uff_E=413.03_out_3	SER497	2.88
155539703_uff_E=413.03_out_4		
155539703_uff_E=413.03_out_5		
155539703_uff_E=413.03_out_6		
155539703_uff_E=413.03_out_7	ARG46	3.15
155539703_uff_E=413.03_out_8		
155539703_uff_E=413.03_out_9		
<b>CHEMBL4519804</b>		
155542101_uff_E=518.72_out		
155542101_uff_E=518.72_out_1	ASP64	3.13
155542101_uff_E=518.72_out_2		
155542101_uff_E=518.72_out_3	SER497	2.79
155542101_uff_E=518.72_out_4	GLU453   GLU453   SER231	2.69   3.28   2.94
155542101_uff_E=518.72_out_5		
155542101_uff_E=518.72_out_6	GLN117   LEU5   LEU5	2.95   3.07   2.77
155542101_uff_E=518.72_out_7		
155542101_uff_E=518.72_out_8	LYS204   SER397	2.61   3.05
155542101_uff_E=518.72_out_9		
<b>CHEMBL4574206</b>		
155563682_uff_E=423.90_out		
155563682_uff_E=423.90_out_1		
155563682_uff_E=423.90_out_2		
155563682_uff_E=423.90_out_3	GLY442   TYR62	2.71   3.33
155563682_uff_E=423.90_out_4		
155563682_uff_E=423.90_out_5	ASP64	3.31
155563682_uff_E=423.90_out_6	SER497	2.85

155563682_uff_E=423.90_out_7		
155563682_uff_E=423.90_out_8		
155563682_uff_E=423.90_out_9	SER345   SER345	2.69   3.10
<b>CHEMBL2374044</b>		
16758167_uff_E=329.45_out		
16758167_uff_E=329.45_out_1		
16758167_uff_E=329.45_out_2	ALA157	3.12
16758167_uff_E=329.45_out_3		
16758167_uff_E=329.45_out_4	SER298	2.96
16758167_uff_E=329.45_out_5		
16758167_uff_E=329.45_out_6		
16758167_uff_E=329.45_out_7	TYR62	2.87
16758167_uff_E=329.45_out_8		
16758167_uff_E=329.45_out_9	PHE230   SER423	3.31   3.26
<b>CHEMBL5407683</b>		
455260_uff_E=337.63_out		
455260_uff_E=337.63_out_1		
455260_uff_E=337.63_out_2	ASN33   GLN469	2.96   3.00
455260_uff_E=337.63_out_3	ALA63	2.92
455260_uff_E=337.63_out_4	ASP111   ARG99	2.71   3.24
455260_uff_E=337.63_out_5	LEU5   LEU5   GLY116	2.82   2.85   2.70
455260_uff_E=337.63_out_6		
455260_uff_E=337.63_out_7		
455260_uff_E=337.63_out_8		
455260_uff_E=337.63_out_9	TRP115   ALA113   GLY116   TRP115   VAL3   GLY116	3.20   3.03   3.09   2.94   2.87   3.18
<b>CHEMBL2376099</b>		
71712255_uff_E=471.71_out		
71712255_uff_E=471.71_out_1	SER298	2.91
71712255_uff_E=471.71_out_2		
71712255_uff_E=471.71_out_3	THR36   THR36	2.54   3.06
71712255_uff_E=471.71_out_4	SER497	2.82
71712255_uff_E=471.71_out_5		
71712255_uff_E=471.71_out_6	LYS67	3.02
71712255_uff_E=471.71_out_7	GLY442	3.13
71712255_uff_E=471.71_out_8		
71712255_uff_E=471.71_out_9		
<b>CHEMBL1096627</b>		
9974918_uff_E=529.05_out		
9974918_uff_E=529.05_out_1	THR36	3.09
9974918_uff_E=529.05_out_2		
9974918_uff_E=529.05_out_3		
9974918_uff_E=529.05_out_4		
9974918_uff_E=529.05_out_5		
9974918_uff_E=529.05_out_6		
9974918_uff_E=529.05_out_7		
9974918_uff_E=529.05_out_8	GLU44   ARG47	3.11   3.15
9974918_uff_E=529.05_out_9		

Table 46: Post-Docking Analysis of Secondary Ligands of Carnosic Acid –Hydrophobic Interactions

LIGAND_NAME	Hydrogen_bonds	Hydrogen_bond_distance			
<b>CHEMBL4868012</b>					
101371515_uff_E=452.36_out					
	GLN299   GLN302   GLN302   GLN302   GLN299   GLN299   GLN299   SER298   PRO161   PRO161   SER298   ILE39   ILE39   SER298   LEU295   MET40   SER298   LEU295   ILE39   ILE39   THR36   PRO161   PRO161   MET40	3.77   3.82   3.51   3.63   3.55   3.74   3.81   3.59   3.82   3.69   3.28   3.85   3.51   3.79   3.53   3.80   3.59   3.82   3.82   3.57   3.75   3.79   3.89			
101371515_uff_E=452.36_out_1					
101371515_uff_E=452.36_out_2	ILE467   ILE467   THR465   GLY442   GLY442   GLY442   GLY442   THR465   LEU447   ILE443   GLY442   LEU447   VAL444   VAL444	3.76   3.86   3.81   3.79   3.84   3.41   3.54   3.74   3.87   3.69   3.85   3.70   3.44   3.64			
101371515_uff_E=452.36_out_3	PRO43   PRO309   PRO309   MET40   MET40   LEU168   PRO309   PRO309   PHE310   GLU169   LEU168	3.86   3.86   3.71   3.79   3.89   3.75   3.73   3.65   3.80   3.65   3.68			
101371515_uff_E=452.36_out_4	TYR30   LYS468   LYS468   LYS468   LYS468   LYS468   LYS468   SER74	3.76   3.78   3.86   3.68   3.48   3.69   3.70   3.81			
101371515_uff_E=452.36_out_5	PHE416   PHE416   PHE416   PHE416   LEU412   PHE284   PHE284   PHE284   PHE284   ILE281   PHE284   PHE284   ILE281   PHE284   MET285   ILE281   ILE281   ILE281   ILE281	3.74   3.69   3.83   3.75   3.68   3.50   3.74   3.82   3.69   3.85   3.54   3.70   3.81   3.75   3.60   3.59   3.70   3.80   3.81			
101371515_uff_E=452.36_out_6	GLN2   TYR114   TYR114   TYR114	3.87   3.69   3.53   3.70			
101371515_uff_E=452.36_out_7	LEU194   LEU194   LYS16   LYS16   THR13   LYS16   THR9   THR9   THR13   THR13   LEU194   THR13   THR9   LEU194   LEU194   PHE193   THR9   THR9	3.71   3.47   3.74   3.69   3.85   3.80   3.80   3.84   3.85   3.63   3.75   3.66   3.73   3.69   3.35   3.83   3.70   3.15			
101371515_uff_E=452.36_out_8	ILE494   GLY348   PRO344   TYR501   TYR501   TYR501   ILE498   SER497   TYR501   TYR501   TYR501   TYR501   PRO344   TYR501	3.56   3.72   3.53   3.73   3.50   3.64   3.71   3.86   3.79   3.59   3.62   3.79   3.62   3.79			
101371515_uff_E=452.36_out_9	ASN76   ASN76   GLY54   GLY54   SER31	3.78   3.81   3.67   3.79   3.70			
<b>CHEMBL2333537</b>					
11336941_uff_E=689.97_out					
11336941_uff_E=689.97_out_1	TYR410   TYR410   MET125   MET125   THR32   TYR63   TYR63   MET35   ASN414   LEU294   LEU294   LEU294   MET290   MET290   ALA157   ALA157	3.57   3.67   3.66   3.78   3.70   3.81   3.10   3.73   3.77   3.79   3.74   3.88   3.84   3.60   3.71   3.58			
11336941_uff_E=689.97_out_2	PHE416   PHE416   ILE244   ILE244   PHE230   PHE416   PHE416   PHE416   PHE230   PHE230   SER423   ALA419   SER231   ILE227   VAL420   VAL420   VAL420   PHE230   PHE230   VAL420   VAL420	3.88   3.88   3.75   3.27   3.61   3.62   3.49   3.86   3.61   3.67   3.29   3.77   3.82   3.61   3.56   3.85   3.90   3.61   3.23   3.42   3.78			

11336941_uff_E=689.97_out_3	PRO73   PHE70   THR213   TRP208   TRP208   TRP208   TRP208   ILE210   ILE210   TRP208   TRP208   THR213   TRP208   TRP208   TRP208   TRP208   TRP208   TRP208   TRP208   TRP208	3.54   3.86   3.64   3.79   3.86   3.75   3.89   3.66   3.44   3.49   3.88   3.84   3.63   3.68   3.75   3.77   3.70   3.70   3.90   3.81   3.33   3.85   3.89		
11336941_uff_E=689.97_out_4	PHE159   ILE163   PHE159   PHE159   PHE159   PHE29   PHE29   PHE29   PHE29   PHE29   ILE155   VAL26   ALA152   ILE151   VAL148   ILE155   PHE29   PHE29   ILE151   ILE151   MET324	3.80   3.87   3.80   3.46   3.79   3.48   3.81   3.63   3.82   3.90   3.86   3.74   3.66   3.84   3.50   3.28   3.60   3.68   3.65   3.79   3.59		
11336941_uff_E=689.97_out_5	GLN302   GLN302   GLN299   PRO161     PRO161   MET40   ILE39   ILE39   THR36   ILE39   LEU295   ILE39   PRO161   SER298	3.66   3.80   3.67   3.61   3.70   3.70   3.67   3.66   3.56   3.78   3.60   3.78   3.82   3.67		
11336941_uff_E=689.97_out_6	LEU107   LEU107   LEU447   ILE443   LEU447   LEU61   LEU61   LEU61   LEU61   THR465	3.65   3.81   3.83   3.84   3.71   3.69   3.66   3.69   3.61   3.43		
11336941_uff_E=689.97_out_7	GLN302   VAL456   GLN299   GLN302     GLN302   GLN302   GLN299   GLN302   ILE39   PRO161   SER298   MET40   SER298   PRO309	3.67   3.62   3.75   3.56   3.84   3.83   3.64   3.76   3.72   3.89   3.04   3.57   3.72   3.74		
11336941_uff_E=689.97_out_8	MET409   LEU412   LEU223   MET220     ILE248   LEU412   LEU412   PHE416     PHE416   PHE284   PHE416   PHE416   PHE284   PHE284   PHE284     PHE284   PHE416   PHE416   PHE284   PHE284   PHE284   PHE284	3.79   3.76   3.51   3.57   3.72   3.83   3.48   3.78   3.70   3.52   3.66   3.81   3.75   3.67   3.48   3.62   3.72   3.68   3.76   3.75   3.52   3.84		
11336941_uff_E=689.97_out_9	THR213   TRP208   TRP208   TRP208     TRP208   TRP208   TRP208   PHE77     PHE77   LEU74   TRP208   PHE77   PHE77   LEU74   ILE119   PHE77   PHE77   LEU74   ILE119   LEU74	3.60   3.57   3.63   3.89   3.84   3.62   3.79   3.56   3.77   3.53   3.50   3.83   3.77   3.72   3.29   3.88   3.83   3.88   3.78   3.33		
<b>CHEMBL479111</b>				
13654835_uff_E=506.73_out				
13654835_uff_E=506.73_out_1	LEU295   ILE39   MET35   ALA157   LEU295   ILE39   LEU295   ILE39   LEU295   ILE39   ILE39   MET40   MET40   PRO161   THR36	3.76   3.81   3.42   3.71   3.57   3.60   3.39   3.43   3.60   3.89   3.83   3.58   3.76   3.71   3.77		
13654835_uff_E=506.73_out_2	LEU333   LEU333   LEU333   ILE329   LEU333   ILE329   VAL342   ALA381   ALA381   ALA330   LEU333   LEU333     ALA330   ILE329   ILE329   ALA378     ALA378   ALA378   ILE349   PHE326     ALA330   ALA330   GLY346   ILE349     PHE326   PHE326	3.90   3.56   3.39   3.62   3.65   3.59   3.80   3.78   3.83   3.63   3.47   3.79   3.75   3.01   3.80   3.08   3.87   3.73   3.76   3.82   3.78   3.48   3.38   3.37   3.55   3.55		
13654835_uff_E=506.73_out_3	THR213   PRO73   TRP208   TRP208   PHE77   LEU74   PRO73   PRO73   TRP208   PHE77   TRP208   TRP208   TRP208   THR213   TRP208   TRP208	3.79   3.62   3.58   3.50   3.88   3.39   3.70   3.59   3.89   3.79   3.77   3.75   3.84   3.78   3.73   3.75		

	TRP208   ILE210   ILE210   TRP208   TRP208   TRP208   TRP208   TRP208	3.90   3.61   3.73   3.34   3.73   3.81   3.41   3.81		
13654835_uff_E=506.73_out_4	VAL456   GLN302   GLN302   GLN299   GLN299   GLN302   GLN302   GLN299   GLN302   GLN302   GLN302   GLN299   GLN302   PRO161   SER298   PRO161   PRO161   PRO161   PRO309	3.75   3.71   3.67   3.66   3.89   3.69   3.51   3.83   3.87   3.76   3.64   3.87   3.76   3.75   3.90   3.74   3.87   3.66		
13654835_uff_E=506.73_out_5	PHE355   PHE359   PHE359   PHE355   PHE355   PHE355   PHE355   PHE355   PHE359   PHE359   PHE359   PHE355   PHE355   PHE359   PHE359   PHE359   PHE359   PHE359   PHE359   PHE355   PHE355   PHE355   PHE359   PHE359   PHE359   PHE359   ILE356   ILE356   ILE356   PHE359   PHE359   PHE359   ILE356	3.82   3.60   3.64   3.79   3.84   3.53   3.80   3.50   3.48   3.57   3.81   3.78   3.34   3.80   3.74   3.83   3.81   3.37   3.28   3.35   3.71   3.58   3.78   3.59   3.66   3.80   3.55   3.89   3.77   3.61   3.73   3.14   3.80		
13654835_uff_E=506.73_out_6	VAL420   PHE416   PHE416   PHE416   ILE227   ILE227   LEU235   PHE230   PHE230   PHE230   PHE230   PHE230   PHE230   ILE248   VAL245   ILE244   ILE244   ILE244   ILE244   ILE244   TRP241   ILE244   TRP241   TRP241   TRP241   ILE244	3.55   3.78   3.71   3.76   3.88   3.87   3.85   3.77   3.81   3.61   3.70   3.80   3.61   3.60   3.67   3.63   3.79   3.78   3.60   3.63   3.86   3.73   3.49   3.62   3.89   3.46		
13654835_uff_E=506.73_out_7	TRP241   TRP241   TRP241   TRP241   TRP241   PHE230   PHE230   PHE230   VAL420   PHE230   PHE230   LEU235   PHE230   PHE230   PHE230   PHE230   PHE230   ILE227   LEU235   VAL420   PHE230   PHE230   PHE230	3.61   3.62   3.80   3.82   3.78   3.57   3.40   3.59   3.89   3.59   3.75   3.79   3.84   3.78   3.66   3.56   3.67   3.71   3.84   3.43   3.48   3.72   3.51		
13654835_uff_E=506.73_out_8	ARG46   TRP115   TRP115   ARG46   ARG46   PHE38   PHE38   PHE38   PHE38   ARG46   ARG46   PHE38   PHE38   ALA48   PHE38   PHE112   ASP111   PHE38   TRP59   ASP111   ALA48	3.76   3.80   3.75   3.35   3.80   3.63   3.64   3.44   3.90   3.66   3.73   3.58   3.88   3.74   3.76   3.68   3.50   3.76   3.58   3.73   3.75		
13654835_uff_E=506.73_out_9	LEU107   ASP64   GLY442   LEU107   LEU107   LEU447   LEU61   LEU61   LEU61   LEU61   LEU61   LEU61   THR465	3.54   3.69   3.88   3.83   3.44   3.76   3.82   3.67   3.60   3.69   3.53   3.81   3.73		
<b>CHEMBL4436108</b>				
155511438_uff_E=428.22_out				
155511438_uff_E=428.22_out_1	LEU107   LEU107   SER440   SER440   VAL444   VAL444   GLY442   LEU61   THR465   LYS67   TYR62   ALA63	3.90   3.59   3.70   3.86   3.62   3.63   3.78   3.78   3.75   3.44   3.87   3.73		
155511438_uff_E=428.22_out_2	PHE416   PHE416   PHE416   LEU412   LEU412   ILE227   LEU223   LEU223   PHE271   PHE271   PHE271   PHE271   PHE271   LEU412   PHE284   PHE284   PHE284   MET285	3.71   3.38   3.48   3.59   3.77   3.90   3.28   3.78   3.78   3.86   3.87   3.83   3.63   3.81   3.85   3.71   3.79   2.97   3.81   3.78		

	MET285   PHE284   ILE281   ILE281   PHE284   PHE284   THR280   PHE284   ILE281   ILE281   MET409   PHE284	3.88   3.50   3.75   3.82   3.68   3.60   3.72   3.23   3.56   3.75		
155511438_uff_E=428.22_out_3	SER345   ILE341   PRO344   PRO344   ILE494   ILE498   ILE494   ILE498   TYR501   TYR501   TYR501   TYR501   TYR501   TYR501   TYR501   ILE498   TYR501   TYR501   ILE498   TYR501   TYR501	3.73   3.89   3.64   3.83   3.54   3.69   3.78   3.85   3.74   3.72   3.69   3.75   3.67   3.82   3.80   3.39   3.32   3.79   3.66   3.53   3.81		
155511438_uff_E=428.22_out_4	ILE341   ILE341   ILE494   GLY348   ILE494   TYR501   TYR501   TYR501   TYR501   ILE498   ILE498   ILE498   ILE498   TYR501   TYR501   TYR501   PRO344   TYR501   TYR501   ILE498   SER497   TYR501   PRO344   TYR501   TYR501	3.78   3.57   3.68   3.86   3.69   3.71   3.67   3.78   3.87   3.49   3.82   3.81   3.59   3.56   3.81   3.85   3.61   3.73   3.29   3.76   3.77   3.61   3.79   3.84   3.77		
155511438_uff_E=428.22_out_5	GLY222   TRP58   TRP58   ILE111   TRP58   TRP58   ILE111   ILE62   TRP58   TRP58   ILE62   TRP58   TRP58   TRP58   TRP58   TRP58   TRP58   TRP58   TRP58   ILE221   ILE221   PHE70   ILE221   ILE62   VAL66   ILE62   ILE221   LEU65   ILE221	3.77   3.76   3.67   3.67   3.71   3.75   3.84   3.76   3.68   3.74   3.75   3.80   3.67   3.78   3.71   3.60   3.86   3.83   3.88   3.63   3.58   3.73   3.53   3.26   3.70   3.81   3.68   3.67   3.58		
155511438_uff_E=428.22_out_6	SER345   PRO344   PRO344   ILE498     ILE498   ILE498   ILE498   ILE498   ILE498   TYR501   TYR501   TYR501   TYR501   TYR501   TYR501   TYR501   ILE498   TYR501   TYR501   TYR501   ILE498   TYR501   TYR501   TYR501	3.80   3.63   3.78   3.78   3.75   3.88   3.59   3.77   3.81   3.80   3.75   3.70   3.74   3.67   3.80   3.78   3.44   3.86   3.24   3.72   3.68   3.88   3.46   3.75		
155511438_uff_E=428.22_out_7	TRP241   TRP241   TRP241   TRP241     VAL420   TRP241   TRP241   PHE230   PHE230   PHE230   PHE230     PHE230   VAL420   LEU235   PHE230   PHE230   PHE230   PHE230     VAL420   ILE227   LEU235   PHE230     PHE230   PHE230   PHE230	3.51   3.54   3.77   3.85   3.68   3.88   3.84   3.62   3.46   3.61   3.72   3.79   3.51   3.77   3.89   3.79   3.75   3.63   3.70   3.78   3.86   3.55   3.60   3.81   3.49		
155511438_uff_E=428.22_out_8	TRP225   TRP225   GLY222   PHE115     PHE115   PHE115   ILE62   ILE221   ILE221   ILE221   ILE221   PHE70   PHE70   ILE221   PHE115   VAL66   ILE221   PHE115   PHE70   VAL66   ILE221   ILE221	3.78   3.88   3.65   3.41   3.63   3.87   3.84   3.89   3.75   3.79   3.64   3.83   3.68   3.62   3.88   3.42   3.63   3.72   3.66   3.87   3.63   3.60		
155511438_uff_E=428.22_out_9	VAL456   LEU295   ILE39   ILE39   THR36   ILE39   ILE39   ILE39   ILE39     GLN299   SER298   GLN302   GLN302   GLN299   GLN299   SER298     SER298	3.76   3.31   3.53   3.74   3.61   3.68   3.72   3.76   3.79   3.72   3.80   3.77   3.90   3.74   3.77   3.39   3.72		
<b>CHEMBL4451825</b>				
155521642_uff_E=557.43_out				

155521642_uff_E=557.43_out_1	ASP64   THR465   LEU61   THR465   LEU107   LEU107   LEU107   LEU61   LEU61   LEU61   LYS67   LYS67   LYS67   TYR62   TYR62   TYR62   VAL444	3.51   3.79   3.77   3.67   3.32   3.67   3.71   3.84   3.85   3.52   3.28   3.81   3.87   3.54   3.48   3.72   3.65
155521642_uff_E=557.43_out_2	TRP208   TRP208   THR213   ILE214   PHE70   PHE70   PHE70   PHE70   TRP208   TRP208   TRP208   TRP208     TRP208   PHE77   TRP208   TRP208     TRP208   PRO73   TRP208   LEU74   THR213   TRP208   TRP208   TRP208     TRP208   TRP208	3.66   3.73   3.55   3.53   3.84   3.88   3.79   3.51   3.86   3.74   3.67   3.73   3.53   3.83   3.66   3.89   3.88   3.57   3.79   3.48   3.85   3.54   3.18   3.61   3.53   3.72
155521642_uff_E=557.43_out_3	LEU266   LEU266   PHE254   MET409     VAL405   PHE271   PHE271   PHE271   PHE271   THR280   PHE271     VAL255   VAL255   PHE271   PHE271   VAL268   VAL268   VAL255     VAL255   PHE271   PHE271   VAL255   VAL255   VAL255   VAL255     VAL255   VAL255	3.72   3.70   3.55   3.89   3.60   3.88   3.74   3.70   3.58   3.34   3.86   3.68   3.23   3.49   3.78   3.41   3.64   3.83   3.73   3.84   3.70   3.86   3.68   3.79   3.90   3.57   3.60
155521642_uff_E=557.43_out_4	TRP225   TRP225   GLY222   TRP58   TRP58   TRP58   TRP58   ILE111   ILE111   ILE221   ILE221   ILE221   ILE221   ILE221   PHE70   PHE70   ILE221   PHE115   VAL66   ILE221   PHE115   PHE70   VAL66   ILE221   ILE221	3.76   3.80   3.60   3.61   3.85   3.73   3.83   3.84   3.50   3.90   3.86   3.72   3.79   3.61   3.84   3.69   3.62   3.88   3.45   3.68   3.69   3.68   3.89   3.62   3.60
155521642_uff_E=557.43_out_5	ILE39   ILE39   PRO43   PRO43   PRO43   PRO43   MET40   MET40   PRO309   LEU295   ILE39   PRO161   PRO161   SER298	3.89   3.39   3.85   3.79   3.68   3.57   3.83   3.77   3.57   3.70   3.74   3.47   3.52   3.33
155521642_uff_E=557.43_out_6	VAL456   VAL456   VAL456   GLN299     GLN299   GLN299   LEU295   LEU295   PRO161   THR36   PRO161     THR36   ILE39   PRO309   MET40   MET40   PRO309   PRO43   MET40	3.81   3.74   3.45   3.55   3.80   3.61   3.84   3.66   3.80   3.63   3.73   3.81   3.89   3.54   3.57   3.80   3.83   3.73   3.78
155521642_uff_E=557.43_out_7	PHE416   LEU412   LEU223   LEU412     PHE271   PHE271   MET409   ILE281   ILE281   ILE496   MET285   PHE284   ILE281   ILE281   PHE284   ILE281   ILE281   ILE281   ILE281   PHE284   PHE284	3.68   3.89   3.48   3.76   3.62   3.70   3.73   3.89   3.78   3.84   3.31   3.88   3.71   3.40   3.66   3.76   3.82   3.88   3.50   3.49   3.81
155521642_uff_E=557.43_out_8	PHE355   PHE359   PHE355   PHE355     PHE359   PHE359   PHE360   PHE360   PHE360   PHE360   PHE360     PHE359   PHE359   PHE359   PHE359   PHE359   PHE359   PHE359     PHE359   PHE355   PHE355   PHE359   ILE356   ILE352   PHE359   ILE356   PHE355   PHE355   ILE356   ILE356   ILE356	3.56   3.51   3.78   3.67   3.86   3.84   3.77   3.68   3.75   3.34   3.77   3.47   3.84   3.74   3.77   3.78   3.68   3.52   3.64   3.63   3.74   3.86   3.70   3.55   3.79   3.77   3.62   3.68   3.77   3.69   3.67

155521642_uff_E=557.43_out_9	PRO161   PRO161   PRO161   MET40   MET40   THR36   GLN302   GLN299   VAL456   GLN299   GLN299   VAL456   VAL456   SER454   MET40   MET40   ILE39   PRO43   MET40   ILE39   PRO309	3.78   3.87   3.90   3.45   3.62   3.49   3.74   3.87   3.74   3.28   3.61   3.42   3.69   3.74   3.74   3.86   3.70   3.84   3.72   3.77   3.63		
<b>CHEMBL4468065</b>				
155532943_uff_E=441.09_out				
155532943_uff_E=441.09_out_1	TRP208   TRP208   ILE210   ILE214   THR213   TRP208   LEU74   THR213   TRP208   TRP208   TRP208   TRP208   TRP208   TRP208   TRP208   TRP208   TRP208   TRP208	3.68   3.66   3.70   3.79   3.82   3.75   3.81   3.67   3.64   3.73   3.53   3.71   3.86   3.90   3.90   3.55   3.84   3.55   3.79   3.57   3.20   3.59   3.57   3.77		
155532943_uff_E=441.09_out_2	ASP64   LEU107   LEU107   LEU61   LEU61   LEU61   LYS67   LYS67   LYS67   ILE443   LYS67   TYR62   TYR62   TYR62   LEU447   VAL444	3.66   3.75   3.76   3.89   3.78   3.80   3.54   3.11   3.82   3.76   3.76   3.82   3.58   3.57   3.79   3.83   3.68		
155532943_uff_E=441.09_out_3	SER345   PRO344   PRO344   ILE494   ILE498   ILE498   TYR501   TYR501   TYR501   TYR501   TYR501   TYR501   TYR501   ILE498   TYR501   TYR501	3.75   3.62   3.76   3.76   3.86   3.65   3.79   3.74   3.69   3.73   3.62   3.75   3.82   3.42   3.32   3.79   3.67   3.46   3.75		
155532943_uff_E=441.09_out_4	VAL456   VAL303   GLN302   GLN302   GLN299   GLN299   GLN299   GLN299   GLN299   GLN302   GLN302   GLN299   GLN302   GLN299   SER298   PRO309   MET40   PRO161   PRO161   PRO309	3.57   3.89   3.72   3.47   3.65   3.73   3.63   3.82   3.35   3.83   3.67   3.68   3.89   3.21   3.76   3.85   3.80   3.83   3.78   3.86   3.81   3.43		
155532943_uff_E=441.09_out_5	LEU107   LEU107   VAL444   GLY442   THR465   LYS67   ALA63	3.88   3.58   3.79   3.85   3.86   3.49   3.71		
155532943_uff_E=441.09_out_6	TYR501   ILE498   ILE498   ILE498   ILE498   TYR501   TYR501   TYR501   TYR501   TYR501   TYR501   TYR501   TYR501   ILE494   ILE352   ILE352   ILE494	3.83   3.60   3.86   3.90   3.68   3.79   3.63   3.61   3.75   3.70   3.50   3.75   3.67   3.88   3.76   3.61   3.61   3.82   3.41   3.76		
155532943_uff_E=441.09_out_7	ILE341   ILE341   GLY348   TYR501   TYR501   TYR501   ILE498   ILE498   ILE498   TYR501   TYR501   TYR501   PRO344   TYR501   TYR501   ILE498   SER497   TYR501   PRO344   TYR501   TYR501	3.70   3.40   3.73   3.71   3.64   3.85   3.41   3.78   3.78   3.61   3.86   3.58   3.82   3.84   3.68   3.78   3.32   3.60   3.69   3.60   3.74   3.89   3.78		
155532943_uff_E=441.09_out_8	PHE355   PHE359   PHE355   PHE355   PHE360   PHE359   PHE359   PHE359   PHE359   PHE359   PHE359   PHE359   PHE359   PHE359   ILE352   ILE356   PHE355   PHE355   PHE359   ILE356   ILE352   ILE356   ILE356   ILE356   PHE359   ILE356   ILE356   ILE356	3.66   3.57   3.78   3.70   3.76   3.54   3.74   3.89   3.75   3.84   3.75   3.66   3.81   3.66   3.73   3.75   3.77   3.65   3.63   3.85   3.58   3.73   3.81   3.73   3.62   3.61		

155532943_uff_E=441.09_out_9	MET40   MET40   THR36   PRO161   VAL456   VAL456   VAL456   GLN299   GLN302   GLN302   GLN299   MET40   ILE39   ILE39   PRO309   PRO309	3.61   3.50   3.29   3.79   3.84   3.90   3.71   3.76   3.76   3.89   3.71   3.84   3.71   3.56   3.88   3.51
<b>CHEMBL4471445</b>		
155535100_uff_E=518.38_out		
155535100_uff_E=518.38_out_1	SER345   PRO344   PRO344   PRO344   TYR501   TYR501   TYR501   TYR501   TYR501   TYR501   TYR501   TYR501   TYR501   ILE498   TYR501   TYR501   TYR501   TYR501   ILE498   ILE498   TYR501   TYR501	3.82   3.68   3.82   3.89   3.76   3.69   3.70   3.70   3.59   3.74   3.81   3.67   3.53   3.48   3.38   3.78   3.88   3.46   3.90   3.61   3.79
155535100_uff_E=518.38_out_2	PHE359   PHE355   PHE355   ILE352   PHE359   PHE359   PHE355   PHE359   PHE359   PHE359   PHE355   PHE355   PHE359   PHE359   PHE359   PHE359   PHE359   PHE355   PHE359   PHE359   PHE359   PHE359   PHE359   LEU487   LEU487   PHE359   PHE355   PHE355   PHE355   PHE359   PHE359   PHE359   PHE359   LEU487   LEU487   LEU487   LEU487   PHE359   PHE359   PHE359   PHE359	3.64   3.70   3.75   3.64   3.84   3.83   3.71   3.79   3.48   3.46   3.17   3.60   3.62   3.41   3.64   3.89   3.78   3.44   3.88   3.53   3.72   3.72   3.84   3.67   3.63   3.81   3.48   3.76   3.54   3.88   3.30
155535100_uff_E=518.38_out_3	TRP208   TRP208   LEU74   PRO73   PRO73   THR213   PRO73   TRP208   ILE210   ILE210   TRP208	3.63   3.54   3.38   3.67   3.58   3.78   3.69   3.79   3.73   3.84   3.85   3.68   3.88   3.79   3.87   3.87   3.65   3.73   3.33   3.72   3.89   3.79   3.44   3.82
155535100_uff_E=518.38_out_4	LEU107   LEU107   LEU107   GLY442   LEU107   LEU107   LEU61   LEU61   ALA63   ALA63	3.59   3.75   3.76   3.70   3.82   3.67   3.76   3.89   3.87   3.82
155535100_uff_E=518.38_out_5	PRO43   PRO309   PRO309   SER298   SER298   PRO309   PRO309   MET40   LEU295   MET40   MET40   ILE39	3.60   3.77   3.67   3.84   3.76   3.64   3.71   3.90   3.60   3.70   3.75   3.76
155535100_uff_E=518.38_out_6	ALA330   ALA381   ALA330   PHE326   PHE326   PHE326   ILE349   LEU333   LEU333   LEU333   ILE329   LEU333   LEU333   LEU333   LEU333   LEU333	3.65   3.85   3.81   3.51   3.85   3.84   3.85   3.57   3.88   3.67   3.11   3.60   3.66   3.73
155535100_uff_E=518.38_out_7	THR213   TRP208   TRP208   TRP208   PRO73   TRP208   TRP208   LEU74   THR89   PHE77   PHE77   PHE77   PHE77   PHE77   ILE119   PHE77   PHE77   ILE119   LEU123   ILE119   PHE77   PHE77   ILE119   LEU74   LEU74   PHE77	3.69   3.75   3.31   3.88   3.70   3.73   3.81   3.74   3.63   3.50   3.65   3.75   3.71   3.90   3.87   3.68   3.27   3.51   3.68   3.75   3.52   3.37   3.80   3.80
155535100_uff_E=518.38_out_8	VAL385   SER382   SER382   ALA330   ALA381   ALA330   LEU333   LEU333   VAL342   VAL342   ILE349   LEU333   VAL342   VAL342   LEU333   LEU333   LEU333   LEU333   ILE349	3.82   3.87   3.54   3.60   3.58   3.40   3.74   3.67   3.88   3.60   3.55   3.51   3.83   3.84   3.26   3.55   3.86   3.46

155535100_uff_E=518.38_out_9	GLY313   ALA312   ALA312   SER298   PRO161   PRO161   THR36   ILE39   ILE39   ILE39   LEU295   MET40   MET40   ILE39   SER298	3.59   3.90   3.89   3.87   3.47   3.75   3.83   3.86   3.55   3.69   3.69   3.71   3.83   3.77   3.65				
<b>CHEMBL4471914</b>						
155535609_uff_E=406.55_out_1	TRP208   TRP208   ILE214   THR213   TRP208   TRP208   TRP208   TRP208   TRP208   TRP208   TRP208   PRO73   TRP208   LEU74   THR213   TRP208   TRP208   TRP208   TRP208   TRP208   TRP208	3.67   3.64   3.71   3.74   3.75   3.80   3.65   3.62   3.72   3.51   3.68   3.85   3.90   3.59   3.84   3.58   3.79   3.60   3.24   3.62   3.57   3.76				
155535609_uff_E=406.55_out_2	LEU107   LEU107   LEU107   GLY442   LEU107   LEU107   LEU61   THR465   LYS67   ALA63	3.66   3.73   3.64   3.78   3.85   3.73   3.82   3.82   3.69   3.71				
155535609_uff_E=406.55_out_3	SER345   PRO344   PRO344   ILE498   ILE498   TYR501   ILE498   TYR501   TYR501   TYR501   ILE498   TYR501   TYR501   ILE498   TYR501   TYR501	3.76   3.61   3.76   3.85   3.62   3.79   3.74   3.70   3.73   3.63   3.75   3.81   3.43   3.31   3.78   3.66   3.45   3.75				
155535609_uff_E=406.55_out_4	LEU61   LEU447   LEU447   ILE443   LEU107   ASP64   THR465   LEU61   THR465   LEU107	3.64   3.85   3.47   3.90   3.78   3.69   3.73   3.81   3.89   3.78				
155535609_uff_E=406.55_out_5	GLN4   GLN4   GLN4   GLN4   GLN4   TYR114   TYR114	3.82   3.60   3.82   3.62   3.81   3.71   3.50				
155535609_uff_E=406.55_out_6	TYR501   GLY348   SER345   ILE352   ILE494   ILE494   ILE352   ILE352   ILE494   ILE494   ILE352   ILE494	3.80   3.73   3.81   3.65   3.74   3.66   3.89   3.68   3.86   3.72   3.86   3.60   3.78   3.83   3.65   3.58   3.87   3.49   3.66   3.85   3.60   3.72   3.53   3.61				
155535609_uff_E=406.55_out_7	THR465   LEU447   ILE443   GLY442   LEU61   LEU61   LEU447   VAL444   VAL444   VAL444   LYS67   ASP64   LYS67   LYS67   LYS67   ASP64	3.71   3.63   3.72   3.84   3.76   3.69   3.67   3.89   3.84   3.39   3.68   3.79   3.67   3.76   3.59   3.60				
155535609_uff_E=406.55_out_8	PHE183   PHE183   PHE183   ILE163   PHE183   PHE29   PHE29   PHE29   PHE29   PHE29   PHE29   PHE159   ILE155   PHE29   PHE29   PHE29   PHE29   PHE29   PHE29   PHE29   PHE29   PHE29	3.65   3.69   3.81   3.77   3.71   3.62   3.86   3.64   3.73   3.71   3.86   3.65   3.40   3.66   3.80   3.86   3.32   3.58				
155535609_uff_E=406.55_out_9	PRO395   GLU393   GLU393   GLU393   GLU137   GLU137   GLN513   GLN513	3.63   3.80   3.81   3.86   3.83   3.60   3.62   3.86				
<b>CHEMBL4515503</b>						
155539703_uff_E=413.03_out						
155539703_uff_E=413.03_out_1	PHE355   PHE355   ILE352   PHE359   PHE355   PHE355   PHE355   PHE355   PHE355   PHE355   PHE359   PHE359   PHE359   PHE355   PHE355   PHE355   PHE355   PHE355   PHE355   PHE359   PHE359   PHE355   PHE355	3.70   3.70   3.65   3.52   3.86   3.88   3.47   3.85   3.88   3.87   3.69   3.81   3.54   3.56   3.89   3.13   3.61   3.68   3.47   3.74   3.74   3.46   3.65   3.76				

	LEU487   PHE359   PHE355   PHE355   PHE359   PHE359   LEU487   LEU487   PHE359   PHE359	3.84   3.71   3.71   3.73   3.67   3.82   3.84   3.38
155539703_uff_E=413.03_out_2	TRP241   VAL245   ILE244   TRP241   PHE416   PHE416   ILE244   TRP241   TRP241   TRP241   ILE244   PHE416   PHE230   TRP241   TRP241   PHE230   PHE416   PHE416   ILE227   PHE230   ILE244   ILE244   PHE230   PHE230   PHE230	3.67   3.86   3.82   3.69   3.86   3.89   3.63   3.50   3.83   3.84   3.34   3.75   3.52   3.62   3.69   3.74   3.40   3.48   3.59   3.77   3.88   3.78   3.89   3.47   3.65
155539703_uff_E=413.03_out_3	SER345   PRO344   PRO344   PRO344   ILE498   ILE498   TYR501   TYR501   TYR501   TYR501   TYR501   TYR501   TYR501   ILE498   TYR501   TYR501   TYR501   ILE498   TYR501   TYR501   TYR501	3.86   3.82   3.60   3.74   3.55   3.75   3.81   3.74   3.69   3.74   3.56   3.69   3.87   3.64   3.87   3.31   3.85   3.76   3.85   3.41   3.76
155539703_uff_E=413.03_out_4	LEU107   LEU107   THR465   LYS67   ALA63	3.80   3.64   3.66   3.48   3.58
155539703_uff_E=413.03_out_5	TRP241   TRP241   TRP241   TRP241   TRP241   TRP241   PHE230   PHE230   PHE230   VAL420   PHE230   LEU235   PHE230   PHE230   PHE230   PHE230   VAL420   LEU235   PHE230   PHE230   PHE230   PHE230	3.63   3.58   3.80   3.83   3.76   3.75   3.62   3.42   3.66   3.60   3.75   3.85   3.79   3.78   3.74   3.69   3.66   3.81   3.63   3.57   3.80   3.45
155539703_uff_E=413.03_out_6	TRP208   TRP208   TRP208   TRP208   PRO73   LEU116   LEU74   LEU74   THR89   PHE77   PHE77   PHE77   PHE77   LEU74   LEU123   ILE119   PHE77   LEU123   ILE119   LEU74   PHE77	3.68   3.87   3.67   3.30   3.54   3.83   3.80   3.52   3.74   3.66   3.65   3.70   3.74   3.80   3.73   3.74   3.76   3.52   3.88   3.70   3.68
155539703_uff_E=413.03_out_7	TRP115   ARG46   TRP115   TRP115   ARG46   ARG46   PHE38   PHE38   PHE38   PHE38   ARG46   ARG46   PHE38   PHE38   ALA48   PHE38   PHE112   ASP111   PHE38   TRP59   ALA48	3.75   3.84   3.78   3.72   3.32   3.80   3.62   3.65   3.43   3.88   3.62   3.77   3.59   3.87   3.78   3.78   3.75   3.65   3.74   3.81   3.63
155539703_uff_E=413.03_out_8	VAL420   PHE416   PHE416   PHE416   ILE227   PHE230   PHE230   ILE227   ILE227   VAL420   PHE230   PHE230   PHE416   PHE230   PHE230   ILE248   ILE244   PHE230   TRP241   ILE244   TRP241   TRP241   PHE230   ILE244	3.36   3.65   3.75   3.75   3.29   3.78   3.20   3.61   3.87   3.72   3.65   3.73   3.71   3.84   3.82   3.67   3.19   3.79   3.61   3.87   3.81   3.85   3.72   3.68
155539703_uff_E=413.03_out_9	VAL420   PHE416   PHE416   PHE416   PHE416   ILE227   PHE230   PHE230   PHE230   PHE230   PHE230   ILE248   ILE248   VAL245   ILE244   ILE244   ILE244   ILE244   TRP241   TRP241   TRP241   ILE244   ILE244   ILE244   TRP241   TRP241   TRP241   ILE244	3.80   3.59   3.62   3.67   3.86   3.71   3.46   3.63   3.87   3.78   3.52   3.29   3.58   3.64   3.82   3.84   3.79   3.54   3.89   3.64   3.78   3.75   3.74   3.81   3.50   3.62   3.81   3.42

CHEMBL4519804

155542101_uff_E=518.72_out						
155542101_uff_E=518.72_out_1	LEU61   LEU447   LEU447   ILE443   THR465   THR465   LEU61   LEU61   LEU107	3.78   3.73   3.46   3.68   3.84   3.73   3.48   3.77   3.37				
155542101_uff_E=518.72_out_2	ILE39   ILE39   THR36   PRO161   PRO161   MET40   THR36   ILE39   MET40   MET40   ILE39   PRO161   SER298	3.64   3.70   3.74   3.57   3.74   3.75   3.79   3.83   3.72   3.81   3.69   3.77   3.52				
155542101_uff_E=518.72_out_3	SER345   PRO344   PRO344   PRO344   TYR501   TYR501   TYR501   TYR501   TYR501   TYR501   TYR501   LEU502   TYR501   ILE498   TYR501   TYR501   TYR501   ILE498   ILE498   TYR501   TYR501	3.82   3.68   3.82   3.89   3.76   3.69   3.71   3.70   3.58   3.73   3.81   3.66   3.52   3.45   3.39   3.78   3.87   3.44   3.87   3.61   3.79				
155542101_uff_E=518.72_out_4	PHE478   PHE478   TYR429   SER425   PHE478   PHE478   VAL455   TYR429   TYR429   SER426   SER426	3.56   3.76   3.68   3.80   3.49   3.69   3.73   3.87   3.45   3.61   3.65				
155542101_uff_E=518.72_out_5	PHE355   ILE352   PHE359   PHE359   PHE359   PHE355   PHE359   PHE359   PHE359   PHE355   PHE355   PHE355   PHE359   PHE359   PHE355   PHE355   LEU487   PHE359   PHE355   PHE355   PHE355   PHE359   PHE359   PHE359   LEU487   LEU487   PHE359   PHE359	3.81   3.72   3.62   3.79   3.82   3.82   3.76   3.48   3.53   3.22   3.70   3.76   3.42   3.67   3.80   3.50   3.67   3.73   3.84   3.67   3.87   3.65   3.68   3.86   3.59   3.74   3.86   3.33				
155542101_uff_E=518.72_out_6	GLN4   GLN4   GLN4   GLN4   GLN4   TYR114   GLN4   TYR114   TYR114   TYR114	3.75   3.46   3.71   3.57   3.86   3.86   3.70   3.40   3.88   3.84				
155542101_uff_E=518.72_out_7	VAL420   PHE416   PHE416   PHE416   PHE416   PHE416   ILE227   PHE230   PHE230   ILE227   VAL420   PHE230   PHE230   PHE416   PHE230   PHE230   ILE248   ILE244   ILE244   PHE230   TRP241   TRP241   ILE244   TRP241   TRP241   PHE230   ILE244	3.46   3.52   3.66   3.61   3.88   3.84   3.28   3.83   3.30   3.66   3.72   3.58   3.72   3.68   3.75   3.77   3.74   3.15   3.84   3.76   3.70   3.88   3.84   3.84   3.84   3.66   3.60				
155542101_uff_E=518.72_out_8	ASP267   ASP263   SER397   LEU200   LYS398   LYS398   ASP267   ASP267   LYS398   LEU200   ASP263   ASP263   ASP263	3.69   3.60   3.62   3.35   3.48   3.72   3.59   3.25   3.67   3.57   3.59   3.83   3.72				
155542101_uff_E=518.72_out_9	TRP241   TRP241   TRP241   VAL420   TRP241   TRP241   PHE230   PHE230   PHE230   PHE230   PHE230   LEU235   PHE230   PHE230   PHE230   PHE230   PHE230   ILE227   LEU235   VAL420   PHE230   PHE230   PHE230	3.53   3.63   3.81   3.86   3.88   3.80   3.50   3.36   3.52   3.66   3.76   3.81   3.80   3.71   3.71   3.58   3.59   3.76   3.84   3.46   3.55   3.78   3.58				
<b>CHEMBL4574206</b>						
155563682_uff_E=423.90_out						
155563682_uff_E=423.90_out_1	TRP208   TRP208   TRP208   TRP208   TRP208   TRP208   TRP208   TRP208   TRP208   TRP208   PRO73   TRP208	3.66   3.62   3.75   3.79   3.64   3.63   3.74   3.52   3.68   3.87   3.62   3.88				

	LEU74   THR213   TRP208   TRP208   TRP208   TRP208   TRP208	3.59   3.79   3.61   3.25   3.63   3.58   3.76		
155563682_uff_E=423.90_out_2	PRO43   PRO309   PRO309   SER298   MET40   MET40   ILE39   GLN299	3.63   3.89   3.79   3.81   3.70   3.66   3.83   3.72		
155563682_uff_E=423.90_out_3	ASP64   LEU61   LEU61   LEU61   LYS67   LYS67   LYS67   ILE443   LYS67   TYR62   TYR62   TYR62   LEU447   VAL444	3.64   3.75   3.77   3.48   3.08   3.80   3.75   3.76   3.78   3.54   3.58   3.76   3.80   3.68		
155563682_uff_E=423.90_out_4	VAL456   VAL303   GLN302   GLN299   GLN299   GLN299   GLN299   VAL456   MET40   MET40   GLN302   GLN302   GLN299   GLN302   PRO309   PRO309	3.49   3.88   3.67   3.63   3.74   3.72   3.86   3.83   3.87   3.42   3.64   3.57   3.23   3.60   3.60   3.37		
155563682_uff_E=423.90_out_5	LEU447   ILE443   LEU61   LEU447   ASP64   LEU61   THR465   THR465   LEU61   LEU61   LEU107   LEU107	3.45   3.54   3.89   3.72   3.78   3.89   3.73   3.71   3.36   3.71   3.47   3.82		
155563682_uff_E=423.90_out_6	PRO344   SER345   PRO344   PRO344   TYR501   TYR501   TYR501   TYR501   TYR501   TYR501   TYR501   ILE498   TYR501   TYR501   TYR501   ILE498   TYR501   TYR501   TYR501	3.85   3.84   3.60   3.74   3.83   3.75   3.70   3.74   3.58   3.70   3.85   3.59   3.87   3.30   3.82   3.73   3.84   3.39   3.73		
155563682_uff_E=423.90_out_7	PHE359   PHE355   PHE355   ILE352   PHE359   PHE359   PHE355   PHE359   PHE359   PHE359   PHE355   PHE355   PHE355   PHE359   PHE359   PHE355   PHE355   LEU487   TYR358   PHE359   PHE355   PHE359   PHE359   LEU487   LEU487   LEU487   PHE359   PHE359   PHE359   PHE359	3.59   3.71   3.71   3.63   3.87   3.85   3.69   3.79   3.48   3.47   3.17   3.60   3.63   3.40   3.64   3.79   3.46   3.48   3.78   3.66   3.77   3.67   3.64   3.62   3.81   3.66   3.83   3.31   3.85   3.88		
155563682_uff_E=423.90_out_8	LEU107   LEU107   THR465   LYS67   ALA63	3.76   3.58   3.64   3.52   3.63		
155563682_uff_E=423.90_out_9	ALA330   ALA381   ALA330   PHE326   PHE326   PHE326   ILE349   LEU333   ILE329   LEU333   LEU333   LEU333   LEU333	3.52   3.58   3.86   3.38   3.74   3.82   3.77   3.65   3.16   3.57   3.89   3.73   3.75		
<b>CHEMBL2374044</b>				
16758167_uff_E=329.45_out				
16758167_uff_E=329.45_out_1	PHE416   ILE244   PHE416   PHE416   PHE416   PHE416   PHE230   SER423   ALA419   SER231   ILE227   PHE230   LEU235   PHE230   PHE230   PHE230   PHE230   PHE230   PHE230   PHE230   VAL420	3.77   3.53   3.74   3.87   3.45   3.73   3.77   3.56   3.63   3.75   3.48   3.67   3.70   3.86   3.44   3.67   3.81   3.18   3.75   3.84   3.80		
16758167_uff_E=329.45_out_2	MET35   MET35   LEU295   ILE39   THR36   LEU295   ILE39   LEU295   ILE39   SER298   ILE39	3.90   3.88   3.55   3.73   3.80   3.45   3.59   3.73   3.48   3.67   3.45		
16758167_uff_E=329.45_out_3	VAL456   GLN302   GLN302   GLN299   GLN299   VAL456   GLN302   PRO309   GLN302   GLN302   GLN302   GLN302   GLN299   GLN302	3.54   3.79   3.67   3.72   3.88   3.84   3.69   3.83   3.49   3.70   3.90   3.67   3.38   3.79   3.70   3.36		

	LEU295   PRO161   PRO161   GLN299   SER298   ILE39   SER298   SER298	3.79   3.59   3.63   3.71   3.83   3.67
16758167_uff_E=329.45_out_4	GLN302   GLN302   GLN299   LEU295   PRO161   THR36   ILE39   ILE39   THR36   ILE39   ILE39   ILE39   ILE39	3.64   3.86   3.68   3.62   3.48   3.62   3.80   3.76   3.65   3.61   3.60   3.51   3.50   3.74
16758167_uff_E=329.45_out_5	VAL268   VAL255   PHE271   PHE271   MET409   PHE271   PHE271   VAL268   VAL268   VAL255   PHE271   VAL268   VAL255   LEU266   PHE254   ILE72   MET409   MET220   VAL268   VAL268   LEU266   VAL255   VAL255   ILE251   ILE251   MET220   VAL268   LEU266   VAL255   PHE254   ILE251   MET220   VAL255   ILE251	3.84   3.74   3.59   3.80   3.70   3.77   3.78   3.78   3.73   3.88   3.73   3.80   3.54   3.58   3.70   3.77   3.42   3.82   2.79   3.68   3.77   3.83   3.83   3.70   3.77   3.70   3.90   3.84   3.73
16758167_uff_E=329.45_out_6	LEU447   LEU447   LEU61   LEU61   LEU61   THR465   LEU107	3.57   3.86   3.54   3.53   3.67   3.89   3.56
16758167_uff_E=329.45_out_7	SER108   LEU107   LEU107   LEU107   LEU61   LEU61   LEU61   GLY442   GLY442   LEU61   LEU61   THR465	3.74   3.68   3.88   3.84   3.49   3.72   3.80   3.70   3.65   3.67   3.86   3.77
16758167_uff_E=329.45_out_8	PHE230   PHE230   ILE227   ILE227   ILE227   PHE416   PHE416   PHE416   PHE230   ILE244   ILE244   TRP241   TRP241   TRP241   PHE230   ILE244   VAL245   VAL245   ILE244   TRP241   VAL245   VAL245   ILE248   ILE244	3.74   3.28   3.15   3.87   3.71   3.57   3.64   3.87   3.33   3.63   3.76   3.90   3.71   3.67   3.67   3.55   3.77   3.66   3.73   3.78   3.39   3.68   3.69   3.41
16758167_uff_E=329.45_out_9	PHE416   PHE230   PHE230   ILE227   PHE416   PHE230   VAL420   LEU235   SER423   VAL420   VAL420   LEU235	3.78   3.58   3.47   3.70   3.59   3.79   3.72   3.41   3.53   3.66   3.81   3.73

### CHEMBL5407683

455260_uff_E=337.63_out		
455260_uff_E=337.63_out_1	LEU223   PHE416   PHE416   LEU412   LEU223   LEU412   LEU223   PHE284   PHE284   PHE284   ILE281   ILE281   ILE496   MET285   PHE284   PHE284   PHE284   ILE281   ILE281   ILE281   PHE284   PHE284   MET285   PHE284   ILE281   ILE281   ILE281   PHE284   PHE284	3.70   3.47   3.63   3.64   3.52   3.51   3.78   3.82   3.72   3.79   3.70   3.61   3.72   3.67   3.68   3.74   3.85   3.75   3.46   3.64   3.63   3.90   3.73   3.77   3.87   3.60   3.53   3.82
455260_uff_E=337.63_out_2	ILE467   ILE467   TYR52   GLN72	3.72   3.62   3.85   3.64
455260_uff_E=337.63_out_3	LEU107   LYS67   LYS67   VAL444   VAL444   VAL444	3.69   3.74   3.89   3.56   3.72   3.54
455260_uff_E=337.63_out_4	GLU47   ARG46   ARG46   PHE38   PHE38   ARG46   PHE112   PHE38   ALA48   PHE38   ALA48   ALA48	3.77   3.68   3.78   3.72   3.76   3.72   3.73   3.52   3.83   3.67   3.67   3.62
455260_uff_E=337.63_out_5	GLN4   GLN4   GLN4   GLN4   GLN4   TYR114   TYR114   GLN4	3.82   3.57   3.82   3.64   3.73   3.64   3.61   3.85
455260_uff_E=337.63_out_6	PHE159   PHE159   PHE159   PHE29   PHE159   PHE159   PHE159   PHE29	3.81   3.52   3.78   3.45   3.66   3.52   3.79   3.85

	VAL148   ALA152   VAL148   ALA25   ALA25   PHE29   PHE29   PHE29   PHE29   ILE151   ILE151   ILE151   ILE151   VAL148   MET324   ILE151	3.76   3.73   3.83   3.21   3.76   3.54   3.78   3.45   3.86   3.74   3.52   3.74   3.80   3.79   3.88   3.80		
455260_uff_E=337.63_out_7	LEU246   LEU246   VAL243   VAL243     GLY222   LEU65   TRP58   GLY222   ILE221   TRP225   TRP225   TRP225   ILE221   TRP225   TRP225   TRP225   TRP58	3.75   3.59   3.57   3.70   3.87   3.61   3.54   3.41   3.74   3.75   3.75   3.86   3.66   3.54   3.80   3.73   3.70		
455260_uff_E=337.63_out_8	LEU123   PHE77   PHE77   LEU74   PHE77   PHE77   LEU74   LEU74   LEU74   THR213   THR213   TRP208   TRP208   TRP208   TRP208   TRP208     TRP208   TRP208   TRP208   TRP208	3.19   3.47   3.76   3.71   3.84   3.70   3.42   3.83   3.67   3.52   3.87   3.90   3.73   3.72   3.35   3.51   3.86   3.76   3.58   3.76		
455260_uff_E=337.63_out_9	TYR114   TYR114   TYR114   TYR114     TYR114   GLN4   GLN4   GLN4	3.72   3.83   3.79   3.74   3.81   3.40   3.66   3.76		
<b>CHEMBL2376099</b>				
71712255_uff_E=471.71_out				
71712255_uff_E=471.71_out_1	MET35   MET35   MET35   LEU295   ILE39   THR36   LEU295   ILE39   ILE39   LEU295   ILE39   ILE39   MET40   MET40   PRO161   THR36   ILE39	3.82   3.74   3.86   3.63   3.59   3.80   3.57   3.71   3.80   3.86   3.56   3.78   3.75   3.81   3.47   3.71   3.88		
71712255_uff_E=471.71_out_2	PHE355   PHE355   ILE352   PHE359   PHE359   PHE355   PHE359   PHE359     PHE359   PHE355   PHE355   PHE355   PHE359   PHE359   PHE359     PHE355   PHE355   PHE355   LEU487   LEU487   PHE359   PHE359     PHE355   PHE355   PHE359   PHE359   PHE355   PHE359   LEU487     LEU487   PHE359   PHE359   PHE359	3.69   3.75   3.68   3.69   3.86   3.84   3.88   3.44   3.33   3.30   3.65   3.51   3.47   3.53   3.71   3.78   3.30   3.81   3.58   3.63   3.60   3.76   3.60   3.68   3.89   3.76   3.86   3.81   3.68   3.68   3.89   3.41   3.85		
71712255_uff_E=471.71_out_3	ALA157   ALA157   TYR410   MET125     MET125   LEU67   LEU294   LEU294     VAL418   LEU295   ALA291   ASN414   LEU295   MET35	3.23   3.65   3.76   3.72   3.87   3.48   3.42   3.76   3.58   3.89   3.73   3.63   3.29   3.82		
71712255_uff_E=471.71_out_4	SER345   PRO344   PRO344   TYR501     TYR501   TYR501   TYR501   TYR501     TYR501   TYR501   LEU502   TYR501     ILE498   TYR501   TYR501   ILE498   TYR501   TYR501	3.79   3.60   3.83   3.71   3.66   3.71   3.73   3.61   3.80   3.81   3.62   3.60   3.51   3.35   3.79   3.46   3.60   3.81		
71712255_uff_E=471.71_out_5	VAL456   GLN302   GLN302   GLN299     GLN299   GLN299   GLN302   GLN302   GLN302   GLN302   GLN302     GLN299   GLN302   PRO161   SER298   PRO161   PRO161   PRO161     PRO309	3.79   3.72   3.62   3.58   3.85   3.77   3.68   3.51   3.79   3.86   3.74   3.61   3.88   3.72   3.74   3.88   3.74   3.85   3.63		
71712255_uff_E=471.71_out_6	LEU61   LEU447   LEU447   LEU107   LEU61   LEU61   LEU61   THR465	3.76   3.67   3.76   3.68   3.77   3.62   3.84   3.69		

71712255_uff_E=471.71_out_7	LEU61   LEU447   LEU447   ILE443   LEU61   THR465   THR465   LEU61   LEU61   LEU61   LEU107   LEU107	3.90   3.81   3.52   3.53   3.85   3.68   3.72   3.31   3.73   3.90   3.33   3.59		
71712255_uff_E=471.71_out_8	PHE183   PHE183   PHE29   ILE155   PHE29   PHE29   PHE29   PHE29   PHE29   PHE159   PHE159   ILE155   PHE29   PHE29   VAL26   ILE155   PHE29   PHE29   PHE29	3.61   3.66   3.58   3.77   3.90   3.80   3.57   3.56   3.82   3.71   3.53   3.44   3.67   3.70   3.88   3.82   3.54   3.60   3.75		
71712255_uff_E=471.71_out_9	ILE244   TRP241   TRP241   TRP241   TRP241   PHE230   PHE230   PHE230     TRP241   PHE230   PHE230   PHE230   PHE230   PHE230   PHE230   LEU235     VAL420   PHE230   PHE230   PHE230   PHE230	3.72   3.75   3.84   3.69   3.71   3.60   3.34   3.83   3.86   3.71   3.63   3.76   3.75   3.74   3.80   3.59   3.42   3.80   3.60		
<b>CHEMBL1096627</b>				
9974918_uff_E=529.05_out				
9974918_uff_E=529.05_out_1	VAL418   LEU295   MET35   LEU295   ILE39   LEU295   ILE39   ILE39   LEU295   ILE39   ILE39   LEU295   ILE39   MET40   THR36   MET40   THR36   ILE39	3.41   3.70   3.69   3.64   3.82   3.41   3.63   3.84   3.48   3.56   3.78   3.80   3.66   3.57   3.84   3.86   3.29   3.42		
9974918_uff_E=529.05_out_2	PHE355   PHE355   ILE352   PHE359   PHE359   PHE359   PHE359   PHE355     PHE359   PHE359   PHE359   PHE355   PHE355   PHE355   PHE359     PHE359   PHE355   PHE355   LEU487   LEU487   PHE359   PHE355     PHE355   PHE359   PHE359   LEU487   LEU487   LEU487   PHE359	3.72   3.82   3.69   3.59   3.74   3.85   3.82   3.67   3.78   3.50   3.48   3.15   3.58   3.63   3.43   3.69   3.76   3.45   3.89   3.61   3.75   3.76   3.88   3.68   3.64   3.46   3.71   3.52   3.35		
9974918_uff_E=529.05_out_3	VAL456   GLN302   GLN302   GLN299     GLN299   GLN299   GLN302   GLN302   GLN302   GLN302   GLN299     GLN302   PRO161   SER298   PRO161   PRO161   PRO309	3.77   3.73   3.63   3.59   3.85   3.78   3.73   3.50   3.78   3.76   3.57   3.83   3.75   3.74   3.78   3.90   3.64		
9974918_uff_E=529.05_out_4	PHE416   LEU223   PHE416   PHE416     LEU412   LEU412   ILE227   LEU223     LEU223   LEU412   PHE284   PHE284   PHE284   ILE281   MET285     PHE284   ILE281   ILE281   PHE284     PHE284   THR280   ILE281   ILE281     MET409	3.68   3.89   3.33   3.41   3.62   3.76   3.84   3.30   3.73   3.82   3.79   3.67   3.74   3.81   3.41   3.54   3.78   3.75   3.60   3.69   3.67   3.27   3.55   3.43		
9974918_uff_E=529.05_out_5	ILE341   ILE341   SER497   TYR501   TYR501   TYR501   TYR501   TYR501     TYR501   TYR501   TYR501   LEU502     TYR501   ILE498   TYR501   TYR501     TYR501   ILE498   ILE498   TYR501   TYR501	3.85   3.82   3.80   3.79   3.80   3.71   3.77   3.89   3.54   3.73   3.87   3.75   3.55   3.25   3.41   3.74   3.80   3.47   3.80   3.52   3.70		
9974918_uff_E=529.05_out_6	VAL420   PHE416   PHE416   PHE416     PHE416   PHE416   ILE227   PHE230     ILE227   VAL420   PHE230   PHE230     PHE416   PHE416   ILE227   PHE230	3.39   3.62   3.72   3.68   3.86   3.83   3.19   3.33   3.58   3.63   3.68   3.83   3.59   3.84   3.85   3.84		

	PHE230   ILE248   ILE244   ILE244   PHE230   TRP241   TRP241   ILE244   PHE230   ILE244	3.80   3.85   3.09   3.84   3.84   3.68   3.88   3.82   3.65   3.60
9974918_uff_E=529.05_out_7	ILE244   PHE230   PHE230   ILE227   PHE416   ILE248   LEU223   ILE244   ILE244   PHE230   ILE244   VAL245   TRP241   ILE244   TRP241   TRP241   TRP241   PHE230   ILE244   TRP241   TRP241   TRP241	3.84   3.80   3.69   3.28   3.66   3.90   3.61   3.73   3.54   3.44   3.62   3.53   3.72   3.56   3.57   3.50   3.90   3.83   3.70   3.74   3.64   3.75
9974918_uff_E=529.05_out_8	MET40   PRO309   PRO43   PRO309   PRO309   MET40   PRO43   PRO309   LEU168   GLU169   MET40   LEU168     LEU168	3.68   3.74   3.57   3.63   3.87   3.73   3.64   3.71   3.82   3.56   3.50   3.67   3.87
9974918_uff_E=529.05_out_9	LEU93   LEU123   LEU93   PHE77   PHE77   LEU74   ILE217   PRO73   PHE70   PHE70   ILE119   LEU74   LEU74   TRP208   TRP208   LEU74   PHE70   PHE70   TRP208   PHE77   LEU74   LEU74   LEU74	3.84   3.49   3.47   3.80   3.87   3.79   3.80   3.61   3.57   3.36   3.64   3.71   3.85   3.19   3.45   3.87   3.74   3.79   3.86   3.86   3.67   3.83   3.34

Table 47: Post Docking Analysis – Secondary Ligands of Carnosol – Hydrogen Bonds

LIGAND_NAME	Hydrogen_bonds	Hydrogen_bond_distance
<b>CHEMBL483017</b>		
10215621_uff_E=647.14_out		
10215621_uff_E=647.14_out_1	THR36   THR36   THR32	3.16   2.98   3.15
10215621_uff_E=647.14_out_2	ASN414   THR36   THR36	2.81   2.77   3.13
10215621_uff_E=647.14_out_3	THR36   MET290   ASN411	2.63   3.13   3.09
10215621_uff_E=647.14_out_4	SER440   SER439	2.81   3.10
10215621_uff_E=647.14_out_5	ALA63   TYR62   LYS67   VAL444   VAL444   VAL444	2.95   3.13   2.83   2.88   2.91   2.80
10215621_uff_E=647.14_out_6	SER497   ILE341   SER497	3.12   3.03   3.05
10215621_uff_E=647.14_out_7	GLN72   GLN72   ASN33   ASN33   TYR52	3.04   3.07   2.77   2.97   2.83
10215621_uff_E=647.14_out_8	SER298	2.99
10215621_uff_E=647.14_out_9	SER426   VAL455   SER425	2.91   3.32   3.01
<b>CHEMBL483017</b>		
13820510_uff_E=641.77_out		
13820510_uff_E=641.77_out_1	GLU453	3.22
13820510_uff_E=641.77_out_2		
13820510_uff_E=641.77_out_3	SER231   SER231   GLN299   SER426	2.98   2.89   3.04   3.21
13820510_uff_E=641.77_out_4	SER497	3.28
13820510_uff_E=641.77_out_5	ARG46   TRP59	2.70   2.98
13820510_uff_E=641.77_out_6	PHE183   PRO182	2.82   3.01
13820510_uff_E=641.77_out_7	THR465	2.84
13820510_uff_E=641.77_out_8	SER497   SER497	3.30   3.19
13820510_uff_E=641.77_out_9	SER497	2.75
<b>CHEMBL494659</b>		
13820511_uff_E=526.64_out		

13820511_uff_E=526.64_out_1	ASN414   ASN411   THR36	2.90   2.74   3.31
13820511_uff_E=526.64_out_2	LYS67   ALA63   TYR62   TYR62	3.10   2.95   2.99   2.84
13820511_uff_E=526.64_out_3	THR213	2.71
13820511_uff_E=526.64_out_4	GLY442   GLY442   SER439   LYS67	3.29   3.04   2.84   2.90
13820511_uff_E=526.64_out_5		
13820511_uff_E=526.64_out_6	TYR62   LYS67	3.25   3.03
13820511_uff_E=526.64_out_7	LEU192   THR6   LEU195   LYS84	3.34   2.81   3.20   3.22
13820511_uff_E=526.64_out_8	SER425	2.64
13820511_uff_E=526.64_out_9		

#### CHEMBL491879

13855851_uff_E=512.74_out		
13855851_uff_E=512.74_out_1	TYR62   LYS67	3.09   3.06
13855851_uff_E=512.74_out_2	PHE183   PRO182	2.76   3.16
13855851_uff_E=512.74_out_3	THR36	3.04
13855851_uff_E=512.74_out_4		
13855851_uff_E=512.74_out_5		
13855851_uff_E=512.74_out_6	ASP64	3
13855851_uff_E=512.74_out_7	THR213	2.79
13855851_uff_E=512.74_out_8	THR6   LEU195   LYS84	2.87   2.86   3.16
13855851_uff_E=512.74_out_9	SER497	2.95

#### CHEMBL4544522

13855852_uff_E=512.74_out		
13855852_uff_E=512.74_out_1	TYR62   TYR62   TYR62	3.19   2.88   2.86
13855852_uff_E=512.74_out_2		
13855852_uff_E=512.74_out_3	SER345	3.11
13855852_uff_E=512.74_out_4	SER345	3.1
13855852_uff_E=512.74_out_5	ARG46	3.2
13855852_uff_E=512.74_out_6	PHE183   PRO182	2.72   3.15
13855852_uff_E=512.74_out_7	SER440	2.93
13855852_uff_E=512.74_out_8	ALA157   THR36	3.29   3.04
13855852_uff_E=512.74_out_9	TYR410	3.13

#### CHEMBL507166

13966122_uff_E=514.97_out		
13966122_uff_E=514.97_out_1	ASN414   ASN411	2.80   2.93
13966122_uff_E=514.97_out_2		
13966122_uff_E=514.97_out_3	ALA157   THR36	2.72   2.74
13966122_uff_E=514.97_out_4	THR213	2.96
13966122_uff_E=514.97_out_5	THR36   ASN414	2.65   3.08
13966122_uff_E=514.97_out_6	GLN299   GLU453   SER426	2.93   3.18   3.08
13966122_uff_E=514.97_out_7	THR36   SER298	3.18   3.15
13966122_uff_E=514.97_out_8	GLN302	2.71
13966122_uff_E=514.97_out_9	ASN414   ASN414   THR36	3.09   3.03   3.04

#### CHEMBL464376

23243692_uff_E=545.61_out		
23243692_uff_E=545.61_out_1	THR213	2.94
23243692_uff_E=545.61_out_2		
23243692_uff_E=545.61_out_3	THR36   SER298	3.17   3.16
23243692_uff_E=545.61_out_4	GLN469   ASP32   LYS441	3.14   3.19   2.90
23243692_uff_E=545.61_out_5		

23243692_uff_E=545.61_out_6	SER497	3.06
23243692_uff_E=545.61_out_7	LYS67	2.98
23243692_uff_E=545.61_out_8		
23243692_uff_E=545.61_out_9		
<b>CHEMBL2376097</b>		
23243694_uff_E=513.07_out		
23243694_uff_E=513.07_out_1	THR36   THR32   THR32	2.98   2.81   2.99
23243694_uff_E=513.07_out_2	THR36   THR32   ASN414   THR32	2.66   2.96   2.87   2.73
23243694_uff_E=513.07_out_3		
23243694_uff_E=513.07_out_4	THR213	2.91
23243694_uff_E=513.07_out_5	SER426	3.01
23243694_uff_E=513.07_out_6	THR36   SER298	3.24   3.19
23243694_uff_E=513.07_out_7	ASN414	2.95
23243694_uff_E=513.07_out_8		
23243694_uff_E=513.07_out_9		
<b>CHEMBL491307</b>		
44566424_uff_E=484.58_out		
44566424_uff_E=484.58_out_1	ASN414   ASN411	2.81   3.11
44566424_uff_E=484.58_out_2	THR36	2.73
44566424_uff_E=484.58_out_3		
44566424_uff_E=484.58_out_4	SER440	2.87
44566424_uff_E=484.58_out_5	ASP32   LYS441	3.16   3.20
44566424_uff_E=484.58_out_6	THR6   LEU195   MET12   THR9	2.97   2.91   2.98   3.08
44566424_uff_E=484.58_out_7	SER77   SER74	2.95   2.72
	TYR28   SER31   TYR28   SER77	
44566424_uff_E=484.58_out_8	LYS76	2.91   3.09   2.72   2.96   3.23
44566424_uff_E=484.58_out_9		
<b>CHEMBL1514916</b>		
455264_uff_E=464.37_out		
455264_uff_E=464.37_out_1	SER298	2.73
455264_uff_E=464.37_out_2	GLN302   GLN302	2.96   3.02
455264_uff_E=464.37_out_3		
455264_uff_E=464.37_out_4	TYR62	3.12
455264_uff_E=464.37_out_5		
455264_uff_E=464.37_out_6		
455264_uff_E=464.37_out_7	SER497	3.24
455264_uff_E=464.37_out_8		
455264_uff_E=464.37_out_9	GLU169   LEU168	3.21   2.98
<b>CHEMBL1081338</b>		
46883406_uff_E=550.72_out		
46883406_uff_E=550.72_out_1		
46883406_uff_E=550.72_out_2	THR213	3
46883406_uff_E=550.72_out_3	ALA157   SER298	2.97   3.01
46883406_uff_E=550.72_out_4		
46883406_uff_E=550.72_out_5	LYS67	2.96
46883406_uff_E=550.72_out_6		
46883406_uff_E=550.72_out_7	SER497	3.01
46883406_uff_E=550.72_out_8	SER440	2.91
46883406_uff_E=550.72_out_9		

CHEMBL1079367		
636675_uff_E=605.58_out		
636675_uff_E=605.58_out_1	THR36   THR36	3.19   2.76
636675_uff_E=605.58_out_2	SER345	3.11
636675_uff_E=605.58_out_3	TYR62	3.2
636675_uff_E=605.58_out_4	SER345	2.77
636675_uff_E=605.58_out_5	THR394   ARG133	3.09   2.89
636675_uff_E=605.58_out_6		
636675_uff_E=605.58_out_7		
636675_uff_E=605.58_out_8		
636675_uff_E=605.58_out_9	THR213	2.79
CHEMBL519970		
65158_uff_E=609.95_out		
65158_uff_E=609.95_out_1	THR32	3.15
65158_uff_E=609.95_out_2	ASN414	2.8
65158_uff_E=609.95_out_3		
65158_uff_E=609.95_out_4		
65158_uff_E=609.95_out_5	SER440	2.88
65158_uff_E=609.95_out_6	GLN302   GLN302	3.06   3.04
65158_uff_E=609.95_out_7		
65158_uff_E=609.95_out_8	ARG142   THR394   LEU392   ARG133	2.82   2.87   2.89   3.24
65158_uff_E=609.95_out_9		

Table 48: Post-Docking Analysis Results – Secondary Ligands of Carnosol - Hydrophobic Interactions

LIGAND_NAME	Hydrogen_bonds	Hydrogen_bond_distance
CHEMBL483017		
10215621_uff_E=647.14_out		
10215621_uff_E=647.14_out_1	ILE39   LEU294   LEU295   ALA157   ALA157   ALA157   ASN414   ASN414   TYR410   MET287   ALA157   TYR410   TYR410	3.75   3.45   3.74   3.84   3.76   3.86   3.44   3.52   3.59   3.77   3.73   3.49   3.74
10215621_uff_E=647.14_out_2	LEU294   LEU294   LEU295   ALA157   MET35   ALA157   LEU67     TYR63   ASN414	3.68   3.72   3.86   3.60   3.45   3.68   3.83   3.86   3.81
10215621_uff_E=647.14_out_3	LEU294   MET290   MET290   ALA157   LEU295   ALA157   ALA157   TYR410   MET125   MET125   MET125   MET125   LEU67   ASN414   ASN414   THR32     THR32   MET35   TYR410	3.79   3.75   3.41   3.84   3.47   3.66   3.88   3.85   3.50   3.83   3.26   3.70   3.47   3.34   3.76   3.83   3.78   3.62   3.35
10215621_uff_E=647.14_out_4	SER440   SER440   VAL444   GLY442     LEU447   LEU447   THR465   VAL444	3.82   3.61   3.68   3.80   3.41   3.71   3.90   3.41
10215621_uff_E=647.14_out_5	LEU447   ILE443   LYS67   LYS67   LYS67   VAL444   ASP64	3.62   3.75   3.88   3.75   3.48   3.67   3.69
10215621_uff_E=647.14_out_6	PRO344   PRO344   PRO344   TYR501   TYR501   TYR501   TYR501	3.88   3.42   3.82   3.81   3.65   3.68   3.68   3.40   3.70

	TYR501   TYR501   ILE498   TYR501   TYR501   TYR501   TYR501   TYR501   TYR501	3.76   3.80   3.87   3.73   3.81   3.39   3.78
10215621_uff_E=647.14_out_7	TYR52   TYR52   TYR52   ILE467   ILE467   ILE467   LYS468	3.82   3.72   3.62   3.73   3.54   3.79   3.78
10215621_uff_E=647.14_out_8	PRO43   PRO43   PRO309   PRO309   MET40   MET40   ILE39   THR36   THR36   THR36   PRO161   MET40   LEU295   MET40   MET40   LEU295   THR36	3.90   3.88   3.65   3.74   3.29   3.69   3.32   3.41   3.86   3.80   3.78   3.73   3.53   3.37   3.56   3.26   3.86
10215621_uff_E=647.14_out_9	SER454   PHE478   SER426   SER426	3.67   3.81   3.62   3.87
<b>CHEMBL483017</b>		
13820510_uff_E=641.77_out		
13820510_uff_E=641.77_out_1	PHE478   PHE478   TYR429   SER425   PHE478   PHE478   VAL455   TYR429   TYR429   SER426   SER426	3.45   3.61   3.61   3.86   3.57   3.72   3.73   3.75   3.36   3.58   3.63
13820510_uff_E=641.77_out_2	PRO309   PRO309   MET40   MET40   MET40   MET40   MET40   PRO309   MET40   SER298   LEU295   PRO161   THR36   ILE39   LEU295	3.67   3.83   3.43   3.75   3.83   3.78   3.73   3.33   3.80   3.77   3.63   3.71   3.77   3.45   3.81
13820510_uff_E=641.77_out_3	SER425   GLY422   LEU296   LEU296   GLY422   GLY422   LYS232   LYS232   SER426	3.56   3.63   3.67   3.89   3.76   3.68   3.82   3.84   3.68
13820510_uff_E=641.77_out_4	TYR501   TYR501   ILE498   ILE498   ILE498   TYR501   TYR501   TYR501   TYR501   TYR501   TYR501   SER345   SER345   PRO344	3.70   3.48   3.76   3.67   3.73   3.85   3.71   3.86   3.81   3.67   3.90   3.56   3.70   3.82
13820510_uff_E=641.77_out_5	TRP59   TRP59   ALA48   ALA48   ALA48   TRP115   TRP115   ARG46   PHE38   ASP111   PHE38   ASP111   PHE38   PHE38   PHE38   GLU47	3.75   3.83   3.68   3.74   3.83   3.52   3.82   3.87   3.89   3.76   3.61   3.76   3.27   3.51   3.90   3.86
13820510_uff_E=641.77_out_6	ILE186   PHE183   PHE183   ILE186   ILE186   PHE183   PHE183   PHE183   VAL26   VAL22   VAL23   ILE186   ILE186   VAL23   PHE183   VAL26   ILE186	3.74   3.84   3.73   3.65   3.73   3.84   3.80   3.83   3.49   3.86   3.34   3.47   3.89   3.86   3.75   3.65   3.86
13820510_uff_E=641.77_out_7	ILE467   LEU61   LEU61   LEU61   THR465   LEU61   GLY442   GLY442	3.62   3.76   3.55   3.76   3.70   3.83   3.78   3.42
13820510_uff_E=641.77_out_8	SER345   PRO344   PRO344   TYR501   TYR501   TYR501   TYR501   TYR501   TYR501   TYR501   ILE498   TYR501   TYR501   TYR501   TYR501   TYR501   TYR501	3.89   3.78   3.34   3.78   3.71   3.65   3.68   3.70   3.79   3.51   3.69   3.66   3.79   3.84   3.82   3.37   3.80
13820510_uff_E=641.77_out_9	ILE352   GLY348   ILE352   TYR501   TYR501   TYR501   TYR501   TYR501	3.82   3.62   3.86   3.78   3.81   3.64   3.76   3.57
<b>CHEMBL494659</b>		
13820511_uff_E=526.64_out		

13820511_uff_E=526.64_out_1	MET125   TYR410   MET125   MET35   LEU295   ALA291   MET290   MET35   ALA157   VAL418   LEU295   MET35   ALA157	3.87   3.85   3.72   3.41   3.71   3.66   3.44   3.85   3.65   3.82   3.76   3.66   3.21
13820511_uff_E=526.64_out_2	LEU447   ILE443   LEU447   LEU447   LEU447   VAL444   LYS67   LYS67   ASP64   VAL444   VAL444   LYS67   LYS67   LYS67   ASP64   LYS67	3.43   3.58   3.87   3.79   3.88   3.86   3.78   3.88   3.88   3.73   3.63   3.64   3.67   3.64   3.62   3.88
13820511_uff_E=526.64_out_3	ILE210   TRP208   TRP208   TRP208   TRP208   TRP208   PHE77   PHE77   PRO73   TRP208   TRP208   LEU74   THR213   TRP208   TRP208   TRP208   TRP208	3.72   3.82   3.89   3.77   3.88   3.78   3.64   3.78   3.75   3.37   3.67   3.72   3.63   3.64   3.84   3.69   3.81
13820511_uff_E=526.64_out_4	THR465   GLY442   THR465   GLY442   GLY442   VAL444   SER440   SER439   VAL444   VAL444   VAL444   VAL444   VAL444   VAL444	3.57   3.67   3.58   3.87   3.87   3.85   3.68   3.88   3.85   3.66   3.71   3.71   3.77   3.58
13820511_uff_E=526.64_out_5	PRO309   PRO309   PRO309   MET40   MET40   MET40   MET40   MET40   MET40   PRO309   MET40   LEU295   THR36   LEU295   LEU295   ILE39	3.77   3.54   3.73   3.47   3.88   3.85   3.75   3.67   3.59   3.46   3.60   3.76   3.65   3.90   3.69   3.79
13820511_uff_E=526.64_out_6	LYS67   LYS67   LYS67   LEU107   THR465   LEU107   THR465	3.74   3.53   3.81   3.64   3.63   3.52   3.80
13820511_uff_E=526.64_out_7	LEU195   THR9   LEU194   LEU194   THR13   LEU195   LEU194   LEU194   THR9   THR9   PHE5   PHE5   THR6   PHE5   PHE5	3.75   3.84   3.62   3.40   3.42   3.82   3.68   3.79   3.73   3.75   3.74   3.79   3.33   3.33   3.64
13820511_uff_E=526.64_out_8	VAL455   SER454   TYR429   SER454   TYR429   TYR429   TYR429   VAL418   LEU295   VAL418	3.81   3.79   3.85   3.76   3.78   3.31   3.71   3.87   3.43   3.52
13820511_uff_E=526.64_out_9	GLN302   GLN302   PRO161   PRO161   MET40   THR36   ILE39   ILE39   PRO309   PRO161   MET40   SER298   MET40   MET40   ILE39	3.59   3.81   3.65   3.88   3.87   3.61   3.37   3.64   3.61   3.54   3.69   3.48   3.68   3.78   3.87
<b>CHEMBL491879</b>		
13855851_uff_E=512.74_out		
13855851_uff_E=512.74_out_1	LYS67   LYS67   LYS67   LYS67   LEU107   LEU61   THR465   LEU107   THR465   THR465	3.88   3.89   3.90   3.66   3.61   3.71   3.64   3.44   3.64   3.77
13855851_uff_E=512.74_out_2	PHE183   PHE183   PHE183   ILE186   ILE186   PHE183   PHE183   PHE183   PHE183   VAL26   VAL23   VAL22   VAL23   VAL26   VAL23   PHE183   PHE183   VAL26   PHE183   ILE186   ILE186	3.63   3.56   3.90   3.72   3.75   3.83   3.73   3.73   3.85   3.82   3.86   3.88   3.59   3.62   3.70   3.75   3.70   3.61   3.83   3.70   3.73
13855851_uff_E=512.74_out_3	MET35   ILE39   MET35   MET35   MET35   LEU295   LEU295   ILE39   LEU294   MET40   MET40   LEU295   SER298   SER298   PRO161   ILE39	3.82   3.60   3.73   3.89   3.59   3.82   3.42   3.58   3.84   3.39   3.84   3.48   3.80   3.59   3.47   3.43

	VAL456   VAL456   GLN299	
	VAL456   GLN302   GLN302	3.79   3.45   3.66   3.48   3.70
	GLN302   GLN299   GLN302	3.70   3.67   3.67   3.73
	GLY313   SER298   PRO309   MET40	3.82   3.86   3.88   3.67   3.53
	MET40   PRO309   MET40	3.68   3.65   3.87   3.59
13855851_uff_E=512.74_out_4	SER298   PRO309   SER298   SER298	2.89   3.88
13855851_uff_E=512.74_out_5	PRO309   PRO309   PRO309   MET40   MET40   PRO309   MET40   MET40   ILE39   THR36   LEU295   LEU295   ILE39   ILE39   ILE39	3.71   3.63   3.86   3.68   3.85   3.68   3.51   3.87   3.66   3.34   3.75   3.87   3.80   3.87   3.72
13855851_uff_E=512.74_out_6	LEU107   LEU107   LEU107   LEU107   LEU107   ILE443   GLY442   LEU61   LEU61   LEU61   LEU447   GLY442   THR465   THR465	3.63   3.86   3.67   3.78   3.49   3.85   3.78   3.71   3.88   3.67   3.73   3.61   3.49   3.18
13855851_uff_E=512.74_out_7	ILE210   ILE210   TRP208   TRP208   TRP208   TRP208   TRP208   PHE77   PHE77   PHE77   TRP208   TRP208   LEU74   THR213   TRP208   TRP208   TRP208   TRP208	3.78   3.45   3.75   3.87   3.77   3.68   3.79   3.75   3.47   3.78   3.43   3.86   3.83   3.89   3.81   3.86   3.75   3.77
13855851_uff_E=512.74_out_8	LEU195   THR9   LEU194   LEU194   THR13   LEU195   LEU194   LEU194   PHE5   PHE5   THR6   PHE5   PHE5	3.78   3.85   3.69   3.47   3.33   3.89   3.67   3.77   3.79   3.81   3.30   3.45   3.73
13855851_uff_E=512.74_out_9	SER345   TYR501   TYR501   ILE341   PRO344   TYR501   TYR501   TYR501   TYR501   ILE498   ILE498   ILE498   ILE498   TYR501   TYR501   TYR501   TYR501   TYR501	3.67   3.84   3.83   3.62   3.48   3.65   3.69   3.69   3.85   3.68   3.72   3.76   3.59   3.61   3.38   3.89   3.78   3.79
<b>CHEMBL4544522</b>		
13855852_uff_E=512.74_out		
13855852_uff_E=512.74_out_1	LEU447   ILE443   LEU447   LEU447   LEU447   VAL444   LYS67   ASP64   LYS67   LYS67   VAL444   VAL444   LYS67   ASP64   LYS67	3.49   3.50   3.78   3.73   3.86   3.81   3.78   3.84   3.60   3.60   3.70   3.60   3.70   3.64   3.89
13855852_uff_E=512.74_out_2	ILE244   PHE230   PHE230   PHE230   LEU235   PHE230   PHE230   PHE230   VAL420   SER231   PHE230   PHE230   VAL420   PHE230   VAL420   LEU235   PHE230   PHE230	3.75   3.77   3.85   3.53   3.87   3.86   3.86   3.84   3.86   3.85   3.83   3.65   3.76   3.56   3.59   3.63   3.68   3.86
13855852_uff_E=512.74_out_3	LEU333   LEU333   LEU333   PHE326   PHE326   PHE326   ALA378   ALA378   ALA378   ILE349   GLY346   VAL342   GLY346   LEU333   ILE329   VAL342   PHE326   PHE326	3.68   3.75   3.82   3.70   3.79   3.54   3.31   3.69   3.89   3.58   3.55   3.51   3.53   3.86   3.81   3.16   3.56   3.60
13855852_uff_E=512.74_out_4	ILE349   SER345   ALA330   PHE326   PHE326   ILE349   VAL342   LEU333   ALA330   ALA330   VAL342   ALA330   LEU333   PHE326   VAL342   LEU333   ILE349   PHE326   PHE326	3.58   3.89   3.80   3.71   3.81   3.71   3.34   3.72   3.86   3.61   3.76   3.69   3.76   3.67   3.71   3.70   3.55   3.67   3.69

13855852_uff_E=512.74_out_5	TRP115   ARG46   TRP115   TRP115   ARG46   ARG46   PHE38   PHE38   PHE38   PHE38   ARG46   ARG46   PHE38   ALA48   TRP59   ASP111   PHE112   PHE112   PHE38	3.78   3.83   3.78   3.72   3.34   3.81   3.62   3.64   3.43   3.88   3.60   3.75   3.77   3.65   3.72   3.69   3.48   3.69   3.82
13855852_uff_E=512.74_out_6	PHE183   PHE183   ILE186   ILE186   PHE183   PHE183   PHE183   PHE183   VAL26   VAL23   VAL23   VAL23   VAL26   ILE186   VAL23   PHE183   PHE183   VAL26   ILE186   PHE183   ILE186   VAL23   ILE186	3.65   3.57   3.69   3.71   3.85   3.75   3.74   3.84   3.84   3.73   3.81   3.49   3.66   3.90   3.70   3.81   3.74   3.59   3.87   3.87   3.70   3.90   3.64
13855852_uff_E=512.74_out_7	SER440   SER440   SER440   VAL444   GLY442   LEU447   LEU447   LEU447   VAL444	3.77   3.78   3.68   3.84   3.73   3.24   3.61   3.84   3.38
13855852_uff_E=512.74_out_8	MET35   ILE39   MET35   MET35   MET35   LEU295   ILE39   LEU294   MET40   MET40   LEU295   SER298   SER298   LEU295   PRO161   ILE39	3.86   3.64   3.74   3.85   3.52   3.48   3.57   3.79   3.37   3.85   3.50   3.76   3.64   3.85   3.44   3.40
13855852_uff_E=512.74_out_9	MET125   LEU295   LEU294   LEU294   LEU294   ALA157   ASN414   MET35   MET35   MET290   ALA157	3.66   3.09   3.76   3.73   3.02   3.69   3.88   3.66   3.70   3.61   3.28   3.87   3.88   3.82
<b>CHEMBL507166</b>		
13966122_uff_E=514.97_out		
13966122_uff_E=514.97_out_1	LEU67   MET125   LEU67   MET35   MET35   MET35   LEU294   MET290   MET290   LEU295   ALA157   VAL418   LEU295   LEU295   ALA157	3.66   3.61   3.81   3.72   3.80   3.42   3.50   3.85   3.38   3.55   3.61   3.86   3.84   3.76   3.24
13966122_uff_E=514.97_out_2	TRP241   ILE244   TRP241   TRP241   PHE230   PHE230   PHE230   PHE230   PHE230   VAL420   VAL420   PHE230   PHE230   VAL420   VAL420   ILE227   PHE230   PHE230   PHE230   PHE230   PHE230   PHE230	3.87   3.62   3.67   3.68   3.85   3.77   3.67   3.87   3.50   3.71   3.38   3.79   3.67   3.76   3.82   3.43   3.61   3.77   3.57   3.62   3.89   3.49
13966122_uff_E=514.97_out_3	ILE39   LEU295   ILE39   LEU295   LEU295   LEU295   ILE39   ALA157   LEU295   LEU295   LEU294   LEU294   MET35   LEU295   MET35   MET35   ALA157   ALA157	3.88   3.52   3.58   3.77   3.87   3.36   3.56   3.79   3.75   3.83   3.81   3.86   3.72   3.50   3.75   3.63   3.22   3.83
13966122_uff_E=514.97_out_4	ILE210   TRP208   TRP208   TRP208   TRP208   TRP208   TRP208   PHE77   PHE77   PRO73   TRP208   TRP208   LEU74   THR213   TRP208   TRP208   TRP208   TRP208	3.88   3.80   3.81   3.52   3.59   3.77   3.70   3.81   3.78   3.64   3.59   3.72   3.54   3.71   3.73   3.58   3.66   3.85   3.53   3.66
13966122_uff_E=514.97_out_5	MET125   LEU67   THR32   LEU295   MET35   MET35   MET35   LEU294   ALA157	3.58   3.44   3.86   3.32   3.49   3.48   3.80   3.28   3.63

13966122_uff_E=514.97_out_6	PHE478   VAL455   TYR429   PHE478   PHE478   TYR429   TYR429   TYR429   SER426   SER425   PHE478   SER426   SER426	3.74   3.79   3.81   3.69   3.79   3.67   3.81   3.44   3.89   3.88   3.58   3.81   3.62
13966122_uff_E=514.97_out_7	VAL418   MET35   MET35   ILE39   LEU295   ILE39   LEU295   ILE39   ILE39   LEU295   ILE39   PRO161   PRO161   LEU295   MET40   PRO161   THR36   ILE39	3.74   3.78   3.75   3.70   3.64   3.59   3.29   3.68   3.71   3.34   3.87   3.50   3.74   3.71   3.46   3.74   3.57   3.55
13966122_uff_E=514.97_out_8	VAL456   VAL456   GLN302   SER298   MET40   MET40   PRO309   MET40   PRO309   SER298	3.75   3.54   3.79   3.54   3.33   3.53   3.89   3.71   3.66   3.35
13966122_uff_E=514.97_out_9	VAL418   ILE39   LEU295   ILE39   MET290   ALA157   MET35   MET35   MET35   LEU295   ILE39   LEU294   ALA157   LEU295   ALA157	3.84   3.82   3.46   3.47   3.77   3.27   3.77   3.86   3.68   3.74   3.86   3.30   3.46   3.60   3.83
<b>CHEMBL464376</b>		
23243692_uff_E=545.61_out		
23243692_uff_E=545.61_out_1	TRP208   TRP208   TRP208   TRP208   TRP208   TRP208   TRP208   TRP208   PHE77   PHE77   PRO73   TRP208   TRP208   LEU74   THR213   TRP208   TRP208   TRP208   TRP208	3.88   3.82   3.56   3.65   3.88   3.70   3.84   3.84   3.66   3.57   3.64   3.56   3.73   3.65   3.58   3.62   3.89   3.56   3.72
23243692_uff_E=545.61_out_2	PRO161   THR36   ILE39   LEU295   LEU295   LEU295   ILE39   ILE39   SER298   PRO161   PRO161   PRO161   MET40   ILE39   SER298	3.77   3.58   3.62   3.59   3.76   3.78   3.66   3.88   3.74   3.68   3.73   3.82   3.59   3.86   3.89
23243692_uff_E=545.61_out_3	VAL418   MET35   MET35   ILE39   LEU295   ILE39   LEU295   ILE39   ILE39   ILE39   LEU295   ILE39   PRO161   PRO161   LEU295   MET40   PRO161   THR36   ILE39	3.76   3.75   3.73   3.69   3.64   3.59   3.30   3.68   3.88   3.71   3.34   3.87   3.50   3.75   3.71   3.47   3.75   3.57   3.55
23243692_uff_E=545.61_out_4	ASP73   ASP73   GLN72   GLN72   GLN72   ASP32   ASP32   THR58   TYR52   THR58   TYR52   TYR52	3.70   3.83   3.86   3.46   3.73   3.85   3.70   3.80   3.75   3.68   3.85   3.73
23243692_uff_E=545.61_out_5	GLN299   LEU295   LEU295   GLN299   VAL456   GLN302   GLN302   GLN299   GLN302   GLN302   GLN299   GLN302   MET40   MET40   PRO161   PRO309	3.89   3.52   3.70   3.88   3.71   3.80   3.76   3.66   3.71   3.82   3.80   3.82   3.43   3.82   3.80   3.48
23243692_uff_E=545.61_out_6	PRO344   PRO344   PRO344   TYR501   TYR501   TYR501   TYR501   TYR501   TYR501   TYR501   TYR501   TYR501   TYR501   TYR501   ILE498   TYR501   TYR501   TYR501   TYR501	3.84   3.42   3.81   3.86   3.82   3.68   3.84   3.58   3.60   3.71   3.84   3.82   3.81   3.72   3.76   3.85   3.75   3.32   3.77
23243692_uff_E=545.61_out_7	ASP64   LYS67   ASP64   LYS67   LYS67   LYS67   THR465   LEU61   THR465   LEU107	3.84   3.68   3.64   3.56   3.79   3.88   3.86   3.62   3.70   3.54

23243692_uff_E=545.61_out_8	TYR501   TYR501   TYR501   ILE498   ILE498   ILE498   ILE498   ILE498   ILE498   TYR501   TYR501   TYR501     TYR501   ILE341   TYR501   TYR501   TYR501   TYR501   TYR501     TYR501   SER345   SER345   TYR501	3.74   3.21   3.89   3.74   3.74   3.57   3.55   3.80   3.84   3.87   3.77   3.81   3.84   3.66   3.71   3.79   3.63   3.80   3.89   3.78   3.65   3.79   3.89
23243692_uff_E=545.61_out_9	MET40   GLN302   GLN302   GLN302   GLN302   GLN302   MET40   ILE39   ILE39   PRO161   PRO161   MET40   PRO309   SER298   SER298   PRO309	3.77   3.74   3.69   3.70   3.69   3.77   3.77   3.21   3.55   3.55   3.62   3.79   3.45   3.71   3.29   3.74
<b>CHEMBL2376097</b>		
23243694_uff_E=513.07_out		
23243694_uff_E=513.07_out_1	LEU294   LEU295   LEU295   ALA157   ALA157   TYR410   ALA157   ALA157   ASN414   ASN414   TYR410   TYR410   TYR410   ALA157   TYR410   ASN414   ASN414   MET287	3.67   3.63   3.80   3.81   3.79   3.75   3.67   3.77   3.76   3.68   3.86   3.13   3.79   3.68   3.81   3.44   3.87   3.67
23243694_uff_E=513.07_out_2	LEU295   ILE39   LEU295   LEU67   TYR63   MET35   MET35   MET35   TYR410	3.70   3.70   3.75   3.42   3.42   3.74   3.63   3.58   3.41
23243694_uff_E=513.07_out_3	TRP241   ILE244   TRP241   TRP241   PHE230   PHE230   PHE230   PHE230   PHE230   PHE230   PHE230   VAL420   VAL420   PHE230   PHE230   VAL420   VAL420   ILE227   PHE230   PHE230   PHE230   PHE230   PHE230	3.71   3.62   3.69   3.68   3.80   3.74   3.68   3.79   3.81   3.65   3.74   3.52   3.82   3.70   3.76   3.78   3.47   3.71   3.74   3.51   3.55   3.84   3.54
23243694_uff_E=513.07_out_4	TRP208   TRP208   TRP208   TRP208   TRP208   TRP208   TRP208   TRP208   PHE77   PHE77   PRO73   TRP208   TRP208   LEU74   THR213   TRP208   TRP208   TRP208	3.79   3.77   3.51   3.63   3.80   3.84   3.65   3.80   3.68   3.58   3.64   3.60   3.78   3.59   3.62   3.57   3.53   3.70
23243694_uff_E=513.07_out_5	PHE478   PHE478   TYR429   SER426   SER425   PHE478   TYR429   TYR429   SER426   GLY422	3.63   3.81   3.63   3.89   3.76   3.75   3.77   3.56   3.63   3.89
23243694_uff_E=513.07_out_6	VAL418   LEU295   MET35   MET35   LEU295   ILE39   LEU295   ILE39   LEU295   ILE39   ILE39   LEU295   ILE39   PRO161   PRO161   LEU295   MET40   MET40   PRO161   THR36   ILE39	3.69   3.84   3.83   3.77   3.87   3.75   3.61   3.59   3.38   3.62   3.68   3.44   3.82   3.52   3.75   3.75   3.89   3.38   3.76   3.58   3.45
23243694_uff_E=513.07_out_7	VAL418   VAL418   LEU295   LEU295   LEU295   LEU295   ILE39   MET290   ALA157   MET35   VAL418   LEU295   LEU294   LEU294   ALA157   LEU295   LEU295   LEU295	3.79   3.72   3.77   3.78   3.78   3.49   3.60   3.69   3.33   3.72   3.80   3.54   3.73   3.33   3.72   3.51   3.77   3.89

	VAL456   VAL456   GLN302   GLN302   GLN299   GLN299   GLN299   VAL456   GLN302   GLN302   GLN299   SER298   3.81   3.54   3.79   3.58   3.65 PRO161   PRO161   SER298     3.77   3.71   3.57   3.87   SER298   PRO309   MET40   MET40   3.67   3.56   3.78   3.85   3.84   PRO309   MET40   PRO309     3.33   3.88   3.62   3.50   SER298   3.53   3.79   3.60   3.36   3.33
23243694_uff_E=513.07_out_8	ILE39   LEU295   LEU295   LEU295   3.71   3.71   3.83   3.84   3.60 ILE39   ILE39   SER298   PRO161     3.80   3.83   3.53   3.61   PRO161   PRO161   MET40   ILE39   SER298   3.81   3.57   3.77   3.82
<b>CHEMBL491307</b>	
44566424_uff_E=484.58_out	
44566424_uff_E=484.58_out_1	LEU294   LEU294   MET290   3.72   3.68   3.88   3.76   3.57 LEU294   LEU294   LEU295     3.74   3.67   3.71   3.86   ALA157   ASN414   THR32   THR32     3.76   3.79   3.81   3.37   3.81   LEU67   LEU67   TYR63   MET35   MET35   3.59
44566424_uff_E=484.58_out_2	LEU295   LEU294   MET290   3.53   3.62   3.82   3.56   3.66 MET290   ALA157   ASN414     3.75   3.75   3.59   3.17   TYR410   MET125   MET125     3.75   3.66   3.86   3.78   3.32 MET125   LEU67   ASN414   TYR63     3.78   3.73   3.87   3.44     ASN414   ASN414   MET125   MET35   TYR410   MET125   3.89
44566424_uff_E=484.58_out_3	ARG46   TRP115   TRP115   ARG46   3.74   3.69   3.80   3.66   3.88   PHE38   PHE38   PHE38   PHE38     3.67   3.70   3.58   3.63   ARG46   ALA48   PHE38   PHE38     3.80   3.67   3.85   3.66   3.81 ALA48   TRP59   PHE112   PHE112   PHE38   3.38   3.73   3.82
44566424_uff_E=484.58_out_4	SER440   SER440   SER440   VAL444   3.78   3.73   3.62   3.82   3.76   GLY442   LEU447   LEU447   VAL444     3.37   3.66   3.44
44566424_uff_E=484.58_out_5	ASP32   THR58   3.60   3.68
44566424_uff_E=484.58_out_6	THR9   LEU194   LEU194   THR13   3.85   3.59   3.34   3.61   3.88 THR9   THR9   THR9   THR9   PHE5   3.72   3.66   3.79   3.75     PHE5   THR6   PHE5   PHE5   3.75   3.33   3.37   3.64
44566424_uff_E=484.58_out_7	LYS468   LYS463   SER105   TYR30   3.79   3.78   3.61   3.35   3.75 LYS463   TYR30   LYS468   TYR30     3.66   3.34   3.82
44566424_uff_E=484.58_out_8	SER74   LYS468   TYR30   SER31   3.80   3.86   3.80   3.82
44566424_uff_E=484.58_out_9	PRO309   PRO309   PRO309   MET40   3.71   3.63   3.88   3.70   3.84 MET40   MET40   PRO309   MET40     3.64   3.48   3.86   3.75     MET40   ILE39   THR36   LEU295     3.39   3.88   3.79   3.80   3.87 ILE39   ILE39   ILE39   ILE39     3.65
<b>CHEMBL1514916</b>	
455264_uff_E=464.37_out	
455264_uff_E=464.37_out_1	GLN302   GLN302   GLN302   3.86   3.55   3.69   3.57   3.79 GLN299   GLN299   GLN302     3.87   3.89   3.52   3.77   GLN302   SER298   MET40   MET40   3.30   3.40   3.33   3.70   3.83   THR36   ILE39   SER298   PRO161     3.88   3.72   3.55   3.86

	PRO161   SER298   PRO309   PRO309   THR36   LEU294   PRO161   MET40   PRO161   PRO161	3.47   3.88   3.83   3.47   3.64   3.78
455264_uff_E=464.37_out_2	GLN299   GLN299   GLN302   MET40   SER298   PRO161   PRO161   ILE39	3.81   3.63   3.83   3.82   3.88   3.84   3.73   3.20
455264_uff_E=464.37_out_3	PRO309   PRO43   PRO43   MET40   PRO309   PRO309   PRO309   MET40   PRO309   GLN302   LEU295   PRO309   GLN299   SER298   PRO309   SER298   SER298   SER298	3.74   3.41   3.44   3.74   3.76   3.63   3.62   3.55   3.86   3.86   3.64   3.75   3.64   3.78   3.89   3.63   3.27   3.62
455264_uff_E=464.37_out_4	LEU61   THR465   THR465   LEU447   GLY442   VAL444   LYS67   LYS67	3.73   3.69   3.70   3.59   3.89   3.88   3.63   3.76
455264_uff_E=464.37_out_5	LEU61   THR465   LEU107   GLY442   LYS67   LYS67   ASP64   ASP64   VAL444   LYS67	3.76   3.68   3.87   3.70   3.71   3.47   3.65   3.55   3.85   3.55
455264_uff_E=464.37_out_6	LEU194   LYS16   LYS16   LEU194   LEU194   THR13   THR9   THR9   LEU194   THR13   LEU194   LEU194   THR13   THR9   THR9   THR13   THR9   THR9   THR9	3.27   3.70   3.67   3.69   3.72   3.42   3.78   3.84   3.81   3.73   3.77   3.83   3.53   3.56   3.82   3.66   3.80   3.37   3.79
455264_uff_E=464.37_out_7	TYR501   TYR501   ILE498   ILE498   ILE498   TYR501   TYR501   TYR501   TYR501   SER345   SER345   PRO344	3.71   3.40   3.78   3.60   3.69   3.83   3.87   3.68   3.87   3.62   3.65   3.88
455264_uff_E=464.37_out_8	PRO43   PRO309   PRO309   MET40   MET40   MET40   MET40   PRO309   ILE39   PRO161   ILE39   ILE39   LEU295	3.85   3.67   3.76   3.59   3.80   3.65   3.82   3.59   3.80   3.56   3.72   3.79   3.78
455264_uff_E=464.37_out_9	GLU169   GLU169   GLU169   GLU169   GLU169   GLU169   GLU169   PHE310   PRO309   MET40   GLU169   LEU168   GLY165   LEU168   LEU168   LEU168   MET40	3.60   3.85   3.84   3.84   3.61   3.71   3.83   3.71   3.66   3.86   3.59   3.61   3.77   3.48   3.80   3.59   3.89

### CHEMBL1081338

46883406_uff_E=550.72_out		
46883406_uff_E=550.72_out_1	LEU235   ILE244   TRP241   TRP241   PHE230   PHE230   PHE230   PHE230   PHE230   VAL420   VAL420   PHE230   PHE230   PHE230   VAL420   VAL420   ILE227   PHE230   PHE230   PHE230   PHE230   PHE230	3.59   3.66   3.74   3.78   3.87   3.82   3.72   3.79   3.84   3.42   3.86   3.79   3.68   3.79   3.85   3.58   3.68   3.70   3.51   3.50   3.79   3.51
46883406_uff_E=550.72_out_2	TRP208   TRP208   TRP208   TRP208   TRP208   TRP208   TRP208   TRP208   PHE77   PHE77   TRP208   PRO73   TRP208   TRP208   TRP208   LEU74   THR213   TRP208   TRP208   TRP208	3.74   3.79   3.52   3.60   3.73   3.88   3.65   3.79   3.69   3.61   3.87   3.72   3.88   3.59   3.78   3.64   3.66   3.59   3.49   3.63

46883406_uff_E=550.72_out_3	ILE39   MET35   MET35   MET35   LEU295   ILE39   LEU294   MET40   ILE39   LEU295   ILE39   ILE39   ILE39   PRO161   ILE39   ILE39	3.83   3.71   3.83   3.75   3.68   3.54   3.76   3.90   3.71   3.64   3.85   3.59   3.51   3.47   3.71   3.87
46883406_uff_E=550.72_out_4	LEU295   VAL456   GLN302   GLN302   GLN299   GLN299   GLN299   GLN299   GLN302   GLN302   GLN299   GLN302   SER298   PRO161   PRO309   MET40   MET40   PRO309	3.83   3.60   3.74   3.54   3.62   3.76   3.68   3.80   3.70   3.70   3.41   3.74   3.85   3.83   3.77   3.58   3.80   3.41
46883406_uff_E=550.72_out_5	LYS67   ASP64   LYS67   LYS67   LYS67   LEU61   THR465   LEU107	3.80   3.56   3.58   3.73   3.76   3.67   3.77   3.51
46883406_uff_E=550.72_out_6	PHE183   VAL26   VAL26   ILE163   ILE163   PHE29   PHE29   PHE29   PHE29   PHE29   ALA152   PHE29   VAL26   VAL26   PHE29   VAL26   MET324   ILE155   ILE155   ILE155     PHE29   PHE29   ILE155   ILE155     VAL26   PHE29	3.82   3.67   3.86   3.78   3.64   3.87   3.82   3.60   3.70   3.87   3.71   3.68   3.71   3.54   3.56   3.81   3.70   3.43   3.84   3.86   3.89   3.68   3.54   3.56   3.25   3.88
46883406_uff_E=550.72_out_7	SER345   PRO344   PRO344   TYR501   TYR501   TYR501   TYR501   TYR501   TYR501   TYR501   TYR501   TYR501   TYR501   ILE498   TYR501   TYR501     TYR501   ILE498   TYR501   TYR501   TYR501   TYR501	3.84   3.45   3.83   3.87   3.86   3.73   3.80   3.89   3.84   3.58   3.59   3.85   3.89   3.89   3.81   3.77   3.71   3.66   3.89   3.78   3.32   3.73
46883406_uff_E=550.72_out_8	LYS67   VAL444   SER440   SER440     SER440   VAL444   GLY442   LEU447   LEU447   VAL444   THR465   THR465   LEU447	3.84   3.65   3.67   3.88   3.74   3.79   3.74   3.62   3.83   3.61   3.73   3.89   3.78
46883406_uff_E=550.72_out_9	ILE498   ILE498   TYR501   TYR501     ILE498   TYR501   TYR501   TYR501   TYR501   ILE341   TYR501     SER345   SER345	3.73   3.57   3.72   3.43   3.72   3.85   3.76   3.88   3.80   3.80   3.77   3.61   3.67
<b>CHEMBL1079367</b>		
636675_uff_E=605.58_out		
636675_uff_E=605.58_out_1	LEU294   ALA157   ALA157   ASN414   TYR410   MET125   MET125   MET125   LEU67   TYR63     ASN414   ASN414   MET125   THR32   MET35   MET35   TYR410	3.31   3.63   3.83   3.82   3.78   3.59   3.29   3.80   3.57   3.77   3.33   3.85   3.81   3.89   3.86   3.83   3.59
636675_uff_E=605.58_out_2	ILE349   SER345   ILE329   PHE326     PHE326   ILE349   VAL342   LEU333   ALA330   ALA330   ILE349   PHE326   ALA330   VAL342   LEU333   ILE349     PHE326   PHE326	3.51   3.89   3.89   3.55   3.73   3.62   3.45   3.76   3.76   3.50   3.84   3.62   3.58   3.73   3.70   3.44   3.69   3.72
636675_uff_E=605.58_out_3	LEU447   LEU447   LEU61   VAL444     LYS67   ASP64   VAL444   VAL444     LYS67   LYS67   LYS67   ASP64     LYS67	3.56   3.59   3.69   3.70   3.77   3.81   3.73   3.62   3.66   3.62   3.68   3.61   3.79

636675_uff_E=605.58_out_4	ALA381   ALA330   PHE326   ALA330   PHE326   LEU333   ILE349   PHE326   LEU333   LEU333	3.37   3.75   3.63   3.73   3.58   3.80   3.84   3.48   3.18   3.90
636675_uff_E=605.58_out_5	PRO395   PRO395   PRO395   PRO395   GLU137   GLN513   GLN513   GLN513   GLN513	3.80   3.58   3.77   3.80   3.89   3.68   3.76   3.89   3.82
636675_uff_E=605.58_out_6	GLN302   GLN302   ILE39   PRO161   THR36   PRO309   PRO161   MET40   MET40   PRO161   SER298   ILE39	3.74   3.87   3.58   3.78   3.64   3.65   3.60   3.77   3.88   3.85   3.55   3.59
636675_uff_E=605.58_out_7	VAL418   LEU295   ILE39   LEU294   LEU294   MET290   ALA157   MET35   LEU295   LEU294   LEU294   ALA157   LEU295   VAL418   LEU295   LEU295	3.65   3.52   3.59   3.68   3.68   3.70   3.61   3.68   3.60   3.66   3.34   3.88   3.81   3.58   3.78   3.38
636675_uff_E=605.58_out_8	PRO309   MET40   MET40   PRO43   PRO309   PRO309   PRO309   MET40   PRO309   MET40   ILE39   THR36   THR36   THR36   LEU295   LEU295   ILE39   ILE39   ILE39	3.78   3.73   3.89   3.83   3.79   3.80   3.85   3.83   3.41   3.48   3.52   3.29   3.85   3.83   3.82   3.74   3.64   3.78   3.72
636675_uff_E=605.58_out_9	ILE210   TRP208   TRP208   ILE210   TRP208   TRP208   TRP208   TRP208   PHE77   PHE77   PRO73   TRP208   TRP208   LEU74   THR213   TRP208   TRP208   TRP208	3.17   3.51   3.83   3.69   3.84   3.85   3.75   3.82   3.58   3.64   3.70   3.54   3.80   3.55   3.63   3.70   3.69   3.86
<b>CHEMBL519970</b>		
65158_uff_E=609.95_out		
65158_uff_E=609.95_out_1	LEU294   LEU295   LEU295   ALA157   ALA157   ALA157   ALA157   ASN414   ASN414   TYR410   MET287   ALA157   TYR410   TYR410	3.63   3.65   3.71   3.88   3.75   3.72   3.70   3.41   3.52   3.65   3.82   3.63   3.62   3.75
65158_uff_E=609.95_out_2	LEU295   LEU294   LEU294   LEU294   ALA157   LEU295   ALA157   ASN414   MET125   MET35   LEU67   TYR63   MET35	3.60   3.64   3.70   3.78   3.76   3.86   3.50   3.78   3.86   3.23   3.73   3.63   3.89
65158_uff_E=609.95_out_3	ILE244   ILE244   PHE230   PHE230   PHE230   PHE230   PHE230   LEU235   PHE230   PHE230   PHE230   SER231   PHE230   PHE230   VAL420   LEU235   PHE230	3.69   3.89   3.84   3.73   3.63   3.84   3.70   3.80   3.71   3.71   3.65   3.82   3.67   3.55   3.23   3.50   3.71
65158_uff_E=609.95_out_4	ILE244   TRP241   ILE244   PHE230   PHE230   TRP241   TRP241   PHE230   PHE230   PHE230   LEU235   LEU235   PHE230   LEU235   PHE230   PHE230   PHE230   PHE230   LEU235   LEU235   PHE230   PHE230	3.67   3.82   3.78   3.78   3.74   3.88   3.89   3.64   3.73   3.82   3.72   3.84   3.64   3.90   3.60   3.66   3.70   3.68   3.38   3.83   3.81   3.30

65158_uff_E=609.95_out_5	SER440   SER440   SER440   VAL444   GLY442   LEU447   LEU447   THR465   THR465   VAL444	3.71   3.78   3.64   3.79   3.77   3.38   3.70   3.84   3.80   3.41
65158_uff_E=609.95_out_6	GLN299   GLN299   GLN302   ILE39   ILE39   MET40   ILE39   PRO161   PRO161   ILE39	3.82   3.60   3.84   3.83   3.72   3.75   3.89   3.86   3.57   3.25
65158_uff_E=609.95_out_7	ARG46   TRP115   TRP115   ARG46   PHE38   PHE38   PHE38   ARG46   ARG46   PHE38   ALA48   ASP111   TRP59   PHE112   PHE112	3.63   3.76   3.78   3.51   3.64   3.64   3.49   3.74   3.61   3.79   3.77   3.58   3.60   3.46   3.64
65158_uff_E=609.95_out_8	PRO395   GLU137   PRO139   GLU137   GLU137   GLU137   GLU137   GLN513	3.64   3.65   3.84   3.86   3.76   3.77   3.89   3.82
65158_uff_E=609.95_out_9	ILE39   LEU295   ILE39   LEU295   LEU295   LEU295   ILE39   ILE39   GLY313   SER298   PRO161   PRO161   PRO309   MET40   ILE39   SER298   ILE39   SER298   PRO161	3.70   3.49   3.70   3.62   3.85   3.65   3.54   3.64   3.86   3.87   3.66   3.64   3.71   3.82   3.63   3.89   3.87   3.55   3.74

## **Challenges and Limitations**

Several challenges were encountered during the structure-based virtual screening of potential inhibitors targeting the QaC A protein of *Staphylococcus aureus*, a membrane-associated efflux transporter known for its role in antiseptic resistance. These challenges not only shaped the design of the workflow but also influenced the interpretation of results and the confidence in computational predictions.

One of the earliest and most significant hurdles was obtaining a usable protein structure. Since the high-resolution crystal structure of QaC A was not available, the protein had to be modeled using homology-based techniques. This added a layer of uncertainty and required careful post-processing to ensure the quality of the predicted structure. Tasks such as protonation, energy minimization, removal of extraneous water molecules, and addition of hydrogen atoms were performed with precision to make the model suitable for molecular docking. Even minor errors in structure preparation could propagate and affect downstream predictions.

Defining the active site was equally complex. Unlike well-characterized enzymes, QaC A lacks abundant ligand-bound structural data in public repositories. To address this, tools like CASTp and literature-derived residue mapping were used to predict potential cavities and functional domains. However, ensuring that the chosen grid box corresponded to a biologically meaningful binding site required multiple validation steps. Variations in grid coordinates, size, and center caused inconsistencies in binding scores, reinforcing the sensitivity of docking to the definition of the binding environment.

Another challenge was evaluating the actual quality and relevance of ligand candidates. While the docking software produced ranked lists based on predicted binding affinity, many of the top-scoring ligands, upon visual inspection, displayed either unrealistic binding poses or interactions with non-functional surface residues. Additionally, several compounds that initially appeared promising failed Lipinski's rule checks or were flagged for potential toxicity, metabolism issues, or poor solubility in preliminary ADMET evaluations. This highlighted the need for post-docking filtering and interpretation beyond raw scores.

The rigid-body assumption in most docking tools introduced its own limitations. Proteins like QaC A, especially those involved in transport, are likely to exhibit flexible, dynamic conformational states. Standard docking platforms often ignore these fluctuations, treating both the protein and ligand as mostly static, which may result in false positives or overlook high-affinity ligands that require induced fit. While ensemble docking or molecular dynamics could potentially address this, resource limitations necessitated compromise.

To enrich the ligand space with known or structurally relevant analogs, the ChEMBL API was integrated into the pipeline. This allowed automated retrieval of bioactive compounds linked to similar transport proteins or antimicrobial resistance targets. While this greatly improved the relevance and quality of the ligand set, the output still required manual curation. Several entries had inconsistent SMILES, undefined stereochemistry, or were duplicates across multiple ChEMBL IDs. These issues had to be cleaned before proceeding with docking.

Finally, a fundamental limitation of the study was the absence of experimental or phenotypic validation. Since this was a purely computational investigation, it was not possible to confirm whether the predicted binders could effectively inhibit the function of QaC A in bacterial cells. This means that the results, while promising as a first-pass filter, remain hypothetical until validated in wet-lab conditions through MIC assays or efflux inhibition studies.

## References

1. Melissa H Brown and Ronald A Skurray. Staphylococcal multidrug efflux protein qaca. *Journal of molecular microbiology and biotechnology*, 3(2):163–170, 2001.
2. Feixiong Cheng, Weihua Li, Yadi Zhou, Jie Shen, Zengrui Wu, Guixia Liu, Philip W Lee, and Yun Tang. admetSAR: a comprehensive source and free tool for assessment of chemical admet properties, 2012.
3. Shiela Chetri. The culmination of multidrug-resistant efflux pumps vs. meager antibiotic arsenal era: Urgent need for an improved new generation of epis. *Frontiers in Microbiology*, 14:1149418, 2023.
4. Gordon YC Cheung, Justin S Bae, and Michael Otto. Pathogenicity and virulence of staphylococcus aureus. *Virulence*, 12(1):547–569, 2021.
5. Saurav Das, Santosh Kumar, Pabitra Bhagowati, and Ashish Kumar Singh. An update on plant-derived compounds as potential inhibitors of the bacterial efflux pumps: with reference to staphylococcus aureus and escherichia coli. *Preprints*, 2018.
6. Mark Davies, Michał Nowotka, George Papadatos, Nathan Dedman, Anna Gaulton, Francis Atkinson, Louisa Bellis, and John P Overington. ChEMBL web services: streamlining access to drug discovery data and utilities. *Nucleic acids research*, 43(W1):W612–W620, 2015.
7. Dijun Du, Xuan Wang-Kan, Arthur Neuberger, Hendrik W Van Veen, Klaas M Pos, Laura JV Pid-dock, and Ben F Luisi. Multidrug efflux pumps: structure, function and regulation. *Nature Reviews Microbiology*, 16(9):523–539, 2018.
8. Amit Gaurav, Pervez Bakht, Mahak Saini, Shivam Pandey, and Ranjana Pathania. Role of bacterial efflux pumps in antibiotic resistance, virulence, and strategies to discover novel efflux pump inhibitors. *Microbiology*, 169(5):001333, 2023.
9. Abayeneh Girma. *Staphylococcus aureus: Current perspectives on molecular pathogenesis and virulence*. The Cell Surface, page 100137, 2024.
10. Lokender Kumar, Monish Bisen, Kusum Harjai, Sanjay Chhibber, Shavkatjon Azizov, Hauzel Lalh-lennawia, and Deepak Kumar. Advances in nanotechnology for biofilm inhibition. *ACS omega*, 8(24):21391–21409, 2023.
11. Balaji Maddiboyina, Harekrishna Roy, M Ramaiah, CN Sarvesh, Sahasra Hanuman Kosuru, Ramya Krishna Nakkala, and Bhabani Shankar Nayak. Methicillin-resistant staphylococcus aureus: novel treatment approach breakthroughs. *Bulletin of the National Research Centre*, 47(1):95, 2023.
12. Puja Majumder, Shahbaz Ahmed, Pragya Ahuja, Arunabh Athreya, Rakesh Ranjan, and Aravind Penmatsa. Cryoem structure of qaca, an antibacterial efflux transporter from staphylococcus aureus. *bioRxiv*, pages 2022–07, 2022.
13. Puja Majumder, Shahbaz Ahmed, Pragya Ahuja, Arunabh Athreya, Rakesh Ranjan, and Aravind Penmatsa. Cryo-em structure of antibacterial efflux transporter qaca from staphylococcus aureus reveals a novel extracellular loop with allosteric role. *The EMBO Journal*, 42(16):e113418, 2023.
14. Bernadette A Mitchell, Melissa H Brown, and Ronald A Skurray. Qaca multidrug efflux pump from staphylococcus aureus: comparative analysis of resistance to diamidines, biguanidines, and guanylhydrazones. *Antimicrobial agents and chemotherapy*, 42(2):475–477, 1998.
15. Mansura S Mulani, Ekta E Kamble, Shital N Kumkar, Madhumita S Tawre, and Karishma R Pardesi. Emerging strategies to combat eskape pathogens in the era of antimicrobial resistance: a review. *Frontiers in microbiology*, 10:539, 2019.
16. Kunihiko Nishino, Seiji Yamasaki, Ryosuke Nakashima, Martijn Zwama, and Mitsuko Hayashi-Nishino. Function and inhibitory mechanisms of multidrug efflux pumps. *Frontiers in Microbiology*, 12:737288, 2021. 20

17. Cícera Datiane de Moraes Oliveira-Tintino, Saulo Relison Tintino, Ana Carolina Justino de Araújo, Cristina Rodrigues dos Santos Barbosa, Priscilla Ramos Freitas, José Bezerra de Araújo Neto, Iêda Maria Begnini, Ricardo Andrade Rebelo, Luiz Everson da Silva, Sandro Lucio Mireski, et al. Efflux pump (qaca, qacb, and qacc) and  $\beta$ -lactamase inhibitors? an evaluation of 1, 8-naphthyridines against staphylococcus aureus strains. *Molecules*, 28(4):1819, 2023.
18. Francesca Prestinaci, Patrizio Pezzotti, and Annalisa Pantosti. Antimicrobial resistance: a global multifaceted phenomenon. *Pathogens and global health*, 109(7):309–318, 2015.
19. PubChem. Naphthyridine-3-carboxamide - compound summary. <https://pubchem.ncbi.nlm.nih.gov/compound/Naphthyridine-3-carboxamide>, 2024. Accessed: 2025-07-11.
20. PubChem. Triclocarban (cid 442009) - compound summary. <https://pubchem.ncbi.nlm.nih.gov/compound/442009>, 2024. Accessed: 2025-07-11.
21. RCSB Protein Data Bank. RCSB PDB: 7Y58 – Crystal Structure of QacA, a Drug:H<sup>+</sup> Antiporter. <https://www.rcsb.org/structure/7Y58>, 2022. Accessed: 2025-07-11.
22. Reinsurance Group of America. Antimicrobial resistance (amr) – a global burden, an individual problem. [https://www.rgare.com/knowledge-center/article/antimicrobial-resistance-\(amr\) ---a-global-burden-an-individual-problem](https://www.rgare.com/knowledge-center/article/antimicrobial-resistance-(amr)----a-global-burden-an-individual-problem), 2024. Accessed: 2025-07-11.
23. Md Abdus Salam, Md Yusuf Al-Amin, Moushumi Tabassoom Salam, Jogendra Singh Pawar, Naseem Akhter, Ali A Rabaan, and Mohammed AA Alqumber. Antimicrobial resistance: a growing serious threat for global public health. In *Healthcare*, volume 11, page 1946. Multidisciplinary Digital Publishing Institute, 2023.
24. Sirijan Santajit and Nitaya Indrawattana. Mechanisms of antimicrobial resistance in esophageal pathogens. *BioMed research international*, 2016(1):2475067, 2016.
25. Atin Sharma, Vivek Kumar Gupta, and Ranjana Pathania. Efflux pump inhibitors for bacterial pathogens: From bench to bedside. *Indian Journal of Medical Research*, 149(2):129–145, 2019.
26. Mohaddeseh Sheikhy, Vajihe Karbasizade, Mustafa Ghanadian, and Hossein Fazeli. Evaluation of chlorogenic acid and carnosol for anti-efflux pump and anti-biofilm activities against extensively drug-resistant strains of *staphylococcus aureus* and *pseudomonas aeruginosa*. *Microbiology Spectrum*, 12(9):e03934–23, 2024.
27. Sara M Soto. Role of efflux pumps in the antibiotic resistance of bacteria embedded in a biofilm. *Virulence*, 4(3):223–229, 2013.
28. Jingjing Sun, Ziqing Deng, and Aixin Yan. Bacterial multidrug efflux pumps: mechanisms, physiology and pharmacological exploitations. *Biochemical and biophysical research communications*, 453(2):254–267, 2014.
29. Jan M Tennent, Bruce R Lyon, Melvin Midgley, Gwyn Jones, Amarjit S Purewal, and Ronald A Skurray. Physical and biochemical characterization of the qaca gene encoding antiseptic and disinfectant resistance in *staphylococcus aureus*. *Microbiology*, 135(1):1–10, 1989.
30. Rahima Touaitia, Assia Mairi, Nasir Adam Ibrahim, Nosiba S Basher, Takfarinas Idres, and Abdelaziz Touati. *Staphylococcus aureus*: A review of the pathogenesis and virulence mechanisms. *Antibiotics*, 14(5):470, 2025
31. Guan, L., Yang, H., Cai, Y., Sun, L., Di, P., Li, W., Liu, G., & Tang, Y. (2018). ADMET-score – a comprehensive scoring function for evaluation of chemical drug-likeness. *MedChemComm*, 10(1), 148–157. <https://doi.org/10.1039/c8md00472b>

32. Flores-Holguín, N., Frau, J., & Glossman-Mitnik, D. (2021). In silico Pharmacokinetics, ADMET study and conceptual DFT analysis of two plant cyclopeptides isolated from rosaceae as a computational peptidology approach. *Frontiers in Chemistry*, 9. <https://doi.org/10.3389/fchem.2021.708364>
33. Flores-Holguín, N., Frau, J., & Glossman-Mitnik, D. (2021). Computational Pharmacokinetics report, ADMET study and conceptual DFT-Based estimation of the chemical reactivity properties of marine cyclopeptides. *ChemistryOpen*, 10(11), 1142–1149. <https://doi.org/10.1002/open.202100178>
34. www.wisdomlib.org. (2025, March 5). Ligand preparation: Significance and symbolism. <https://www.wisdomlib.org/concept/ligand-preparation>
35. Agu, P. C., Afiukwa, C. A., Orji, O. U., Ezeh, E. M., Ofoke, I. H., Ogbu, C. O., Ugwuja, E. I., & Aja, P. M. (2023). Molecular docking as a tool for the discovery of molecular targets of nutraceuticals in diseases management. *Scientific Reports*, 13(1). <https://doi.org/10.1038/s41598-023-40160-2>
36. Acharya, Chayan et al. "Recent advances in ligand-based drug design: relevance and utility of the conformationally sampled pharmacophore approach." *Current computer-aided drug design* vol. 7,1 (2011): 10-22. doi:10.2174/157340911793743547
37. Valich, L. (2024, August 28). New ligand-guided technique enhances drug development. News Center. <https://www.rochester.edu/newscenter/what-is-a-ligand-meaning-pharmaceuticals-616372/>
38. Technology, I. I. P. (2024, July 7). The role of protein synthesis in drug discovery and development. *The Role of Protein Synthesis in Drug Discovery and Development*. <https://www.iptonline.com/articles/the-role-of-protein-synthesis-in-drug-discovery-and-development>
39. Qiao, F., Binknowski, T. A., Broughan, I., Chen, W., Natarajan, A., Schiltz, G. E., Scheidt, K. A., Anderson, W. F., & Bergan, R. (2024). Protein structure inspired drug discovery. *bioRxiv* (ColdSpring Harbor Laboratory). <https://doi.org/10.1101/2024.05.17.59463>
40. Konc, J., & Janežič, D. (2022). Protein binding sites for drug design. *Biophysical Reviews*, 14(6), 1413–1421. <https://doi.org/10.1007/s12551-022-01028-3>
41. Agu, P. C., Afiukwa, C. A., Orji, O. U., Ezeh, E. M., Ofoke, I. H., Ogbu, C. O., Ugwuja, E. I., & Aja, P. M. (2023b). Molecular docking as a tool for the discovery of molecular targets of nutraceuticals in diseases management. *Scientific Reports*, 13(1). <https://doi.org/10.1038/s41598-023-40160-2>
42. Meng, X., Zhang, H., Mezei, M., & Cui, M. (2011). Molecular Docking: a powerful approach for Structure-Based drug discovery. *Current Computer - Aided Drug Design*, 7(2), 146–157. <https://doi.org/10.2174/157340911795677602>
43. Dodaro, A., Novello, G., Menin, S., Strascia, C. C., Sturlese, M., Salmaso, V., & Moro, S. (2025). Post-Docking refinement of peptide or Protein-RNA complexes using Thermal Titration Molecular Dynamics (TTMD): a stability insight. *Journal of Chemical Information and Modeling*. <https://doi.org/10.1021/acs.jcim.4c01393>
44. Team, E. W. (n.d.). LigPlot+ home page. <https://www.ebi.ac.uk/thornton-srv/software/LigPlus/>
45. Terefe, E. M., & Ghosh, A. (2022). Molecular Docking, Validation, Dynamics Simulations, and Pharmacokinetic Prediction of Phytochemicals Isolated From Croton dichogamus Against the HIV-1 Reverse Transcriptase. *Bioinformatics and Biology Insights*, 16. <https://doi.org/10.1177/11779322221125605>
46. Agrawal, Raghvendra, H. B. Punarva, Gagan O. Heda, Y. M. Vishesh, and Prashantha Karunakar. "VinaLigGen: a method to generate LigPlots and retrieval of hydrogen and hydrophobic interactions from protein-ligand complexes." *Journal of Biomolecular Structure and Dynamics* (2023): 1-4.

47. Wallace, Andrew C., Roman A. Laskowski, and Janet M. Thornton. "LIGPLOT: a program to generate schematic diagrams of protein-ligand interactions." *Protein engineering, design and selection* 8, no. 2 (1995): 127-134.
48. Dallakyan, Sargis, and Arthur J. Olson. "Small-molecule library screening by docking with PyRx." *Chemical biology: methods and protocols* (2015): 243-250.
49. Volkamer, A., Kuhn, D., Rippmann, F., & Rarey, M. (2012). DoGSiteScorer: a web server for automatic binding site prediction, analysis and druggability assessment. *Bioinformatics*, 28(15), 2074–  
<https://doi.org/10.1093/bioinformatics/bts310>
50. SwissADME: a free web tool to evaluate pharmacokinetics, drug-likeness and medicinal chemistry friendliness of small molecules. *Sci. Rep.* (2017) 7:42717.
51. Xiong, G., Wu, Z., Yi, J., Fu, L., Yang, Z., Hsieh, C., Yin, M., Zeng, X., Wu, C., Lu, A., Chen, X., Hou, T., & Cao, D. (2021). ADMETlab 2.0: an integrated online platform for accurate and comprehensive predictions of ADMET properties. *Nucleic Acids Research*, 49(W1), W5–W14.  
<https://doi.org/10.1093/nar/gkab255>
52. O'Boyle, N. M., Banck, M., James, C. A., Morley, C., Vandermeersch, T., & Hutchison, G. R. (2011). Open Babel: An open chemical toolbox. *Journal of Cheminformatics*, 3(1)  
<https://doi.org/10.1186/1758-2946-3-33>
53. Gaulton, A., Bellis, L. J., Bento, A. P., Chambers, J., Davies, M., Hersey, A., Light, Y., McGlinchey, S., Michalovich, D., Al-Lazikani, B., & Overington, J. P. (2011). ChEMBL: a large-scale bioactivity database for drug discovery. *Nucleic Acids Research*, 40(D1), D1100–D1107.  
<https://doi.org/10.1093/nar/gkr777>
54. The PyMOL Molecular Graphics System, Version 3.0 Schrödinger, LLC.